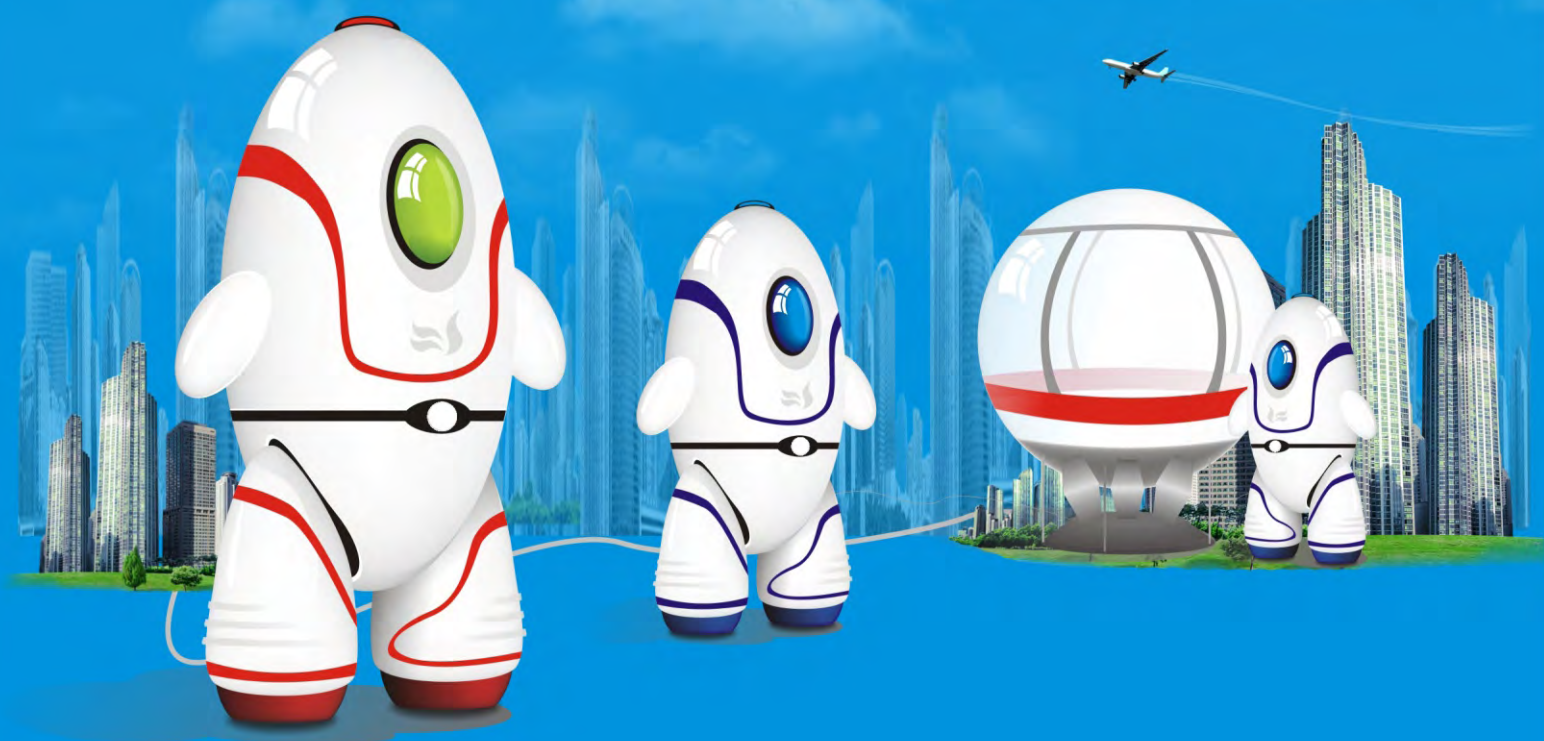


ISSN: 2153-0653 Vol.1, No.1, August 2010



Scientific  
Research

# Intelligent Control and Automation



ISSN: 2153-0653



[www.scirp.org/journal/ica](http://www.scirp.org/journal/ica)

# Journal Editorial Board

ISSN 2153-0653 (Print) ISSN 2153- 0661 (Online)

<http://www.scirp.org/journal/ica>

---

## Editor in Chief

**Prof. Theodore B. Trafalis** University of Oklahoma, USA

## Editorial Board

**Prof. Ramon Vilanova Arbos** Universitat Autònoma de, Brazil  
**Prof. Celal Batur** University of Akron, USA  
**Dr. Derya Birant** Dokuz Eylul University, Turkey  
**Prof. Ru-Xu Du** The Chinese University of Hong Kong, Hong Kong (China)  
**Prof. Vic Grout** Glyndŵr University, UK  
**Prof. Yanxiang He** Wuhan University, China  
**Dr. Tingwen Huang** Texas A&M University, USA  
**Prof. Ali vahidian Kamyad** University of Leeds, UK  
**Prof. Guay Martin** Queen's University, Canada  
**Dr. Peter Mitrouchev** Optimization and Production Laboratory of Grenoble, France  
**Dr. Chang-Woo Park** Korea Electronics Technology Institute, Korea (South)  
**Prof. Dilip Kumar Pratihar** Indian Institute of Technology, India  
**Prof. A. Karim Qayumi** University of British Columbia, Austria  
**Dr. José Reinaldo Silva** University of São Paulo, Brazil  
**Dr. Jue Wang** Chinese Academy of Sciences, China  
**Dr. Rong-Long Wang** University of Fukui, Japan  
**Dr. Wai-keung Wong** Hong Kong Polytechnic University, Hong Kong (China)  
**Prof. Tiaojun Xiao** Nanjing University, China  
**Prof. Vinod Yadava** Motilal Nehru National Institute of Technology, India  
**Dr. Jianfeng Yang** Wuhan University, China  
**Prof. Ruey-fang Yu** National United University, Taiwan (China)

## Editorial Assistant

Nancy Fang

Scientific Research Publishing Email: [ica@scirp.org](mailto:ica@scirp.org)

## TABLE OF CONTENTS

**Volume 1    Number 1**

**August 2010**

**Parametric Tolerance Analysis of Mechanical Assembly by Developing Direct**

**Constraint Model in CAD and Cost Competent Tolerance Synthesis**

G. Jayaprakash, K. Sivakumar, M. Thilak.....1

**Optimal Control Strategy for a Fully Determined HIV Model**

M. Shirazian, M. H. Farahi.....15

**Weightlifting Motion Generation for a Stance Robot with Repeatedly Direct Kinematics**

J. N. Liu, Y. Kamiya, H. Seki, M. Hikizu.....20

**A Nonmonotone Line Search Method for Symmetric Nonlinear Equations**

G. L. Yuan, L. S. Yu.....28

**Stability Analysis and Hadamard Synergic Control for a Class of Dynamical Networks**

X. J. Liu, Y. Zou.....36

**Maximizing of Asymptomatic Stage of Fast Progressive HIV Infected Patient**

**Using Embedding Method**

H. Zarei, A. V. Kamyad, S. Effati.....48

# **Intelligent Control and Automation**

## **Journal Information**

### **SUBSCRIPTIONS**

The *Intelligent Control and Automation* (Online at Scientific Research Publishing, [www.SciRP.org](http://www.SciRP.org)) is published quarterly by Scientific Research Publishing, Inc., USA.

#### **Subscription rates:**

Print: \$50 per copy.

To subscribe, please contact Journals Subscriptions Department, E-mail: [sub@scirp.org](mailto:sub@scirp.org)

### **SERVICES**

#### **Advertisements**

Advertisement Sales Department, E-mail: [service@scirp.org](mailto:service@scirp.org)

#### **Reprints (minimum quantity 100 copies)**

Reprints Co-ordinator, Scientific Research Publishing, Inc., USA.

E-mail: [sub@scirp.org](mailto:sub@scirp.org)

### **COPYRIGHT**

Copyright© 2010 Scientific Research Publishing, Inc.

All Rights Reserved. No part of this publication may be reproduced, stored in a retrieval system, or transmitted, in any form or by any means, electronic, mechanical, photocopying, recording, scanning or otherwise, except as described below, without the permission in writing of the Publisher.

Copying of articles is not permitted except for personal and internal use, to the extent permitted by national copyright law, or under the terms of a license issued by the national Reproduction Rights Organization.

Requests for permission for other kinds of copying, such as copying for general distribution, for advertising or promotional purposes, for creating new collective works or for resale, and other enquiries should be addressed to the Publisher.

Statements and opinions expressed in the articles and communications are those of the individual contributors and not the statements and opinion of Scientific Research Publishing, Inc. We assume no responsibility or liability for any damage or injury to persons or property arising out of the use of any materials, instructions, methods or ideas contained herein. We expressly disclaim any implied warranties of merchantability or fitness for a particular purpose. If expert assistance is required, the services of a competent professional person should be sought.

### **PRODUCTION INFORMATION**

For manuscripts that have been accepted for publication, please contact:

E-mail: [ica@scirp.org](mailto:ica@scirp.org)

# Parametric Tolerance Analysis of Mechanical Assembly by Developing Direct Constraint Model in CAD and Cost Competent Tolerance Synthesis

Govindarajalu Jayaprakash<sup>1</sup>, Karuppan Sivakumar<sup>2</sup>, Manoharan Thilak<sup>3</sup>

<sup>1</sup>Department of Mechanical Engineering, Shivani College of Engineering, Tiruchirapalli, India

<sup>2</sup>Department of Mechanical Engineering, Bannari Amman Institute of Technology, Sathiyamangalam, India

<sup>3</sup>Department of Mechanical Engineering, T. R. P. Engineering College, Tiruchirapalli, India

E-mail: [jpjaya\\_74@yahoo.co.in](mailto:jpjaya_74@yahoo.co.in), [ksk71@rediffmail.com](mailto:ksk71@rediffmail.com), [thilakrep@gmail.com](mailto:thilakrep@gmail.com)

Received February 17, 2010; revised March 21, 2010; accepted June 1, 2010

## Abstract

The objective of tolerance analysis is to check the extent and nature of variation of an analyzed dimension or geometric feature of interest for a given GD & T scheme. The parametric approach to tolerance analysis is based on parametric constraint solving. The accuracy of simulation results is dependent on the user-defined modeling scheme. Once an accurate CAD model is developed, it is integrated with tolerance synthesis model. In order to make it cost competent, it is necessary to obtain the cost-tolerance relationships. The neural network recently has been reported to be an effective statistical tool for determining relationship between input factors and output responses. This study deals development of direct constraint model in CAD, which is integrated to an optimal tolerance design problem. A back-propagation (BP) network is applied to fit the cost-tolerance relationship. An optimization method based on Differential Evolution (DE) is then used to locate the combination of controllable factors (tolerances) to optimize the output response (manufacturing cost plus quality loss) using the equations stemming from the trained network. A tolerance synthesis problem for a motor assembly is used to investigate the effectiveness and efficiency of the proposed methodology.

**Keywords:** Tolerance Analysis, Tolerance Synthesis, CAD Integration, Optimization, Neural Network

## 1. Introduction

Tolerance is the allowable range of variation from design intent in a dimension. As one of many design variables, the role of dimensional tolerances is to restrict the amount of size variation in a manufacturing feature while ensuring functionality. Although the ideal amount of feature variation is zero, it is neither feasible nor economical to meet the ideal due to a variety of process factors including machine tool accuracy, material property variation, process effects, etc. Determining the allowable amount of dimensional variation at design stage impacts the manufacturing costs incurred during the actual processing of the part. Tolerance analysis involves modeling of the relations among variation, tolerance and cost. Tolerance analysis is conducted using variation propagation models that compute how part, subassembly, and process variations propagate to final product variation, which is related to product quality. Variations are typically trans-

lated to tolerances using statistic principles, and analytical models are then used to estimate cost as a function of tolerance. The variation of the analyzed dimension arise from the accumulation of dimensional and/or geometric variations in the tolerance chain. The analysis include: 1) the contributor, *i.e.*, The dimensions or features that causes variations in the analyzed dimension, 2) the sensitivities with respect to each contributor, 3) the percent contribution to variation from each contributor, and 4) worst case variations, statistical distribution, and acceptance rates. Analysis approaches can be classified as 1) one-dimensional (1D), two-dimensional (2D), and three-dimensional (3D), according to dimensionality; 2) worst case (*i.e.*, 100% acceptance rate) and statistical (*i.e.*, less than 100% acceptance rate), according to analysis objective; 3) dimensional and dimensional + geometric, according to the type of variation included; or 4) part level and assembly level, according to the analysis level. Popular analysis methods are manual 1D chart, linearized 2D/3D analysis, and the Monte Carlo simula-

tion.

At the present time, three different and disconnected communities *i.e.*, designers/draftsmen, engineering analysts, and design researchers are using vastly different tools and techniques for tolerance analysis. Cultural and educational differences between these communities have isolated them from one another and made them unaware of the others' techniques. The draftsmen community uses a manual procedure called tolerance charts; but can do only worst-case analysis, and is conducted in only one direction at a time. Meanwhile, the engineering analysis community uses computer-aided tolerancing software CATs. These CAT packages can do both worst-case and statistical analyses. Many researchers [1-4] provided good surveys of GD&T modeling for CATs; Some researcher [5] discussed the simplification of feature based models for tolerance analysis, and used the linear programming approach to tolerance analysis involving geo-metric tolerances [5]; Guilford *et al.* [2] introduced a CAT system using the variation modeling and feasibility space approaches.

## 2. Background

### 2.1. 1D Tolerance Charts

Tolerance charting is a manual bookkeeping procedure for 1D stack calculations. The analyst typically works with engineering drawings [6-7]. Since the method is limited to worst-case analysis, the analyst positions parts in assemblies to yield each of the worst-cases minimum or maximum value of the analyzed dimension, *i.e.*, separate charts have to be constructed for each worst-case. Since no algebraic expression for the analyzed dimension in terms of the contributors is generated by this method, no statistical analysis can be performed. Also, contributors not in the direction of analysis are ignored, which may yield significant errors in most cases. The limitations associated with this method, as practiced today, are as follows. 1) It is done manually, and since each type of tolerance is handled differently, the user must remember all the rules correctly while constructing the charts to obtain correct results, making the process tedious and prone to errors. 2) It deals with one direction at a time, ignoring possible contributions from other directions, which often leads to inaccurate results. 3) The charting procedure is only capable of the worst-case analysis only; no statistical analysis is available. 4) This method has not been widely integrated with existing CAD systems.

### 2.2. Parametric Tolerance Analysis

Most CAT packages take advantage of the same parametric/variational approach used in CAD systems and

apply the Monte Carlo simulation to tolerance analysis [8-10]. This section will give a brief description of parametric approach to tolerance analysis. In the parametric approach, the analyzed dimension is expressed as an algebraic function an equation, or a set of equations that relates the analyzed dimension to those on which it depends *i.e.*, contributors. The function is either linearized or directly used for the Monte Carlo simulation in the nonlinear analysis. Results commonly available are the lists of contributors, sensitivities, and percentage contributions, and the tolerance accumulation for worst-case and statistical cases.

### 2.3. Cost Competent Tolerancing

Aspects such as design for quality, quality improvement and cost reduction, asymmetric quality losses, charts for optimum quality and cost, minimum cost approach, cost of assemblies, development of cost tolerance models [11-15] have been explored in the quality area of tolerance synthesis. Experiments (DOE) approach was used in robust tolerance design, the cases of 'nominal the best', 'smaller the better', 'larger the better', and asymmetric loss function, were investigated [16] and allocation of tolerances of products with asymmetric quality loss was presented [14]. The combined effect of manufacturing cost and quality loss was also investigated under the restraints of process capability limits, design functionality restriction and product quality requirements by using tolerance chart optimization for quality and cost [12]. Relationships between the product cost and tolerances have also been investigated. An analytical method was proposed for determining tolerances for mechanical parts with objectives of minimizing manufacturing costs [17]. Minimizing the cost of assembly was investigated mathematically in which it was observed that widening the tolerance of more expensive part and a tightening of tolerances on cheaper parts could result in major reduction in cost of the assembly [18]. Exhaustive search, zero-one, SQP and Univariate methods were evaluated for performing a combined minimum cost tolerance allocation and process selection [19]. The production cost tolerance and hybrid tolerance models based on empirical cost tolerance data of manufacturing processes like punching, turning, milling, grinding and casting were introduced [20]. The robust design by tolerance allocation considering quality and manufacturing cost and optimizing tolerance allocation based on manufacturing cost were also investigated [21,22]. It involved development of relationship between part tolerances and assembly tolerances to provide a quantitative measure of product quality using the quality loss function concept introduced by Taguchi. Numerical optimization was used to balance manufacturing cost and product quality. The possibility of using statistics and probability methods for

allocation of tolerances has also been explored with a view to developing tools for tolerance synthesis.

Relationship between function and dimensional variation on assembly was considered as logical basis for selection of tolerances [23]. A probabilistic model for tolerance synthesis was developed [24] in which the reliability indices were associated with either assembly condition or component dimension. Strategies to compute small changes or gradient in tolerance values were also developed using probability theory [25]. Tolerance cost models based on the distribution function zone [26], tolerance optimization problem using system of experimental design [27] and using Monte–Carlo simulations [28] approaches, were also investigated in application of statistical methods for tolerance synthesis.

#### 2.4. Neural Network-Based Cost-Tolerance Functions

Neural networks have received a lot of attention in many research and application areas. One of the major benefits of neural networks is the adaptive ability of their generalization of data from the real world. Exploiting this advantage, many researchers apply neural networks for nonlinear regression analysis and have reported positive experimental results in their applications [29]. Recently, neural networks have received a great deal of attention in manufacturing areas. Zhang and Huang [30] presented an extensive review of neural network applications in manufacturing. Neural networks are defined by Rumelhart and McClelland [31] as massively parallel interconnected networks of simple (usually adaptive) elements and their hierarchical organizations which are intended to interact with objects of the real world in the same way as biological nervous systems do. The approach towards constructing the cost tolerance relationships is based on a supervised back-propagation (BP) neural network. Among several well-known supervised neural networks, the BP model is the most extensively used and can provide good solutions for much industrial application [32].

A BP network is a feed-forward network with one or more layers of nodes between the input and output nodes. An imperative item of the BP network is the iterative method that propagates the error terms required to adopt weights back from nodes in the output layer to nodes in lower layers. The training of a BP network involves three stages: the feed forward of the input training pattern, the calculation and BP of the associated error, and the adjustment of the weights. After the network reaches a satisfactory level of performance, it will learn the relationships between input and output patterns and its weights can be used to recognize new input patterns.

**Figure 1** depicts a BP network with one hidden layer. The hidden nodes of the hidden layer perform an impor-

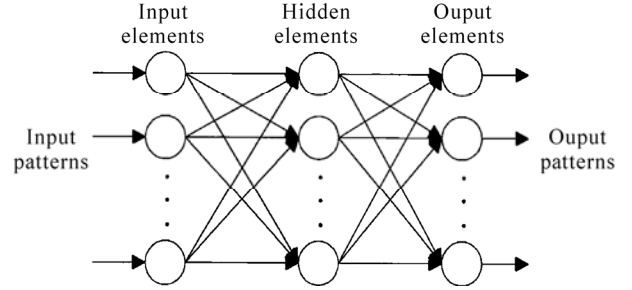


**Figure 1. Architecture of a three-layer BP network.**

tant role in creating internal representation. The following nomenclatures are used for describing the BP learning rule.

$net_{pi}$  = net input to processing unit  $i$  in pattern  $p$  (a pattern corresponding to a vector of factors),

$w_{ij}$  = connection weight between processing unit  $I$  and processing unit  $j$ ,

$a_{pi}$  = activation value of processing unit  $i$  in pattern  $p$ ,

$\delta_{pi}$  = the effect of a change on the output of unit  $I$  in pattern  $p$ ,

$g_{pi}$  = target value of processing unit  $i$ ,

$\varepsilon$  = learning rate.

The net inputs and the activation values of the middle processing nodes are calculated as follows:

$$net_{pi} = \sum_j w_{ij} a_{pj} \quad (1)$$

$$a_{pi} = \frac{1}{1 + \exp(-net_{pi})} \quad (2)$$

The net input is the weighed sum of activation values of the connected input units plus a bias value. Initially, the connection weights are assigned randomly and are varied continuously. The activation values are in turn used to calculate the net inputs and the activation values of the output processing units using the same Equations (1) and (2).

Once the activation values of the output units are calculated, we compare the target value with activation value of each output unit. The discrepancy is propagated using.

$$\delta_{pi} = (g_{pi} - a_{pi}) f'_i (net_{pi}) \quad (3)$$

For the hidden processing units in which the target values are unknown, instead of Equation (3), the following equation is used to calculate the discrepancy. It takes the form

$$\delta_{pi} = f'_i (net_{pi}) \sum_k \delta_{pk} w_{ki} \quad (4)$$

From the results of Equations (3) and (4), the weights between processing units are adjusted using

$$\Delta w_{ij} = \varepsilon \delta_{pi} a_{pj} \quad (5)$$

## 2.5. Differential Evolution (DE)

Differential Evolution is an improved version of Genetic Algorithm for faster optimization [33]. Unlike simple GA that uses binary coding for representing problem parameters, Differential Evolution (DE) uses real coding of floating point numbers. Among the DE's advantages are its simple structure, ease of use, speed and robustness.

The simple adaptive scheme used by DE ensures that the mutation increments are automatically scaled to the correct magnitude. Similarly DE uses a non-uniform crossover in that the parameter values of the child vector are inherited in unequal proportions from the parent vectors. For reproduction, DE uses a tournament selection where the child vector competes against one of its parents. The overall structure of the DE algorithm resembles that of most other population based searches. The parallel version of DE maintains two arrays, each of which holds a population of  $NP$ ,  $D$ -dimensional, real valued vectors. The primary array holds the current vector population, while the secondary array accumulates vectors that are selected for the next generation. In each generation,  $NP$  competitions are held to determine the composition of the next generation. Every pair of vectors ( $X_a$ ,  $X_b$ ) defines a vector differential:  $X_a - X_b$ . When  $X_a$  and  $X_b$  are chosen randomly, their weighted differential is used to perturb another randomly chosen vector  $X_c$ . This process can be mathematically written as  $X'c = Xc + F(Xa - Xb)$ . The scaling factor  $F$  is a user supplied constant in the range ( $0 < F < 1.2$ ). The optimal value of  $F$  for most of the functions lies in the range of 0.4 to 1.0 [33]. Then in every generation, each primary array vector,  $X_i$  is targeted for crossover with a vector like  $X'c$  to produce a trial vector  $X_t$ . Thus the trial vector is the child of two parents, a noisy random vector and the target vector against which it must compete. The non-uniform crossover is used with a crossover constant  $CR$ , in the range  $0 < CR < 1$ .  $CR$  actually represents the probability that the child vector inherits the parameter values from the noisy random vector. When  $CR = 1$ , for example, every trial vector parameter is certain to come from  $X'c$ . If, on the other hand,  $CR = 0$ , all but one trial vector parameter comes from the target vector. To ensure that  $X_t$  differs from  $X_i$  by at least one parameter, the final trial vector parameter always comes from the noisy random vector, even when  $CR = 0$ . Then the cost of the trial vector is compared with that of the target vector, and the vector that has the lowest cost of the two would survive for the next generation. In all, just three factors control evolution under DE, the population size,  $NP$ ; the weight applied to the random differential,  $F$ ; and the crossover constant,  $CR$ .

The general convention used is  $DE/x/y/z$ . DE stands for Differential Evolution,  $x$  represents a string denoting

the vector to be perturbed,  $y$  is the number of difference vectors considered for perturbation of  $x$ , and  $z$  stands for the type of crossover being used (exp:exponential; bin: binomial). Thus, the working algorithm outlined above is the strategy of DE, i.e.,  $DE/rand/1/bin$ . Hence the perturbation can be either in the best vector of the previous generation or in any randomly chosen vector. Similarly for perturbation either single or two vector differences can be used. For perturbation with a single vector difference, out of the three distinct randomly chosen vectors, the weighted vector differential of any two vectors is added to the third one. Similarly for perturbation with two vector differences, five distinct vectors, other than the target vector are chosen randomly from the current population. Out of these, the weighted vector difference of each pair of any four vectors is added to the fifth one for perturbation. In binomial crossover, the crossover is performed on each of the  $D$  variables whenever a randomly picked number between 0 and 1 is within the  $CR$  value.

### 2.5.1. Pseudo Code for DE

The pseudo code of DE used in the present study is given below:

- Choose a seed for the random number generator.
- Initialize the values of  $D$ ,  $NP$ ,  $CR$ ,  $F$  and  $MAXGEN$  (maximum generation).
- Initialize all the vectors of the population randomly. The variables are normalized within the bounds. Hence generate a random number between 0 and 1 for all the design variables for initialization.
  - for  $i = 1$  to  $NP$
  - { for  $j = 1$  to  $D$
  - $X_{i,j} = \text{Lower bound} + \text{random number} * (\text{upper bound} - \text{lower bound})$
- All the vectors generated should satisfy the constraints. Penalty function approach, i.e., penalizing the vector by giving it a large value, is followed only for those vectors, which do not satisfy the constraints.
- Evaluate the objective function of each vector. Here is the value of the objective function to be minimized calculated by a separate function *defunct*. *objective* ()
  - for  $i = 1$  to  $NP$
  - $C_i = \text{defunct. objective} ()$
- Find out the vector with the minimum objective value i.e. the best vector so far.
  - $C_{min} = C_1$  and  $best = 1$
  - for  $i = 2$  to  $NP$
  - { if ( $C_i < C_{min}$ )
  - then  $C_{min} = C_i$  and  $best = i$  }
- Perform mutation, crossover, selection and evaluation of the objective function for a specified number of generations.
  - While ( $gen < MAXGEN$ )
  - { for  $i = 1$  to  $NP$
  - {
  - For each vector  $X_i$  (target vector), select three distinct

vectors  $Xa$ ,  $Xb$  and  $Xc$  (select five, if two vector differences are to be used) randomly from the current population (primary array) other than the vector  $Xi$  do

```
{ r1 = random number * NP
r2 = random number * NP
r3 = random number * NP
} while
(r1 = i) OR (r2 = i) OR (r3 = i) OR (r1 = r2) OR (r2 = r3)
OR (r1 = r3)
· Perform crossover for each target vector  $Xi$  with its
noisy vector  $Xn,i$  and create a trial vector,  $Xt, i$ . Per-
forming mutation creates the noisy vector.
· If  $CR = 0$  inherit all the parameters from the target
vector  $Xi$ , except one which should be from  $Xn, i$ .
· for binomial crossover
{  $p =$  random number
for  $n = 1$  to  $D$ 
{if ( $p < CR$ )
 $Xn, i = Xa, i + F(Xb, i - Xc, i)$ 
 $Xt, i = Xn, i$ 
} else  $Xt, i = Xi, j$ 
}
· Again, the NP noisy random vectors that are generated
should satisfy the constraint and the penalty function
approach is followed as mentioned above.
· Perform selection for each target vector,  $Xi$  by com-
paring its objective value with that of the trial vector,  $Xt, i$ ;
whichever has the minimum objective will survive for the
next generation.
 $Ct, i =$  defunct. Objective ()
if ( $Ct, i < Ci$ )
new  $Xi = Xt, i$ 
else new  $Xi = Xi$ 
/* for  $i = 1$  to NP */
}
```

· Print the results (after the stopping criteria is met).

The stopping criterion is maximum number of genera-  
tions.

### 3. Parametric Approach Using Direct CAD

In the parametric approach, the analyzed dimension is expressed as an algebraic function an equation, or a set of equations that relates the analyzed dimension to those on which it depends, *i.e.*, contributors. The function is either linearized or directly used for the Monte Carlo simulation in the nonlinear analysis. Results commonly available are the lists of contributors, sensitivities, and percentage contributions, and the tolerance accumulation for worst-case and statistical cases.

#### 3.1. Linearized Tolerance Analysis

In this type of analysis, partial derivatives are calculated

for each contributor; the derivatives give the sensitivity for each contributor from which worst case and variance can be determined. In general, the dimension to be analyzed,  $A$ , can be expressed as a function of independent variables (contributors),  $d_i$ , *i.e.*,

$$A = f(d_1, d_2, \dots, d_n) \quad (6)$$

To perform a linearized tolerance analysis, this function  $f$ , usually called the design function, is linearized about the variables nominal values  $\bar{d}_i$ , using the Taylor's series expansion, as follows:

$$A \approx f(\bar{d}_1, \dots, \bar{d}_n) + \sum_{i=1}^n \left( \frac{\partial f}{\partial d_i} \times \Delta d_i \right) \quad (7)$$

After linearization, both worst-case and statistical analyses can be performed. For worst-case analysis, the mean and worst-case variance of  $A$  are computed from equation below

$$\bar{A} = \frac{\partial f}{\partial d_1} \bar{d}_1 + \frac{\partial f}{\partial d_2} \bar{d}_2 + \dots + \frac{\partial f}{\partial d_n} \bar{d}_n \quad (8)$$

$$\Delta A = \frac{\partial f}{\partial d_1} \Delta d_1 + \frac{\partial f}{\partial d_2} \Delta d_2 + \dots + \frac{\partial f}{\partial d_n} \Delta d_n \quad (9)$$

For statistical analysis, the mean of  $A$  is computed using the same equation as (8), but statistical variance of  $A$  is obtained from this equation

$$\sigma_A = \sqrt{\left( \frac{\partial f}{\partial d_1} \right)^2 \sigma_{d1}^2 + \left( \frac{\partial f}{\partial d_2} \right)^2 \sigma_{d2}^2 + \dots + \left( \frac{\partial f}{\partial d_n} \right)^2 \sigma_{dn}^2} \quad (10)$$

The percentage contribution of  $d_i$  is computed as

$$C_i = \left( \frac{S_i \sigma_i}{\sigma_A} \right)^2 \times 100\% \quad (11)$$

The acceptance rate can also be computed if the corresponding design limits of  $A$  are supplied. In the earlier equations,  $S_i = \partial f(\bar{d}_1, \dots, \bar{d}_n) / \partial d_i$  is the sensitivity of  $A$  to the contributor  $d_i$ , and  $\Delta d_i = (d_i - \bar{d}_i)$  represents the contributors' perturbation ranges (tolerances) about their respective nominal values. Tolerance sensitivity is an essential aspect of tolerance analysis for mechanical assemblies in 2D and 3D space while the sensitivity is nonzero constants (usually 1.0) for 1D analysis. The contributors' tolerances are usually assumed to correspond to  $n$  sigma standard deviations (typically  $n = 6$ , *i.e.*,  $\Delta d = 6\sigma$ ) in statistical analysis.  $S_i$  and  $C_i$  are useful measures for redesign.

#### 3.2. Direct Constraint Model in CAD

In parametric CAD systems, constraint equations based

on geometric and dimensional relations are used to model a design. By perturbing the variables in these equations, some kind of sensitivity and tolerance analysis can be performed [32]. The design process using such a system is as follows. 1) First, create the nominal topology to obtain a model exhibiting the desired geometric elements and connectivity between the elements, but without the dimensions. 2) Next, describe the required properties between the model entities in terms of geometric constraints, which define the desired mathematical relationships between the numerical variables of the model entities. 3) Third, the modeling system applies a general solution procedure to the constraints, resulting in an evaluated model where the declared constraints are satisfied. 4) Create variants of the model by changing the values of the constrained variables. After each change, a new instance of the model is created by re-executing the constraint solution procedure.

As can be seen from the earlier process, if the user specifies the dimension of interest, the system solution procedure can also obtain that value for a specific instance of the model. If one variable is perturbed at a time, this variable's sensitivity can be studied by comparing this perturbation's effect on the dimension of interest. With the sensitivities of each variable and their perturbation ranges tolerances, both linearized and non-linearized analyses can be performed. Therefore, tolerance analysis functionality is just an extension or by-product of parametric solid modeling.

#### 4. An Application

In this study, the Pro/E wildfire version 3.0 parametric modeling software package is used to develop the direct constraint model. Linear tolerance analysis (statistical analysis) is carried out for the problem, in which partial derivatives are calculated for each contributor and the derivatives give the sensitivity for each contributor from which variance can be determined. The response variable in this study is Total cost which is sum of manufacturing cost and quality losses and it is expressed as

$$TC_i = \sum_{j=1}^q k_j \left[ (U_{ij} - T_j)^2 + \sigma_{ij}^2 \right] + \sum_{k=1}^m C_M(t_{ik}) \quad (12)$$

where  $m$  is the total number of components from  $q$  assembly dimensions in a finished product,  $K_j$  the cost coefficient of the  $j$ th resultant dimension for quadratic loss function,  $U_{ij}$  the  $j$ th resultant dimension from the  $i$ th experimental results,  $\sigma_{ij}$  the  $j$ th resultant variance of statistical data from the  $i$ th experimental results,  $T_j$  the design nominal value for the  $j$ th assembly dimension,  $t_{ik}$  the tolerance established in the  $i$ th experiment for the  $k$ th component, and  $C_M(t_{ik})$  the manufacturing cost for the tolerance  $t_{ik}$ .

This application is related to motor assembly [13]

which consists of an x-base, crank, shaft and motor base. **Figures 2-7** are graphic representation of the motor assembly with dimensioning and tolerancing schemes. **Table 1** provides some relevant information for these figures. The ordering number in the first row of **Table 1** is also given in **Figures 3-7** for the purpose of easy association. The objective is to determine an appropriate tolerance allocation so that there is sufficient clearance between the crank and x-base.

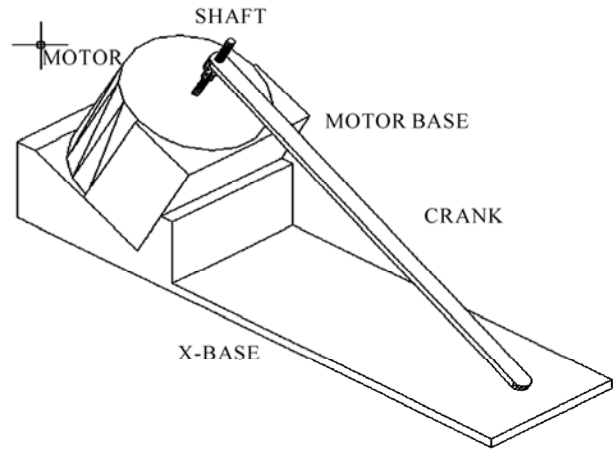


Figure 2. A motor assembly drawing (Jeang, 1999).

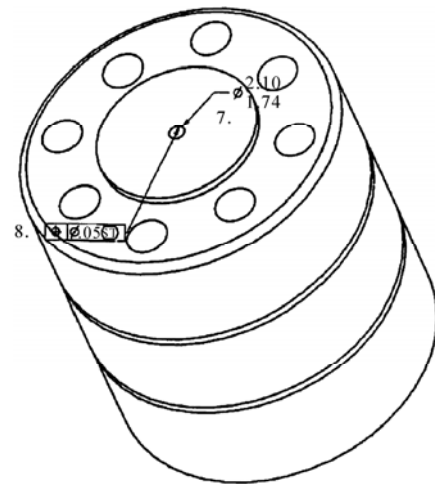


Figure 3. X-base.

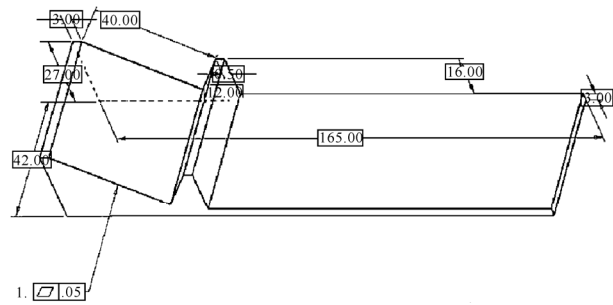
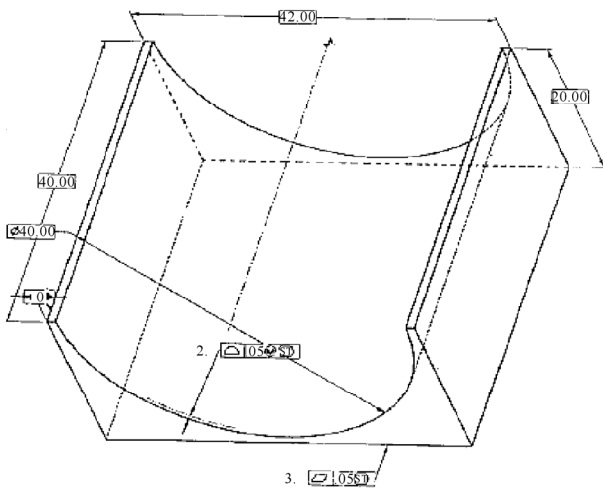


Figure 4. X-base.

**Table 1. Dimensioning and tolerancing schemes for motor assembly.**

| Tolerance and size no.    | 1                       | 2                     | 3                                   | 4   | 5                         | 6                | 7                  | 8                      | 9                  | 10                             |
|---------------------------|-------------------------|-----------------------|-------------------------------------|---|---------------------------|------------------|--------------------|------------------------|--------------------|--------------------------------|
| Component                 | X-base                  | motor base            | motor base                          | motor shaft                                 | motor shaft               | motor shaft      | motor              | motor                  | crank              | crank                          |
| Geometry feature          | flatness                | profile               | flatness                            | size  | perpendicularity          | profile          | size               | position               | size               | Perpendicularity               |
| Illustration              | Surface on X-base       | Surface on motor base | Surface on the bottom of motor base | Size of the shaft (with target value 2.0cm) | Perpendicularity of shaft | Profile of shaft | Hole size of motor | Hole position of motor | Hole size of crank | Hole perpendicularity of crank |
| Possible tolerance levels | 0.050<br>0.075<br>0.100 | –                     | 0.040<br>0.060<br>0.080             | 0.100<br>0.150<br>0.200                     | 0.050<br>0.075<br>0.1     | –                | –                  | –                      | –                  | –                              |
| Influence on clearance?   | yes                     | no                    | yes                                 | yes   | yes                       | no               | no                 | no                     | no                 | no                             |



**Figure 5. Motor base.**

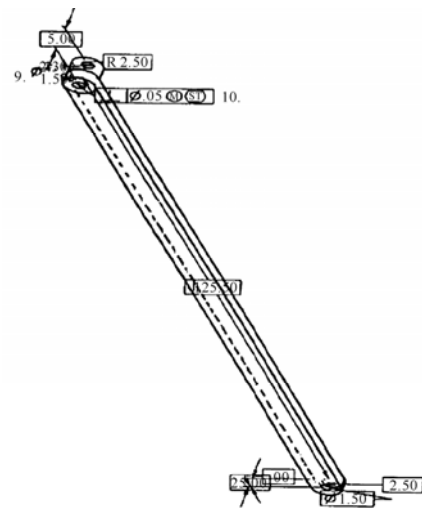


**Figure 7. Crank.**

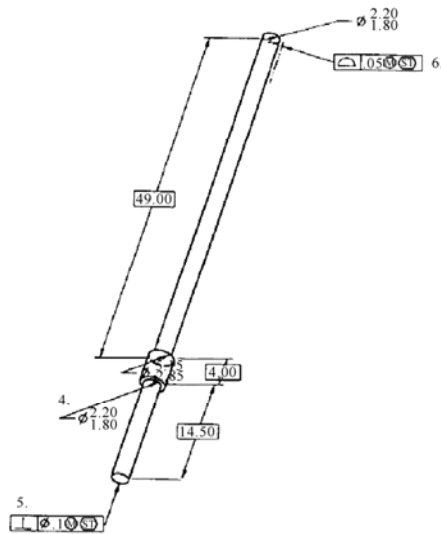


**Figure 6. Shaft.**

A parametric model of motor assembly is created in order to develop constraint equations based on geometric and dimensional relations (**Figure 8**). The direct constraint model in CAD is created as follows. 1) First, a nominal topology to obtain a model exhibiting the desired geometric elements and connectivity between the elements is created, but without the dimensions. 2) Next, the required properties between the model entities is described in terms of geometric constraints, which define the desired mathematical relationships between the numerical variables of the model entities. 3) Thirdly, a general solution procedure is applied to the constraints, which results in an evaluated model where the declared constraints are satisfied. 4) Finally, more variants of the model are created by changing the values of the constrained variables. After each change, a new instance of the model is created by re-executing the constraint solution procedure.

Once the constraint equation is developed (Equation 13), sensitivity and tolerance analysis can be performed by perturbing the variables in that equation. Then, the user has to specify the dimension of interest; the system solution procedure will obtain that value for the specific instance of the model. In this application the dimension of interest is clearance between the crank and x-base which is 0.89 cm (**Figure 9**). The variables are  $X_1$  (motor shaft size),  $X_2$  (motor shaft perpendicularity),  $X_3$  (x-base) and  $X_4$  (motor base flatness). The number of levels for each variable is three. **Table 3** shows the variables and levels of experiment with 27 runs. Each variable's sensitivity can be studied by comparing this perturbation's effect on the dimension of interest by perturbing that variable alone. After determining the sensitivities of each variable and their perturbation ranges tolerances, both linearized analyses can be performed. Thus the tolerance analysis functionality is found to be an extension or by-product of parametric solid modeling.

$$\begin{aligned} & X_1 \times \sin(0.5771) + \frac{X_2 \times \sin(0.5771)}{2} \\ & - \frac{X_3 \times \sin(0.99369)}{2} - \frac{X_4 \times \sin(0.99369)}{2} \quad (13) \\ & \leq 0.116084 \end{aligned}$$

Then neural network model of cost-tolerance function is developed as follows. The 2/3<sup>rd</sup> of experimental results drawn randomly from **Table 3** are used to train the neural network. Before applying the neural network for modeling, the architecture of the network has been decided; *i.e.* the number of hidden layers and the number of neurons in each layer. As there are 4 inputs and 1 output, the number of neurons in the input and output layer has to be set to 4 and 1 respectively. Also, the back propagation architecture with one hidden layer is enough for majority of the applications. Hence only one hidden layer has been adopted. A procedure was employed to optimize the number of neurons in the hidden layer. Accordingly, an experimental approach was adopted, which involves testing the trained neural networks against the remaining 1/3<sup>rd</sup> of experimental results. Experimental and predicted outputs for different number of neurons have been compared. The regression statistics for different architecture are determined and listed in **Table 4** and the same have been plotted against the number of neurons as shown in **Figure 10**. It is observed that the regression statistics were minimized with 7 neurons.

Hence, 4-7-1 is the most suitable network for the task under consideration. The training function used in this research is Gradient descent with momentum back-propagation. The transfer function used in this research is

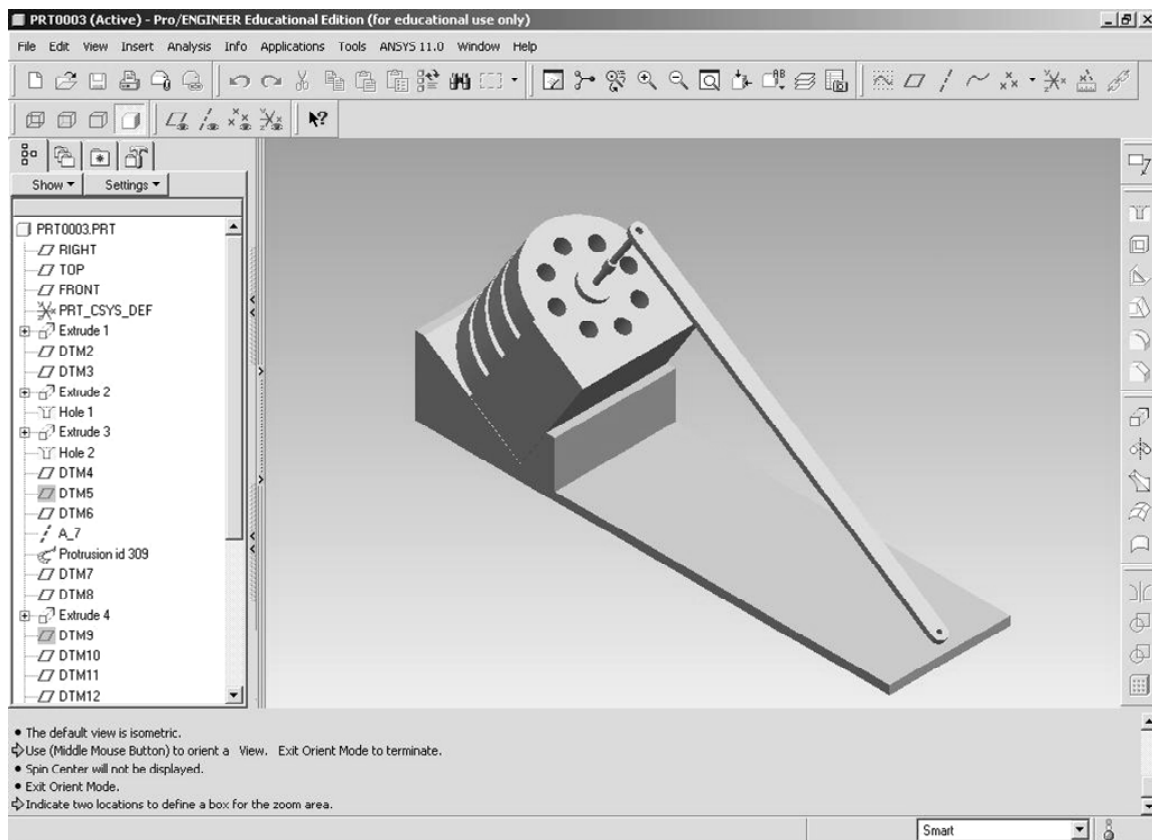


**Figure 8. Motor assembly (Pro/E Wildfire 3.0 model).**

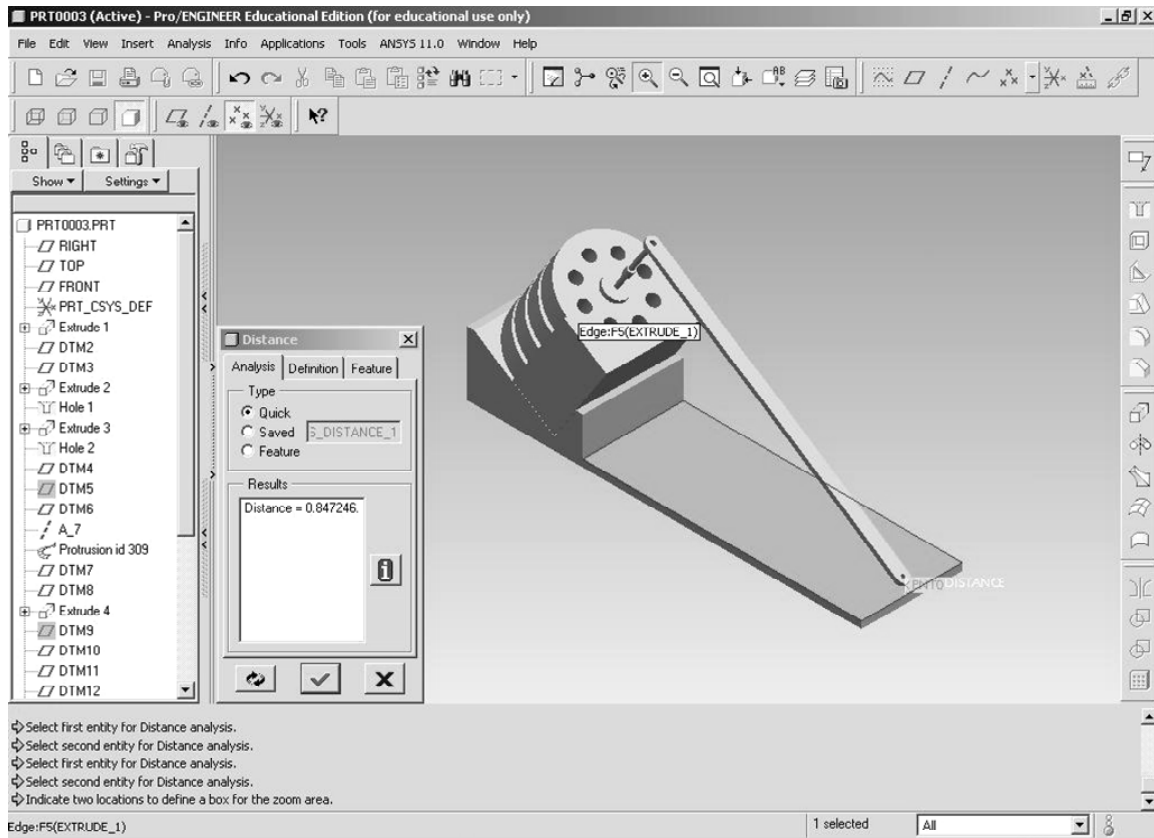


Figure 9. Motor assembly–Value of Clearance.

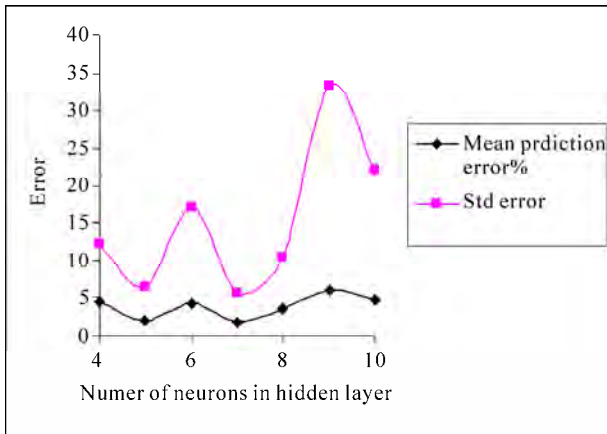


Figure 10. Error versus the number of neurons in a hidden layer.

Table 2. Tolerance costs for each factor at various levels.

|    | Lower level | Middle level | Upper level |
|----|-------------|--------------|-------------|
| x1 | \$18.07     | \$13.63      | \$12.82     |
| x2 | \$35.18     | \$24.68      | \$21.90     |
| x3 | \$279.61    | \$170.39     | \$108.57    |
| x4 | \$29.87     | \$19.62      | \$17.98     |

tan-sigmoid and gradient. Descent w/momentum weight/bias learning function has been used. **Figure 11** shows the schematic diagram of the neural network. The learning rate = 0.7, momentum = 0.65 and training epochs = 2000. The weights (and biases) are randomly initialized between -0.5 and 0.5. Once the neural network gets trained, it can provide the result for any arbitrary value of input data set. **Table 5** shows the experimental result and the model prediction. It is observed that the prediction based on an ANN model is quite close to the experimental observation.

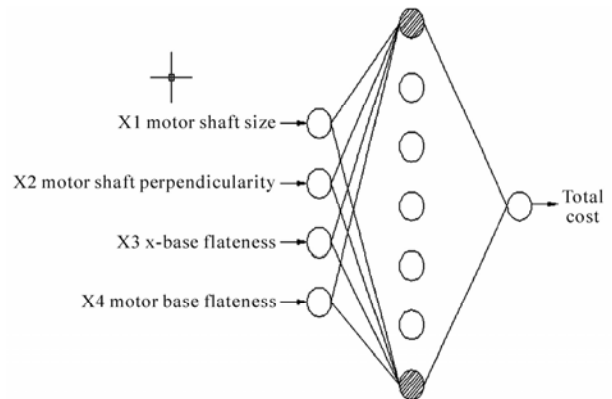


Figure 11. Schematic diagram of the neural network.

**Table 3. Experiment design.**

| Experiment number | X-Base Flatness (x1) | Motor base Flatness (x2) | Motor shaft size (x3) | Motor shaft perpendicularity (x4) | Total cost in \$ TC(X) |
|-------------------|----------------------|--------------------------|-----------------------|-----------------------------------|------------------------|
| 1                 | 0.15                 | 0.075                    | 0.1                   | 0.08                              | 228.9                  |
| 2                 | 0.15                 | 0.075                    | 0.1                   | 0.04                              | 239.5                  |
| 3                 | 0.15                 | 0.075                    | 0.05                  | 0.08                              | 361.3                  |
| 4                 | 0.15                 | 0.075                    | 0.05                  | 0.04                              | 373.0                  |
| 5                 | 0.15                 | 0.1                      | 0.075                 | 0.08                              | 266.1                  |
| 6                 | 0.15                 | 0.1                      | 0.075                 | 0.04                              | 277.6                  |
| 7                 | 0.15                 | 0.05                     | 0.075                 | 0.08                              | 277.2                  |
| 8                 | 0.15                 | 0.05                     | 0.075                 | 0.04                              | 289.0                  |
| 9                 | 0.15                 | 0.1                      | 0.1                   | 0.06                              | 228.4                  |
| 10                | 0.15                 | 0.1                      | 0.05                  | 0.06                              | 361.1                  |
| 11                | 0.15                 | 0.05                     | 0.1                   | 0.06                              | 240.8                  |
| 12                | 0.15                 | 0.05                     | 0.05                  | 0.06                              | 372.5                  |
| 13                | 0.2                  | 0.075                    | 0.075                 | 0.08                              | 274.6                  |
| 14                | 0.2                  | 0.075                    | 0.075                 | 0.04                              | 286.3                  |
| 15                | 0.1                  | 0.075                    | 0.075                 | 0.08                              | 267.0                  |
| 16                | 0.1                  | 0.075                    | 0.075                 | 0.04                              | 278.7                  |
| 17                | 0.2                  | 0.075                    | 0.1                   | 0.06                              | 236.3                  |
| 18                | 0.2                  | 0.075                    | 0.05                  | 0.06                              | 369.9                  |
| 19                | 0.1                  | 0.075                    | 0.1                   | 0.06                              | 228.6                  |
| 20                | 0.1                  | 0.075                    | 0.05                  | 0.06                              | 362.0                  |
| 21                | 0.2                  | 0.1                      | 0.075                 | 0.06                              | 274.6                  |
| 22                | 0.2                  | 0.05                     | 0.075                 | 0.06                              | 290.9                  |
| 23                | 0.1                  | 0.1                      | 0.075                 | 0.06                              | 266.7                  |
| 24                | 0.1                  | 0.05                     | 0.075                 | 0.06                              | 278.3                  |
| 25                | 0.15                 | 0.075                    | 0.075                 | 0.06                              | 271.2                  |
| 26                | 0.15                 | 0.075                    | 0.075                 | 0.06                              | 268.4                  |
| 27                | 0.15                 | 0.075                    | 0.075                 | 0.06                              | 269.9                  |

The neural network model for the above problem is developed as per the approach discussed previously. Based on those discussions, the BP network of 4-7-1 architecture produces the best performance (refer **Table 4**) and the same is adopted to generate the neural network based cost-tolerance function under this case study.

At this point, the relationship between input factors  $X = (x_1, x_2, x_3, x_4) = (x\text{-base flatness, motor base flatness, motor shaft size, motor shaft perpendicularity})$ , and output response  $F(X)$  (total cost defined by Equation 12) can be revealed from the constructed neural network.

The solution of the motor assembly case can be found by solving the following mathematical models:

$$\begin{aligned} \text{Maximize } F(X) &= F(x_1, x_2, x_3, x_4) \\ \text{subject to } &0.1 \leq x_1 \leq 0.2, \\ &0.05 \leq x_2 \leq 0.1, \\ &0.05 \leq x_3 \leq 0.1, \\ &0.04 \leq x_4 \leq 0.08 \end{aligned} \quad (14)$$

A clearance of 0.89 cm has to be maintained between

**Table 4. Regression statistics for each network architecture.**

| Network architecture | Mean Prediction error % | R square value | Standard error |
|----------------------|-------------------------|----------------|----------------|
| 4-4-1                | 4.498492501             | 0.943112       | 12.06117       |
| 4-5-1                | 2.035675506             | 0.987509       | 6.426893       |
| 4-6-1                | 4.100965211             | 0.902752       | 16.94439       |
| 4-7-1                | 1.735294596             | 0.989658       | 5.608395       |
| 4-8-1                | 3.495912167             | 0.96686        | 10.32931       |
| 4-9-1                | 5.935647182             | 0.725488       | 33.33576       |
| 4-10-1               | 4.749441739             | 0.850217       | 22.10918       |

**Table 5. Comparison of experimental results with the ANN model prediction.**

| Total cost in \$ TC(X) Experimental results               | Predicted values by ANN | Prediction error (%) |
|---|-------------------------|----------------------|
| 239.517   | 233.5125993             | 2.506878729          |
| 373.02  | 370.1791799             | 0.761573146          |
| 228.449   | 229.8694101             | 0.621762439          |
| 361.1   | 353.4342438             | 2.12289012           |
| 266.993   | 269.1789878             | 0.818743499          |
| 236.277   | 234.1075089             | 0.918198157          |
| 274.648   | 270.9355255             | 1.351720937          |
| 266.679   | 251.1227928             | 5.833307915          |
| 271.192   | 269.3409074             | 0.682576422          |
| Maximum prediction error for each output in this row in % |                         | 5.833307915          |
| Minimum prediction error for each output in this row in % |                         | 0.621762439          |
| Mean prediction error for each output in this row in %    |                         | 1.735294596          |

**Table 6. The DE specific data.**

| Variable type           | Real variable |
|-------------------------|---------------|
| Population size         | 100           |
| Cross over type         | binomial      |
| No of difference vector | 1             |
| Vector to be perturbed  | random        |
| Total no of generation  | 100           |
| No of variables         | 4             |

motor base and crank. The functional constraint is the constraint equation developed using the parametric model (Equation 13). The Problem (14) is solved by the proposed Differential evolution discussed in the previous section. The outline of the proposed optimization strategy is shown in **Figure 12**.

The optimization strategy is explained as follows. Initially the cost-tolerance function is established by the neural network model. Once the neural network based cost-tolerance function is established, and then optimization of the problem (Equation 14) is carried out using Differential evolution (DE). The DE optimization program determines the set of tolerance with minimum cost. Those tolerance values are assigned to the Direct constraint model in CAD and the clearance value is determined. If the clearance value is less than the desired one,

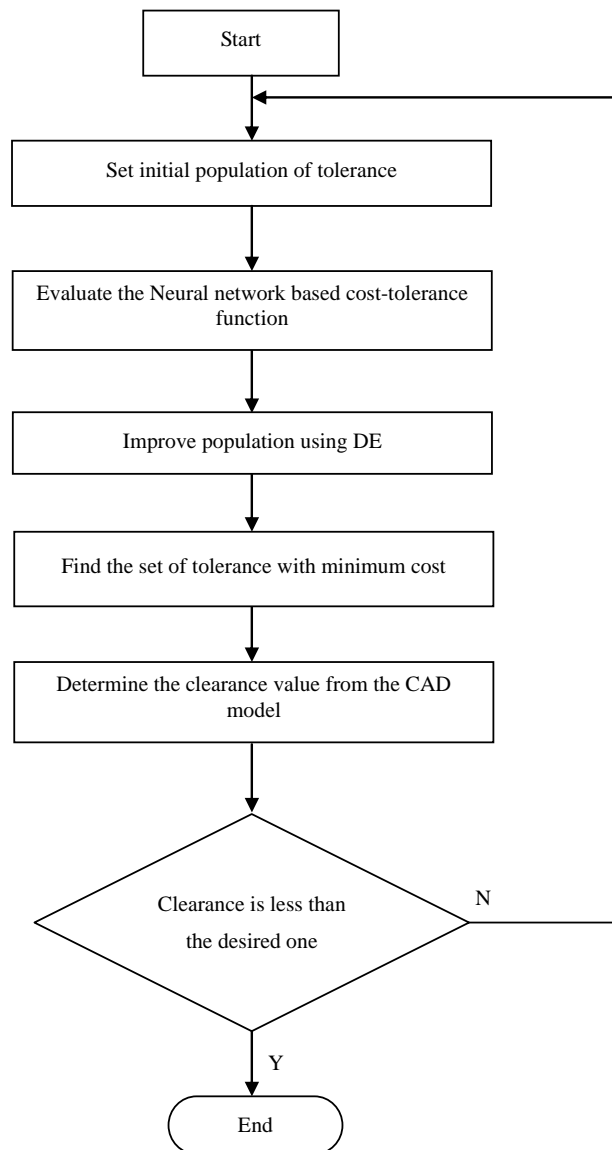


**Figure 12. The outline of the proposed optimization strategy.**

the process terminates, otherwise the process is repeated from the beginning.

The least cost is found to be \$232.1907; the solution converges in the 49<sup>th</sup> generation (**Figure 13**). The value of cost obtained by this method is lesser than that of the value obtained by response surface methodology [13] which was \$238.5191 and the constraint equation provided, ensures that the values of variables satisfies the functional constraint. The values of the variables are as follows.  $x_1$ -base flatness,  $x_1 = 0.1$ , motor base flatness,  $x_2 = 0.081125$ , motor shaft size,  $x_3 = 0.1$ , and the motor shaft perpendicularity,  $x_4 = 0.07799$ . It is found that the proposed hybrid methodology with BP and DE can solve tolerance synthesis problem effectively.

## 5. Discussion

Many products are now routinely designed with the aid of computer modeling. With an input consisting of designable engineering parameters and parameters representing manufacturing process conditions, computer simulation generates an output, which is the product's quality characteristic. Then a standard statistical analysis is performed based on this output. The finite element analysis of mechanical components and the design of electronic circuits are two important application areas where computer modeling is widely used. With the current development of computer aided tolerancing software (CATS) it becomes possible to put tolerance design via computer modeling into practical use. Major CATs use the abstracted feature-parameter model for the Monte Carlo simulation based tolerance analysis. The major problems with these CAT packages are as follows: 1) Cumbersome work is needed in model creation. First, parametric CAD uses a combination of 2D constraint solving with 3D sweep and loft operations; this constraint model is not suitable for tolerance analysis. Second, STEP standards for tolerances exist but vendors do not provide translators, so importing a CAD model with GD & T is only partially achieved, *i.e.*, the GD & T and assembly constraint information is lost after importing. Therefore, the user must recreate the tolerance specs in CATs manually using CAD entities. 2) There is a lack of an underlying mathematical model for geometric variations. First, the quality of the analysis depends on the expertise of the person creating the CATS model; this is a problem. The results should depend on the GD & T scheme only and not by trial and error or any "tricks". Second, the Monte Carlo simulation does not produce a closed form solution; the solution changes with the number of simulations performed; one can never be sure of the worst-case results. Third, since the dependent dimensions cannot be expressed explicitly by one equation in terms of all contributors, the contributors and sensi-

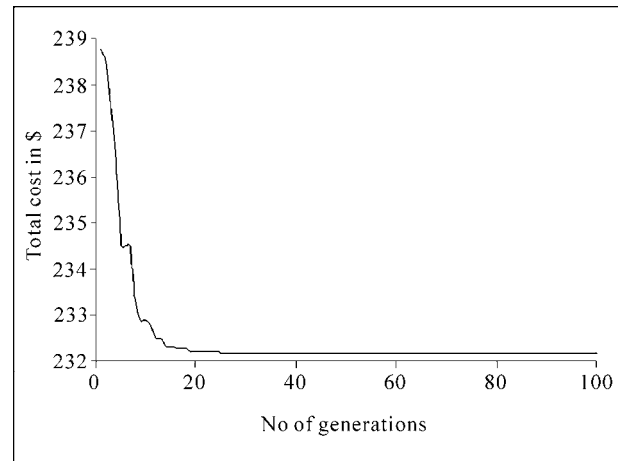


**Figure 13. Solution history.**

tivities are determined numerically by trial and error. In this study, a parametric analysis method based on direct constraint model is proposed which addresses the above problems in using CATs packages. First, the parametric tolerance analysis borrows its concept from the mature parametric CAD; there by it can be easily integrated with CAD system. Second, a constraint equation is developed after developing the direct constraint model, which ensures that dependent dimension can be expressed explicitly in terms of contributors. The constraint equation is then used as a functional constraint in the optimization method. Due to the above reasons, parametric tolerance analysis based on direct constraint model in CAD is more suitable for tolerance analysis of simple problems than that of CATs package.

## 6. Conclusions

In this research, the parametric tolerance analysis of given application problem is performed by developing a direct constraint model in CAD. This method is found to be more suitable for tolerance analysis of simple problems than that of CATs package. And the proposed optimization strategy is found to provide better formulation of cost-tolerance relationships for empirical data. BP network architecture of configuration 4-7-1 generates a suitable model for cost-tolerance relationship of  $R^2$  value 0.99993, there by eliminating errors due to curve fitting in case of regression fitting. And it also generates more robust outcomes of tolerance synthesis. The proposed optimization strategy obtains an optimal solution better than that of Response surface methodology (RSM) (Jeang, 1999). The CAD model developed ensures that the values of variables satisfy the functional constraint. This study proposes a parametric tolerance analysis of mechanical assembly by developing direct constraint model in cad and cost competent tolerance synthesis

based on BP learning and DE based optimization algorithm. The constraint equation developed ensures that the proposed values of controllable factors (tolerances) satisfy the assembly constraint, even before the start of manufacturing process. There by reducing scrap and rework cost.

## 7. References

- [1] J. Turner and A. B. Gangoiti, "Tolerance Analysis Approaches in Commercial Software," *Concurrent Engineering*, Vol. 1, No. 2, 1991, pp.11-23.
- [2] J. Guilford, M. Sethi and J. Turner, "Worst Case and Statistical Tolerance Analysis of the Daughter Card Assembly," *Proceedings of the 1992 ASME International Computers in Engineering Conference*, San Francisco, 2-6 August 1992, pp. 343-350.
- [3] Y. Wu, J. Shah and J. Davidson, "Computer Modeling of Geometric Variations in Mechanical Parts and Assemblies," *ASME Journal Computing and Information Science in Engineering*, Vol. 3, No. 1, 2003, pp. 54-63.
- [4] T. M. K. Pasupathy, E. P. Morse and R. G. Wilhelm, "A Survey of Mathematical Methods for the Construction of Geometric Tolerance Zones," *ASME Journal Computing and Information Science in Engineering, Special Issue on GD & T*, Vol. 3, No. 1, 2003, pp. 64-75.
- [5] P. Martino, "Simplification of Feature Based Models for Tolerance Analysis", *Proceedings of the 1992 ASME International Computers in Engineering Conference & Exposition*, San Francisco, 2-6 August 1992, pp. 329-341.
- [6] Y.-J. Tseng and Y.-S. Terng, "Alternative Tolerance Allocations for Machining Parts Represented with Multiple Sets of Features," *International Journal of Production Research*, Vol. 37, No. 7, 1999, pp. 1561-1579.
- [7] B. K. A. Ngoi and J. M. Ong, "A Complete Tolerance Charting System in Assembly," *International Journal of Production Research*, Vol. 37, No. 11, 1999, pp. 2477-2498.
- [8] U. Prisco and G. Giorleo, "Overview of Current CAT Systems," *Integrated Computer-Aided Engineering*, Vol. 9, No. 4, 2002, pp. 373-387.
- [9] Z. Shen, "Software Review-Tolerance Analysis with EDS/VisVSA," *ASME Journal Computing and Information Science in Engineering, Special Issue on GD & T*, Vol. 3, No. 1, 2003, pp. 95-99.
- [10] F. Chiesi and L. Governi, "Software Review-Tolerance Analysis with eTol-Mate," *ASME Journal Computing and Information Science in Engineering, Special Issue on GD & T*, Vol. 3, No. 1, 2003, pp. 100-105.
- [11] C. X. Feng and A. Kusiak, "Design of Tolerances for Quality," *Design Theory and Methodology-DTM* 94, Vol. 668, ASME, 1994, pp. 19-27.
- [12] A. Jeang, "Tolerance Chart Optimisation for Quality and Cost," *International Journal of Production Research*, Vol. 36, No. 11, 1998, pp. 2969-2983.
- [13] A. Jeang, "Optimal Tolerance Design by Response Surface Methodology," *International Journal of Production Research*, Vol. 37, No. 14, 1999, pp. 3275-3288.
- [14] C. C. Wu and G. R. Tang, "Tolerance Design for Products with Asymmetric Quality Losses," *International Journal of Production Research*, Vol. 36, No. 9, 1998, pp. 2529-2541.
- [15] S. C. Diplaris and M. M. Sfantsikopoulos, "Tolerancing for Enhanced Quality and Optimum Cost," *Proceedings of the 33rd International MATADOR Conference*, Manchester, 1999, pp. 539-544.
- [16] A. Jeang, "An Approach of Tolerance Design for Quality Improvement and Cost Reduction", *International Journal of Production Research*, Vol. 35, No. 5, 1997, pp. 1193-1211.
- [17] F. H. Speckhart, "Calculation of Tolerance Based on Minimum Cost Approach," *Journal of Engineering for Industry-Transactions of the ASME*, Vol. 94, No. 2, 1972, pp. 447-453.
- [18] M. F. Spotts, "Allocation of Tolerances to Minimize Cost of Assembly," *Journal of Engineering for Industry-Transactions of the ASME*, Vol. 95, No. 3, 1973, pp. 762-764.
- [19] K. W. Chase, W. H. Greenwood, B. G. Loosli and L. F. Hauglund, "Least Cost Tolerance Allocation for Mechanical Assemblies with Automated Process Selection," *Manufacturing Review*, Vol. 3, No. 1, 1990, pp. 49-59.
- [20] Z. Dong, W. Hu and D. Xue, "New Production Cost Tolerance Models for Tolerance Synthesis," *Journal of the Engineering Industry*, Vol. 116, 1994, pp. 199-205.
- [21] R. Soderberg, "Robust Design by Tolerance Allocation Considering Quality and Manufacturing Cost," *Advances in Design Automation*, Vol. 69-1, ASME, 1994, pp. 219-226.
- [22] M. Krishnasawamy and R. W. Mayne, "Optimizing Tolerance Allocation Based on Manufacturing Cost," *Advances in Design Automation*, Vol. 69-1, ASME, 1994, pp. 211-217.
- [23] E. M. Mansoor, "The Application of Probability to Tolerances Used in Engineering Design," *Proceedings of the Institution of Mechanical Engineers*, Vol. 178, No. 1, 1963, pp. 29-44.
- [24] E. Santoro, "Probabilistic Model for Tolerance Synthesis: An Analytical Solution, Structural Safety and Reliability," Balkema, Rotterdam, 1994.
- [25] V. J. Skowronski and J. U. Turner, "Estimating Gradients for Statistical Tolerance Synthesis," *Computer-Aided Design*, Vol. 28, No. 12, 1996, pp. 933-941.
- [26] C. Zhang, J. Luo and B. Wang, "Statistical Tolerance Synthesis Using Distribution Function Zones," *International Journal of Production Research*, Vol. 37, No. 17, 1999, pp. 3995-4006.
- [27] M. H. Gaddalah and H.A. ElMaraghy, "The Tolerance Optimization Problem Using a System of Experimental Design," *Advances in Design Automation*, Vol. 69-1, ASME, 1994, pp. 251-264.
- [28] V. J. Skowronski and J. U. Turner, "Using Monte-Carlo Variance Reduction in Statistical Tolerance Synthesis,"

- Computer-Aided Design*, Vol. 29, No. 1, 1997, pp. 63-69.
- [29] H. S. Stern, "Neural Networks in Applied Statistics (with Discussion)," *Technometrics*, Vol. 38, No. 3, 1996, pp. 205-220.
- [30] H.-C. Zhang, H. Huang, "Applications of Neural Networks in Manufacturing: A-State-of-the-Art Survey," *International Journal of Production Research*, Vol. 33, No. 3, 1995, pp. 705-728.
- [31] D. E. Rumelhart and J. L. McClelland, "Parallel Distributed Processing Explorations in the Microstructure of Cognition," MIT Press, Cambridge, 1989.
- [32] R. P. Lippmann, "An Introduction to Computing with Neural Nets," *IEEE ASSP Magazine*, Vol. 4, No. 2, 1987, pp. 4-22.
- [33] K. Price and R. Storn, "Differential Evolution—A Simple Evolution Strategy for Fast Optimization," *Dr. Dobbs' Journal*, Vol. 22, No. 4, pp. 18-24 and 78.

# Optimal Control Strategy for a Fully Determined HIV Model

Mohammad Shirazian<sup>1</sup>, Mohammad Hadi Farahi<sup>1,2</sup>

<sup>1</sup>Department of Applied Mathematics, Ferdowsi University of Mashhad, Mashhad, Iran

<sup>2</sup>The Center of Excellence in Modeling and Computations in Linear and Nonlinear Systems  
Ferdowsi University of Mashhad, Mashhad, Iran

E-mail: [mo.shirazian@stu-mail.um.ac.ir](mailto:mo.shirazian@stu-mail.um.ac.ir), [farahi@math.um.ac.ir](mailto:farahi@math.um.ac.ir)

Received January 25, 2010; revised March 21, 2010; accepted June 22, 2010

## Abstract

This paper shows how mathematical methods can be implemented to formulate guidelines for clinical testing and monitoring of HIV/AIDS disease. First, a mathematical model for HIV infection is presented which the measurement of the CD4<sup>+</sup>T cells and the viral load counts are needed to estimate all its parameters. Next, through an analysis of model properties, the minimal number of measurement samples is obtained. In the sequel, the effect of Reverse Transcriptase enzyme Inhibitor (RTI) on HIV progression is demonstrated by using a control function. Also the total cost of treatment by this kind of drugs has been minimized. The numerical results are obtained by a numerical method in discretization issue, called AVK.

**Keywords:** HIV/AIDS, Mathematical Modeling, System Identification, Control Theory, Immunotherapy

## 1. Introduction

Despite tremendous effort for mathematical modeling of HIV/AIDS (for example, see [1-4]), estimation of model parameters has not been attended a lot. For example, in [2,5,6], only the virus clearance rate and the death rate of infected CD4<sup>+</sup>T cells have been estimated. The importance of parameter estimation in models, is due to predicting “set-points” in the early infection stage for making the desired treatment decisions (See [7]).

One of the objectives of this paper is presenting a realistic model, *i.e.* the basic model of HIV, and estimating all its parameters. It is necessary to mention that one can identify all of the model parameters by using measured output (For more details see [4]).

Another objective is to add a control function to the identified basic model which plays the role of reverse transcriptase enzyme inhibitor drug in disease progression.

In the sequel, the optimal control model of HIV will be solved by a method in discretization issue, called AVK.

Numerical results are obtained using mathematical softwares, LINGO and MATLAB.

## 2. Translating Biological Knowledge to Ordinary Differential Equations (ODE)

To make ODE's from biological knowledge, first we need some syntax. For example, if we denote the count of uninfected and infected CD4<sup>+</sup>T helper cells, with  $a$  and  $b$ , respectively, the syntax “ $a \rightarrow 0$ ” can be used to present this biological descriptions: “Uninfected CD4<sup>+</sup>T cells die” and the syntax “ $a + b \rightarrow b + b$ ” can present: “The reaction between two infected and uninfected CD4<sup>+</sup>T cells produces two infected CD4<sup>+</sup>T cells”. Now, for translating these syntaxes to the corresponding ODE's, we use *Mass action law*. This law says: “The rate of change of products is proportional to the product of reactants concentration”. So if the syntax “ $a + b \rightarrow c$ ” is obtained, according to the mass action law, we can write

$\dot{c} = kab$ , for  $k > 0$ , where  $\frac{dc}{dt}$  is denoted by  $\dot{c}$ . Two

other reactions in the previous syntax is dying  $a$  and  $b$  reactants, while producing  $c$ . So we have also these two ODE's as:  $\dot{a} = -kab$  and  $\dot{b} = -kab$ , for  $k > 0$ . Finally, the desired ODE, corresponding to the syntax “ $a + b \rightarrow c$ ” is

$$\begin{aligned}\dot{c} &= kab, \\ \dot{a} &= -kab, \\ \dot{b} &= -kab.\end{aligned}$$

Obviously, the rate of change of a product is the sum of changes from all reactions.

### 3. HIV Basic Model

The target cells of HIV infection are lymphocyte helper cells, specially CD4<sup>+</sup>T cells. These cells become infected and begin to produce free virions. The main fact about HIV infection, is reducing the count of CD4<sup>+</sup>T cells, which have an essential role in protecting body against different pathogens. So it is important to understand the dynamics of CD4<sup>+</sup>T cell count as a function of time. In HIV infection basic model, three groups of molecules are considered; Uninfected CD4<sup>+</sup>T cells (T), infected CD4<sup>+</sup>T cells (I) and viral load (V). Biological descriptions, translation to reactions and corresponding ODE's are presented in **Table 1**.

Now, according to **Table 1** and Section 2, the complete ODE model, which is sum of contributions from all reactions, is as follows:

$$\begin{aligned}\dot{T} &= s - dT - \beta TV, \\ \dot{I} &= \beta TV - \mu I, \\ \dot{V} &= kI - cV.\end{aligned}\quad (1)$$

### 4. Properties of HIV Basic Model

There are two advantages to show the virus propagation in HIV disease, by the basic model (1).

1) From medical point of view, one important subject is the relative steady viral level during the asymptomatic stage of an HIV infection. This level is called "set-point". When body reaches this level, immune system develops HIV antibodies and begins to attempt to fight the virus. The higher the viral load of the set point, the faster the

virus will progress to full blown AIDS (See [8]).

It can be shown that set-point is the amount of V, in the equilibrium of virus depicted by the model (1), that is

$$V^* = \frac{ks}{\mu c} - \frac{d}{\beta}.$$

2) It can be seen that a model of such a simple nature is able to adequately reflect the disease progression from the initial infection to an asymptomatic stage after the set-point is reached (See [9]).

### 5. Estimation of Models Parameters Using Discretization

In this section, our aim is to estimate all parameters of HIV basic model (1). Clinically all six variables in model (1), can be measured. Since the cost of quantifying the infected cells is much higher, we are going to omit variable I, initially. For this, let  $y_1 = T$  and  $y_2 = V$ . After some calculations, model (1) can be changed to:

$$\dot{y}_1 = \alpha_1 + \alpha_2 y_1 + \alpha_3 y_1 y_2 \quad (2)$$

$$\dot{y}_2 = \alpha_4 y_2 + \alpha_5 y_2 + \alpha_6 y_1 y_2 \quad (3)$$

where

$$\alpha = \begin{bmatrix} \alpha_1 \\ \alpha_2 \\ \alpha_3 \\ \alpha_4 \\ \alpha_5 \\ \alpha_6 \end{bmatrix} = \begin{bmatrix} s \\ -d \\ -\beta \\ -\mu - c \\ -\mu c \\ k\beta \end{bmatrix}.$$

The vector  $\alpha$  defines a one-to-one map for  $\beta \neq 0$  and  $\mu \neq c$ . Therefore the identification of the original parameters of (1) is equivalent to the identification of  $\alpha$ . It is known that for most HIV patients,  $\beta \neq 0$  and  $\mu < c$  (See [7]). In this case, the following inverse map can be defined:

**Table 1. HIV basic model interactions.**

| Biological description                                 | Translation to reactions  | Reaction rate | Translation to ODE                            |
|--|---------------------------|---------------|---|
| CD4 <sup>+</sup> T cells production                    | $0 \rightarrow T$         | $s$           | $\dot{T} = s$                                 |
| CD4 <sup>+</sup> T cells natural death                 | $T \rightarrow 0$         | $d$           | $\dot{T} = -dT$                               |
| CD4 <sup>+</sup> T cells become infected by virus      | $T + V \rightarrow I + V$ | $\beta$       | $\dot{T} = -\beta TV$<br>$\dot{I} = \beta TV$ |
| Infected CD4 <sup>+</sup> T cells death                | $I \rightarrow 0$         | $\mu$         | $\dot{I} = -\mu I$                            |
| Virus replication in infected CD4 <sup>+</sup> T cells | $I \rightarrow I + V$     | $k$           | $\dot{V} = kI$                                |
| Virus natural death                                    | $V \rightarrow 0$         | $c$           | $\dot{V} = -cV$                               |

$$\begin{bmatrix} s \\ d \\ \beta \\ \mu \\ c \\ k \end{bmatrix} = \begin{bmatrix} -\alpha_1 \\ -\alpha_2 \\ -\alpha_3 \\ \frac{-\alpha_4 - \sqrt{\alpha_4^2 + 4\alpha_5}}{2} \\ \frac{-\alpha_4 + \sqrt{\alpha_4^2 + 4\alpha_5}}{2} \\ \frac{\alpha_6}{\alpha_3} \end{bmatrix}. \quad (4)$$

Since there are three unknown parameters in each of Equation (2) and (3), it is necessary to generate at least two other equations based on each of them. This will be achieved by differentiating (2) and (3) more times, and produce upper derivatives of  $y_1$  and  $y_2$ . So one can concludes that at least four measurements of  $y_1$ , CD4<sup>+</sup>T cell count, and five measurements of  $y_2$ , viral load, are needed for a complete determination of model (1) parameters (See [7]).

Assume that the following measurements are available.

By discretization of Equations (2) and (3), and substituting the approximated values of first derivative of  $y_1$  and the first and second derivatives of  $y_2$ , we found that

$$\alpha_1 + y_1^i \alpha_2 + y_1^i y_2^i \alpha_3 = \frac{y_1^{i+1} - y_1^i}{d_{i+1}}, \quad i = 0, 1, 2 \quad (5)$$

$$\begin{aligned} \frac{y_2^{i+1} - y_2^i}{d_{i+1}} \alpha_4 + y_2^i \alpha_5 + y_1^i y_2^i \alpha_6 = \\ \frac{1}{d_{i+1}} \left( \frac{y_2^{i+2} - y_2^{i+1}}{d_{i+2}} - \frac{y_2^{i+1} - y_2^i}{d_{i+1}} \right), \quad i = 0, 1, 2 \end{aligned} \quad (6)$$

Or in matrix form, we have

$$\begin{bmatrix} 1 & y_1^0 & y_1^0 y_2^0 \\ 1 & y_1^1 & y_1^1 y_2^1 \\ 1 & y_1^2 & y_1^2 y_2^2 \end{bmatrix} \begin{bmatrix} \alpha_1 \\ \alpha_2 \\ \alpha_3 \end{bmatrix} = \begin{bmatrix} \frac{y_1^1 - y_1^0}{d_1} \\ \frac{y_1^2 - y_1^1}{d_2} \\ \frac{y_1^3 - y_1^2}{d_3} \end{bmatrix}$$

Similar matrix form can be obtained from (6). Thus, the variables  $\alpha_i, i = 1, 2, \dots, 6$  and then from (4), all of the basic model parameters can be calculated. As an example, we considered the basic model (1), where the following estimated parameters are as Xia [7].

$$\begin{aligned} s = 7, d = 0.007, \beta = 0.00000042163, \\ \mu = 0.0999, c = 0.2, k = 90.67. \end{aligned} \quad (7)$$

**Table 2. Available measurements for the count of CD4<sup>+</sup>T cells and viral load.**

| Time ( $t$ )                  | CD4 <sup>+</sup> T cell count ( $y_1$ ) | Viral load ( $y_2$ ) |
|-------------------------------|---|----------------------|
| $t_0$                         | $y_1^0$                                 | $y_2^0$              |
| $t_0 + d_1$                   | $y_1^1$                                 | $y_2^1$              |
| $t_0 + d_1 + d_2$             | $y_1^2$                                 | $y_2^2$              |
| $t_0 + d_1 + d_2 + d_3$       | $y_1^3$                                 | $y_2^3$              |
| $t_0 + d_1 + d_2 + d_3 + d_4$ | -                                       | $y_2^4$              |

The solution of model (1) for  $t \in [0, 1000]$ , with the initial values  $T_0 = 1000, I_0 = 0$  and  $V_0 = 7000$ , can be determined using the well-known numerical methods like RK4. The graphs of the propagation of healthy CD4<sup>+</sup>T cells, infected CD4<sup>+</sup>T cells and virous loads, respectively, are shown in **Figure 1**.

### 6. HIV Infection Optimal Control Model

There are three convenient groups of drugs for AIDS retroviral therapy; Reverse transcriptase, Protease, and Integrase enzyme inhibitors. In this section, we study the role of reverse transcriptase inhibitors. The main action of this kind of drugs is preventing uninfected lymphocyte cells, to be infected by viral load. According to **Table 1**,

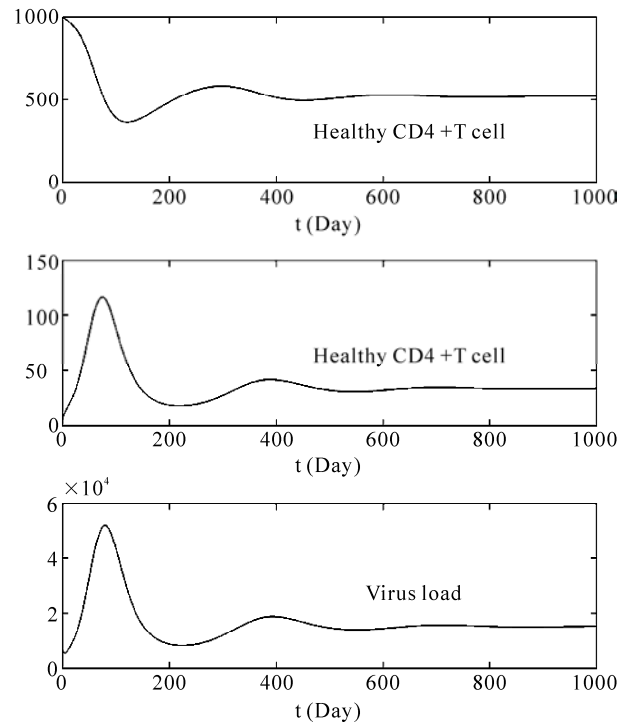


**Figure 1. The solution of basic model of HIV, model (1).**

this action is equivalent to the reaction  $T+V \rightarrow I+V$ . So we control the first equation to prevent the transmission of uninfected cells to infected ones. This control function is called  $u(t)$ , where  $0 \leq u(t) \leq 1$ . The most drug efficiency is in the case  $u \equiv 1$  which means CD4<sup>+</sup>T cells are not infected by viral load anymore. At the other side,  $u \equiv 0$  is the case which the drug does not change the disease progression. By above argument, the control system is as:

$$\begin{aligned} \dot{T} &= s - dT - \beta TV(1-u), \\ \dot{I} &= \beta TV(1-u) - \mu I, \\ \dot{V} &= kI - cV. \end{aligned} \quad (8)$$

Using [10], consider the objective functional to be defined as:

$$J(T, u) = \int_{t_0}^{t_f} \left[ T(t) - \frac{1}{2} \alpha u(t)^2 \right] dt \quad (9)$$

where  $\alpha = 110$ . Our goal is maximizing the objective functional (9) subject to the control system (8); that is, maximizing the total count of CD4<sup>+</sup>T cells and minimizing the costs of treatment by applying some RTI drugs.

The solution of this optimal control problem should be calculated by numerical methods. We have used a special discretization method, called AVK.

For a detailed explanation of this method, see [11].

In AVK method, for solving the optimal control problem,

$$\text{Min } J(x, u) = \int_{t_0}^{t_f} g(x(t), u(t), t) dt \quad (10)$$

Subject to:

$$\begin{aligned} \dot{x}(t) &= f(x(t), u(t), t), \quad t \in [t_0, t_f] \\ x(t_0) &= x_0, \quad x(t_f) = x_f \end{aligned} \quad (11)$$

the following steps should be applied:

**Step 1.** Form the *total error function*  $E_1$  as:

$$E_1(x, u) = \int_{t_0}^{t_f} \left\| \dot{x}(t) - f(x(t), u(t), t) \right\| dt$$

**Step 2.** Combine the total error function with the objective functional (10) as follows:

$$\begin{aligned} \text{Min } \int_{t_0}^{t_f} \left\{ \lambda_1 g(x(t), u(t), t) \right. \\ \left. + \lambda_2 \left\| \dot{x}(t) - f(x(t), u(t), t) \right\| \right\} dt \quad (12) \\ \text{subject to: } x(t_0) = x_0, \quad x(t_f) = x_f \end{aligned}$$

where nonnegative numbers  $\lambda_1$  and  $\lambda_2$  are two given weights and  $\lambda_1 + \lambda_2 = 1$ .

**Step 3.** In order to control the error, add the following constraint,

$$E_1(x, u) \leq \epsilon$$

to the optimal control problem in Step 2. So the modified optimal control problem (10)-(11) can be formulated as:

$$\begin{aligned} \text{Min } \int_{t_0}^{t_f} \left\{ \lambda_1 g(x(t), u(t), t) \right. \\ \left. + \lambda_2 \left\| \dot{x}(t) - f(x(t), u(t), t) \right\| \right\} dt \\ \text{subject to:} \quad (13) \\ \int_{t_0}^{t_f} \left\| \dot{x}(t) - f(x(t), u(t), t) \right\| dt \leq \epsilon \\ x(t_0) = x_0, \quad x(t_f) = x_f \end{aligned}$$

**Step 4.** Calculate  $u(t_i)$  by minimizing the optimal control problem (13) using discretization method.

For example, if the norm function  $\|\cdot\|$ , is norm 1, then one can solve the following optimization problem:

$$\begin{aligned} \text{Min } h \sum_{h=0}^{n-1} \left\{ \lambda_1 g(x_i, u_i, t_i) + \lambda_2 \left\| \dot{x}_i - f(x_i, u_i, t_i) \right\| \right\} \\ \text{subject to: } h \sum_{h=0}^{n-1} \left\| \dot{x}_i - f(x_i, u_i, t_i) \right\|_1 \leq \epsilon \quad (14) \\ x(t_0) = x_0, \quad x(t_f) = x_f \end{aligned}$$

where  $h = \frac{t_f - t_0}{n}$ ,  $t_i = t_0 + ih$ ,  $x_i = x(t_i)$ ,  $u_i = u(t_i)$

and  $\dot{x}_i = \dot{x}(t_i) \approx \frac{x_{i+1} - x_i}{h}$  for  $i = 0, 1, \dots, n-1$  and  $n \in \mathbb{N}$ .

**Step 5.** By the means of  $u(t_i)$  for every  $t_i$ , from (11), it is easy to find  $x(t_i)$ , for any  $i$ ,  $i = 0, 1, \dots, n-1$ .

We use this technique to solve the control problem (8) with the objective functional (9). The parameters used in the basic control model (8) are exactly as (7). Assume that the treatment begins when CD4<sup>+</sup>T cells reach their minimum count, in the absence of drug.

According to **Figure 1**,  $T(129) = 363$  is the minimum count of CD4<sup>+</sup>T cells. So the treatment interval is [129, 1000] day. Also, note that by **Figure 1**, at  $t = 129$ , we have  $I(129) = 57$  and  $V(129) = 28860$ .

Now, we divide [129, 1000] into  $n$  parts with length  $h$ . The discretization form of (14) is:

$$\begin{aligned} \text{Max } h \sum_{h=0}^{n-1} \left\{ \lambda_1 \left[ T_i - \frac{1}{2} \alpha u_i^2 \right] \right. \\ \left. - \lambda_2 \left[ \dot{T}_i - (s - dT_i - \beta T_i V_i (1 - u_i)) \right] \right. \\ \left. + \left| \dot{I}_i - (\beta T_i V_i (1 - u_i) - \mu I_i) \right| \right. \\ \left. + \left| \dot{V}_i - (kI_i - cV_i) \right| \right\} \end{aligned}$$

subject to:  $T_i, I_i, V_i \geq 0$ ,  $0 \leq u_i \leq 1$ ,  $\forall i = 0, 1, 2, \dots, n$

$$T_0 = 363, \quad I_0 = 57, \quad V_0 = 28860$$

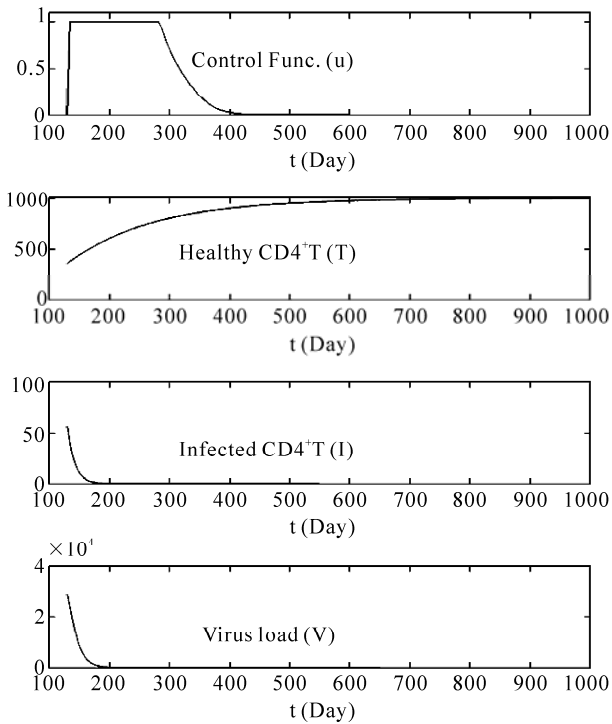


**Figure 1.** The solution of optimal control problem (8)-(9), using AVK method.

where assumed  $\lambda_1 = \lambda_2 = \frac{1}{2}$ .

The results of this optimization problem which obtained by LINGO and MATLAB softwares for  $n = 200$  and  $\epsilon = 10^{-6}$ , are depicted in **Figure 2**.

## 7. Conclusions

In this paper, the parameter of the basic model of HIV/AIDS is estimated only by measurement of the CD4<sup>+</sup>T cells and the viral load count. Since the suggested models for HIV, or infectious diseases like consumption, cholera, influenza and etc., have unknown parameters which should be estimated, one can use the proposed method in this paper to estimate the parameters of such models.

One of the most important kinds of drug treatments for

HIV immunotherapy is assumed. One can investigate the effects of other drugs, like Protease enzyme inhibitors in preventing AIDS progression. In these cases, one can use the described discretization method for solving such optimal control problems.

## 8. References

- [1] D. Covert and D. Kirschner, "Revisiting Early Models of the Host-Pathogen Interactions in HIV Infection," *Comments Theoretical Biology*, Vol. 5, No. 6, 2000, pp. 383-411.
- [2] M. A. Nowak and R.M. May, "Virus Dynamics: Mathematical Principles of Immunology and Virology," Oxford University Press, New York, 2000.
- [3] A. S. Perelson and P. W. Nelson, "Mathematical Analysis of HIV-1 Dynamics in Vivo," *SIAM Review*, Vol. 41, No. 1, 1999, pp. 3-44.
- [4] W.-Y. Tan and H. Wu, "Deterministic and Stochastic Models of AIDS Epidemics and HIV Infections with Intervention," World Scientific, Singapore, 2005.
- [5] M. A. Nowak and C. R. M. Bangham, "Population Dynamics of Immune Responses to Persistent Viruses," *Science*, Vol. 272, No. 5758, 1996, pp. 74-79.
- [6] X. Wei, S. K. Ghosh, M. E. Taylor, V. A. Johnson, E. A. Emini, P. Deutsch and J. D. Lifson, "Viral Dynamics in HIV-1 Infection", *Nature*, Vol. 273, No. 6510, 1995, pp. 117-122.
- [7] X. Xia, "Estimation of HIV/AIDS parameters," *Automatica*, Vol. 39, No. 11, 2003, pp. 1983-1988.
- [8] R. Pattman, M. Snow, P. Handy, K. N. Sankar and B. Elawad, "Oxford Handbook of Genitourinary Medicine, HIV and AIDS," Oxford University Press, USA, 2005.
- [9] X. Xia, "Modelling of HIV Infection: Vaccine Readiness, Drug Effectiveness and Therapeutical Failures," *Journal of Process Control*, Vol. 17, No. 3, 2007, pp. 253-260.
- [10] K. R. Fister and S. Lenhart, "Optimizing Chemotherapy in an HIV Model," *Journal of Differential Equations*, Vol. 1998, No. 32, 1998, pp. 1-12.
- [11] K. P. Badakhshan and A. V. Kamyad, "Numerical Solution of Nonlinear Optimal Control Problems Using Nonlinear Programming," *Applied Mathematics and Computation*, Vol. 187, No. 2, 2007, pp. 1511-1519.

# Weightlifting Motion Generation for a Stance Robot with Repeatedly Direct Kinematics

Jining Liu, Yoshitsugu Kamiya, Hiroaki Seki, Masatoshi Hikizu

*Division of Innovative Technology and Science, Kanazawa University, Kanazawa, Ishikawa, Japan*

*E-mail: kamiya@t.kanazawa-u.ac.jp*

*Received April 1, 2010; revised July 15, 2010; accepted July 20, 2010*

## Abstract

This research focuses on how to control the robot easily and how to generate the better trajectories of the robot with multiple joints to implement weightlifting motion. The purpose of this research is to develop a multi-joint robot can stand up successfully with an object. This research requires the operations with two items. First, when the object is lifted up slowly, the robot could stand up as easily as possible and does not tumble down. Second, the load applied on each joint should be as small as possible. In this article, a motion control method is proposed to evaluate the variations of the load torque and rotated angle of each joint with the geometrical constraints in the procedure and find the best algorithm to generate the trajectory of a weightlifting motion by a stance robot with repeatedly direct kinematics.

**Keywords:** Weightlifting, Trajectory Generation, Load Torque, Repeatedly Direct Kinematics

## 1. Introduction

In recent years, robots that are able to perform work in human daily environment have been successfully developed. Furthermore more and more multi-joint robots have been used to meet the needs of the people and industry in daily. For instant, humanoid robots are placed in dangerous work in some fields such as in medical treatment, architecture, manufacture, and researched in science fields, because the configuration is in similitude of human being.

Today, about 60% of the working population in the world, based on statistics, suffered from different kinds of arthritis, 30% suffer from different kinds of arthrosis, and when it comes to muscle, joint or rheumatic pain, practically every person is familiar with them. Arthralgia is an ailment that lots of teenagers suffer from. Adults also suffer from arthralgia caused by injuries [1]. These situations make us think about that how to reduce the load on the joints to keep away from the arthralgia. Weightlifting is a common action to every person in daily lives, which is hardly avoidable. In this paper, the research is developed, which focuses on how to generate a better trajectory of the robot with multiple joints to simulate human being to realize the weightlifting motion [2].

Regarding trajectory generation, there are two aspects to be considered usually. One is the aim you will achieve.

What a kind of trajectory is generated? Is it collision-free or time-optimal or energy-optimal? The other one is the constraint existing in the process of the trajectory generation [3]. Sometime we want the humanoid robot to work as workhorse without damage. But the joints are the parts, which are easy to damage. So how to make the load on each joint minimum is that we need to consider.

In the following, we try to generate a trajectory that consists of many link postures, each of which makes the load torque of all the joints as low as possible without the dangerousness of tumbling down. Based on the idea above, the algorithm is proposed, and simulations are provided. The trajectories of weightlifting motion for a multi-joint robot with an object are generated, the precision of which depends on the specified motion increment of each link in the calculation.

## 2. Model and Calculations

In this paper, we assume that the system is symmetric during the procedure. Hence from a complicated humanoid robot model with many degrees of freedom, we simplify it to a 5-dof model with 6 links [4], which can move along the horizontal direction. As shown in **Figure 1**, we set the coordinate system so that x-axis is on the floor and z-axis passes through the ankle joint.

Here  $J_i$  represents the joint  $i$ ,  $\theta_i$  represents the angle

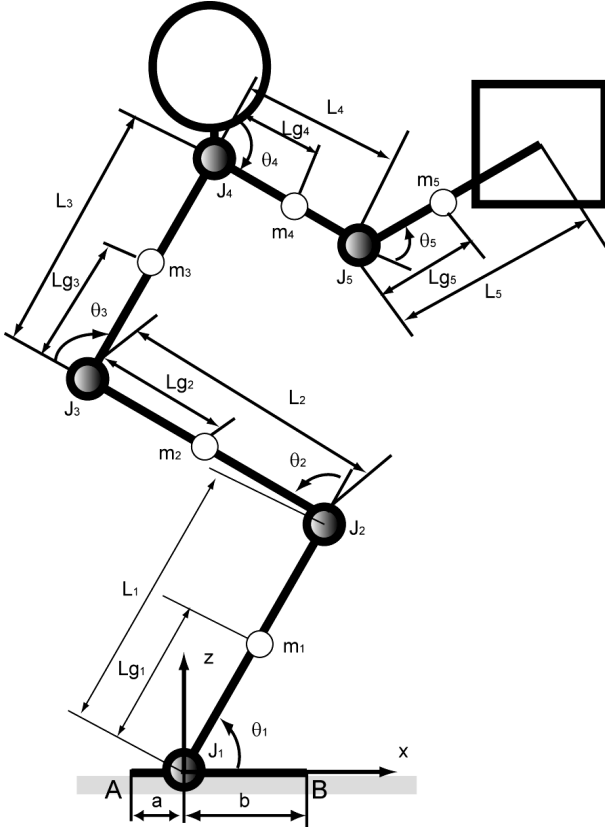


Figure 1. Model of the robot and its geometric parameters.

between the link  $i$  and the link  $i-1$ ,  $a$  represents the length from the ankle joint to the heel (point A),  $b$  represents the length from the ankle joint to the tiptoe (point B),  $L_i$  represents the length of the link, and  $L_{g_i}$  represents the distance from the CoM (Centre of Mass) of the link to the beginning point of the link. The mass of a link is noted as  $m_i$ , and the object's mass is given when a simulation is implemented. The position of the CoM of the elbow link follows the mass of the object. Furthermore,  $g$  denotes the gravity acceleration. The centre of mass of the object is located at the middle point of the object.

As showed in **Table 1** below, the geometric parameters are properly given to estimate the effectiveness of the algorithm applied on the trajectory generation of the robot's weightlifting motion.

We usually research about the robots under dynamic conditions, but which makes the research complicated. The joints of robot are mostly drove by reducers in fact, and the motion of the links is very tiny in this paper, so the static effect is first considered that the dynamic performances could be neglected, Only considering the static influences under some limitations here [5]. The detailed analysis of this matter under a dynamic environment is future works.

To implement the weightlifting motion successfully for a multi-joint robot, the following two requirements or

constraints must be satisfied in this procedure.

First, the robot must maintain its stability or keep its balance so that it will not tumble down, which is called the balance constraint here. To satisfy this condition, the ZMP (Zero Moment Point) or the projection of the CoM of the robot onto the ground must remain within the pre-defined stability region, that is, it should move between the tiptoe and the heel. Because the dynamic performances are neglected, we do not consider the inertial force and influence from external forces. As mentioned above, when the robot is static, the ZMP coincides with the projection point of the CoM on the ground.

Second, the load torque of all the joints must be as low as possible, which is called the load constraint here [6]. When the robot carries an object, generally higher joint-torques is needed, because the object is carried far away from the floor or the base of the robot. Those may cause a saturation of joint-torque to the torque limitation. Since the robot could not avoid withstanding the load of the object, we should make the robot's joints keep away from the torque limits to protect the relatively frailest joint among all the joints. The torque limitations are shown in **Table 1**. The torque limitations of the wrist and the elbow are quite smaller than that of other parts of the model, which is similar to human beings. The multi-joint robots usually have many degrees of freedom. Although we have simplified the complicated humanoid (a 3D model) to the robot model in this paper, which has 5 degrees of freedom, there are still  $3^5$  options to each posture in the weightlifting motion procedure. So how to choose an optimal option from these  $3^5$  options becomes a question we have to face. To satisfy the load constraint, the one is considered among those options, in which the output of the relatively frailest joint is a minimum, comparing with other options'.

According to the model, the load torque of each joint ( $T_1, T_2, T_3, T_4, T_5$ ) and reaction force ( $R_A, R_B$ ) are indicated in the equations below.

$$T_5 = m_5 L_{g5} g \cos(\theta_1 + \theta_2 + \theta_3 + \theta_4 + \theta_5) \quad (1)$$

$$T_4 = (m_4 L_{g4} + m_5 L_4) g \cos(\theta_1 + \theta_2 + \theta_3 + \theta_4) + T_5 \quad (2)$$

$$T_3 = [m_3 L_{g3} + (m_5 + m_4) L_3] g \cos(\theta_1 + \theta_2 + \theta_3) + T_4 \quad (3)$$

Table 1. Geometric parameters of the model.

| Joint           | 1<br>ankle | 2<br>knee | 3<br>waist | 4<br>shoulder | 5<br>elbow |
|-----------------|------------|-----------|------------|---------------|------------|
| $m$ (kg)        | 9.6        | 14.4      | 36         | 8.5           | 8.5        |
| $L$ (mm)        | 463        | 450       | 416        | 300           | 320        |
| $L_g$ (mm)      | 180        | 252       | 392        | 162           | x          |
| $T_{\max}$ (Nm) | 600        | 500       | 550        | 400           | 400        |
| $T_{\min}$ (Nm) | -600       | -500      | -550       | -400          | -400       |

$$T_2 = [m_2 L_{g_2} + (m_5 + m_4 + m_3) L_2] g \cos(\theta_1 + \theta_2) + T_3 \quad (4)$$

$$T_1 = [m_1 L_{g_1} + (m_5 + m_4 + m_3 + m_2) L_1] g \cos \theta_1 + T_2 \quad (5)$$

$$R_A = \frac{T_1 + (m_1 + m_2 + m_3 + m_4 + m_5) g b}{a + b} \quad (6)$$

$$R_B = \frac{(m_1 + m_2 + m_3 + m_4 + m_5) g a - T_1}{a + b} \quad (7)$$

To satisfy the balance constraint,  $R_A$  and  $R_B$  must be both positive. So according to (6) and (7), the load torque of ankle joint  $T_1$  has another limitation, which is called balance limitation here.

$$\begin{aligned} -b(m_1 + m_2 + m_3 + m_4 + m_5) g &\leq T_1 \\ &\leq a(m_1 + m_2 + m_3 + m_4 + m_5) g \end{aligned} \quad (8)$$

The balance limitation is different with the torque limitations initialized in **Table 1**, which avoid the joints overloading to be damaged. Therefore, (9) is provided.

$$H_{T_i} = \begin{cases} \frac{T_i}{T_{i \min}} \times 100\% & (T_i < 0) \\ \frac{T_i}{T_{i \max}} \times 100\% & (T_i > 0) \end{cases} \quad (9)$$

where  $H_{T_i}$  is the output of the torque, which must be less than 1, if each joint of the robot does not overload. The parameter  $H_{T_i}$  can help us analysis the situations that the joint is withstanding the load of the object in the weightlifting motion procedure. As we known, the knee joint and the waist joint often suffer a pain to the aged, so this parameter is available to be used to reduce the load applied on the joints. Considering the conditions above, the following algorithm is proposed to simplify and facilitate the analysis in Section 3.

### 3. Algorithm for Trajectory Generation

The weightlifting motion can be obtained by an approximated optimal algorithm. In this paper, the algorithm is developed, based on the RDK (Repeatedly Direct Kinematics) method for the robot, which is introduced into applying on the trajectory generation of the standing up movements that is a series of motions from an initial posture to the erect posture [7]. In the task, a small increment is given to each joint of the model. Moreover, there are three motion options, + rotation, - rotation and no rotation, to the five joints ( $J_1, J_2, J_3, J_4, J_5$ ) and the model could place the soles backward and forward to keep the ZMP away from the unstable area when the model robot will tumble down. So according to the RDK method, each posture has  $3^5$  options in the weightlifting motion procedure and the option that satisfies the aim and the constraint mentioned in Section 2 is selected as the result of this posture at this time. Such procedure is

reiterated until the erect posture is reached.

The algorithm of the trajectory generation is elaborated as following:

1) Initialize the parameters in **Table 1** and give an initial posture to the robot model.

2) After given an initial posture, if each joint does not overload, give a small increment and then choose the options that the object is lifted from  $3^5$  options of each posture, else the weightlifting motion could not be realized as a result of a bad initial posture or the object's heavy mass.

3) Choose the options that the object is lifted and the robot will not tumble down. If  $R_A \times R_B < 0$  in all the options, the ZMP will move out of the predefined stability region. To keep the balance, we should choose the option that the reaction force  $R_j$  ( $j = A$  or  $B$ ) is increased which is negative. That means the robot model will walk forward or backward. At this time, the object is tried to be held without motion. Go back to Step 2.

4) Choose the options that  $R_A$  and  $R_B$  are positive. Calculate the output of each joint of the chosen options.

5) Compare the outputs of the five joints of each one of the chosen options to memory the joint that has maximum output of each chosen option. This joint is the one we called the relatively frailest joint.

6) Compare the output of the relatively frailest joint of each chosen option, the option that has the minimum output of the relatively frailest joint is the result we need. Memory this posture and give it a same increment. Go back to Step 2.

7) If the object could not reach a higher position, end the program.

The operations are implemented iteratively until the object could not be held at a higher position. The weightlifting motion is finished and the simulations for the trajectory generations are provided in Section 4.

### 4. Simulations for Algorithm Proposed

To evaluate the effectiveness of the algorithm proposed above, the following simulations are provided, where the motion trajectories are showed with every 20 postures. When lifting an object to the top, the robot always stands up completely at last as we known. So a criterion that the increase of the height of the object in the z-direction must be first satisfied is defined to make sure the robot can implement the standing up motion to the last. The wrist point (the middle of the object) is chosen as the datum of the weightlifting motion.

**Figure 2** shows Simulation 1 in the case that the mass of the 20 kg's object is held. As shown in the graph (c), the robot has no motion in the x-direction, because the ZMP moves within the predefined stability region between the tiptoe (200 mm) and the heel (-60 mm), in the graph (d).

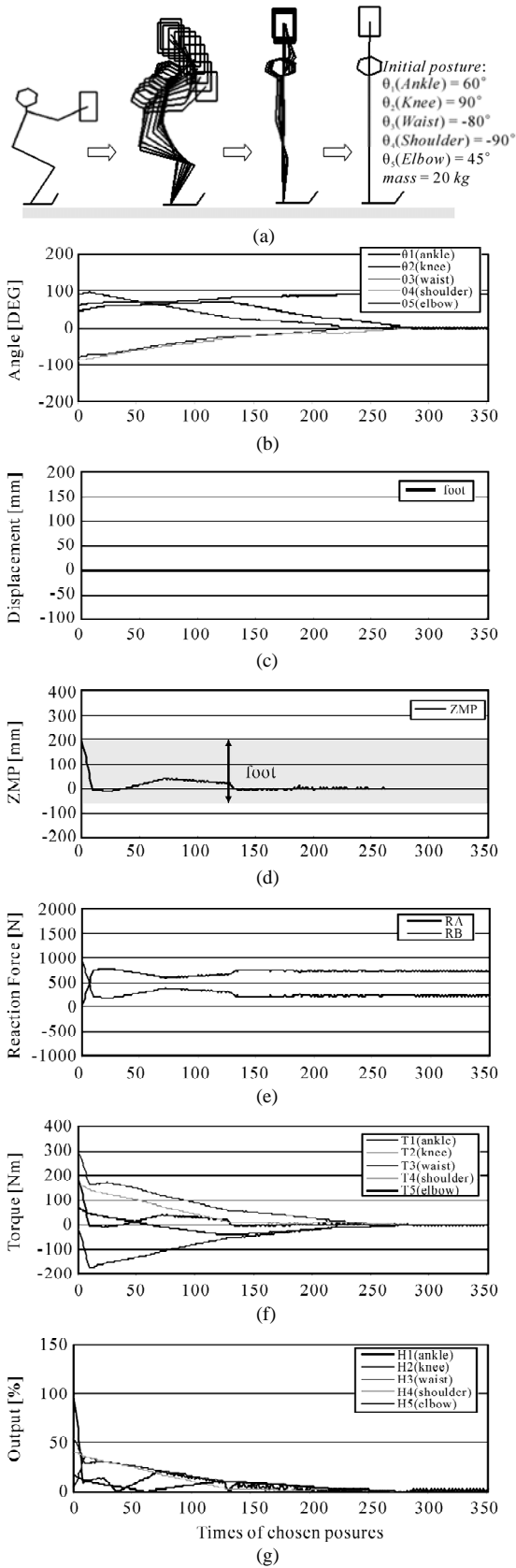


Figure 2. Simulation 1 of weightlifting.

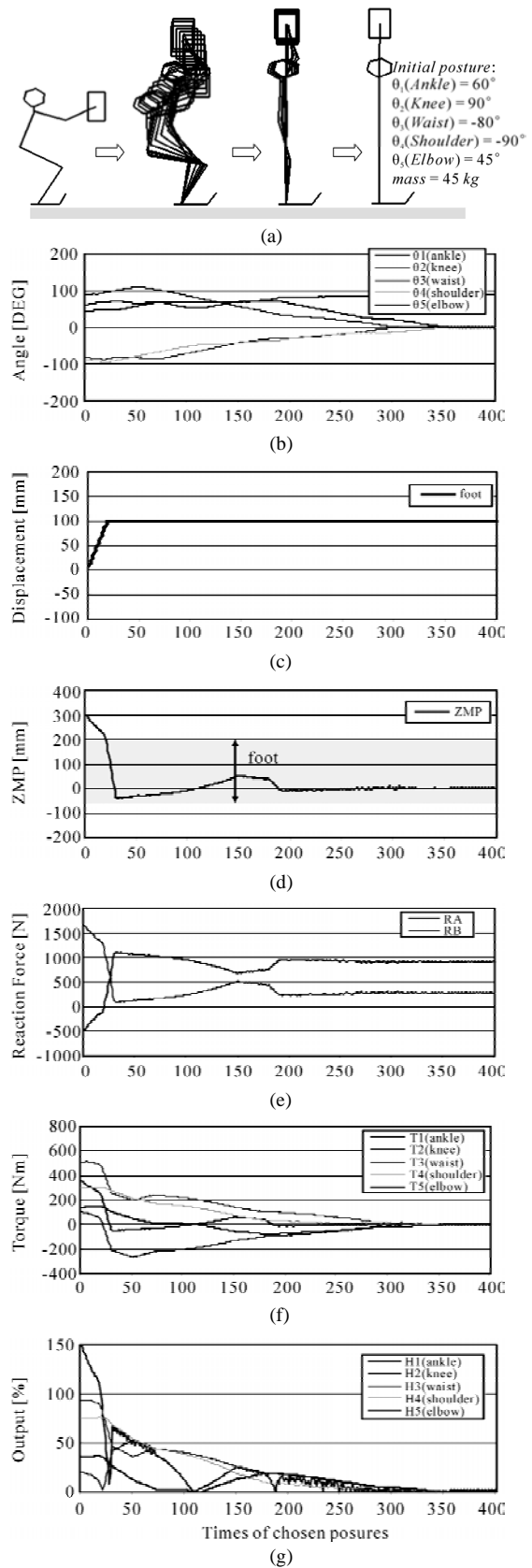


Figure 3. Simulation 2 of weightlifting.

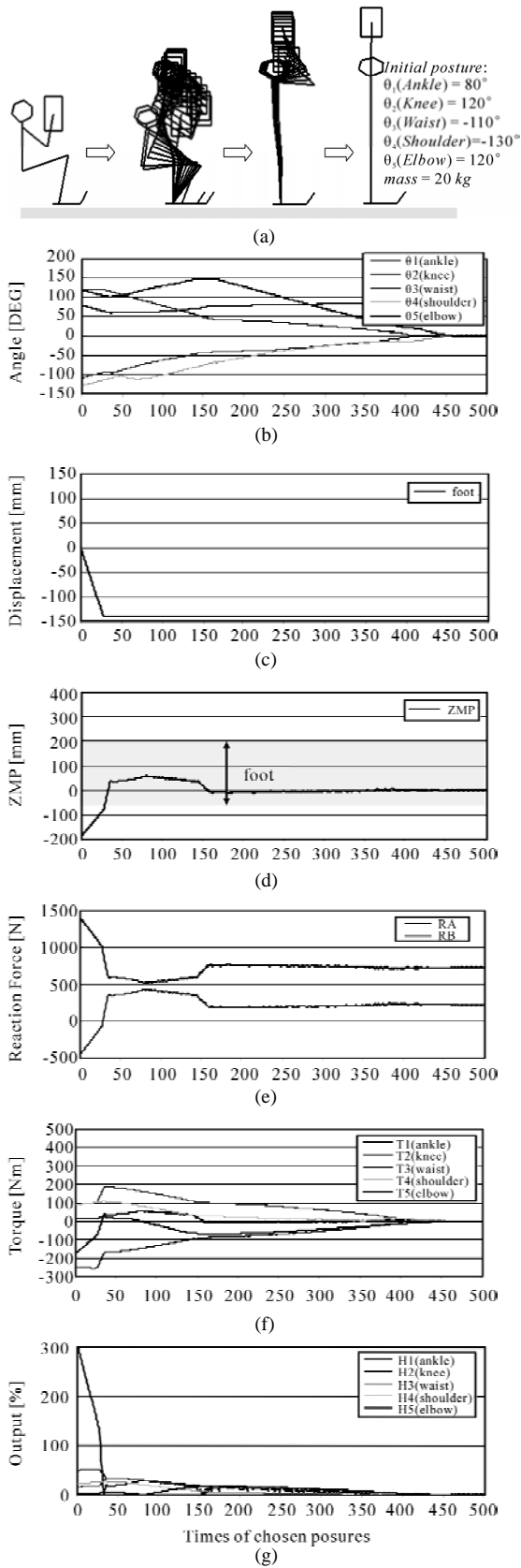


Figure 4. Simulation 3 of weightlifting.

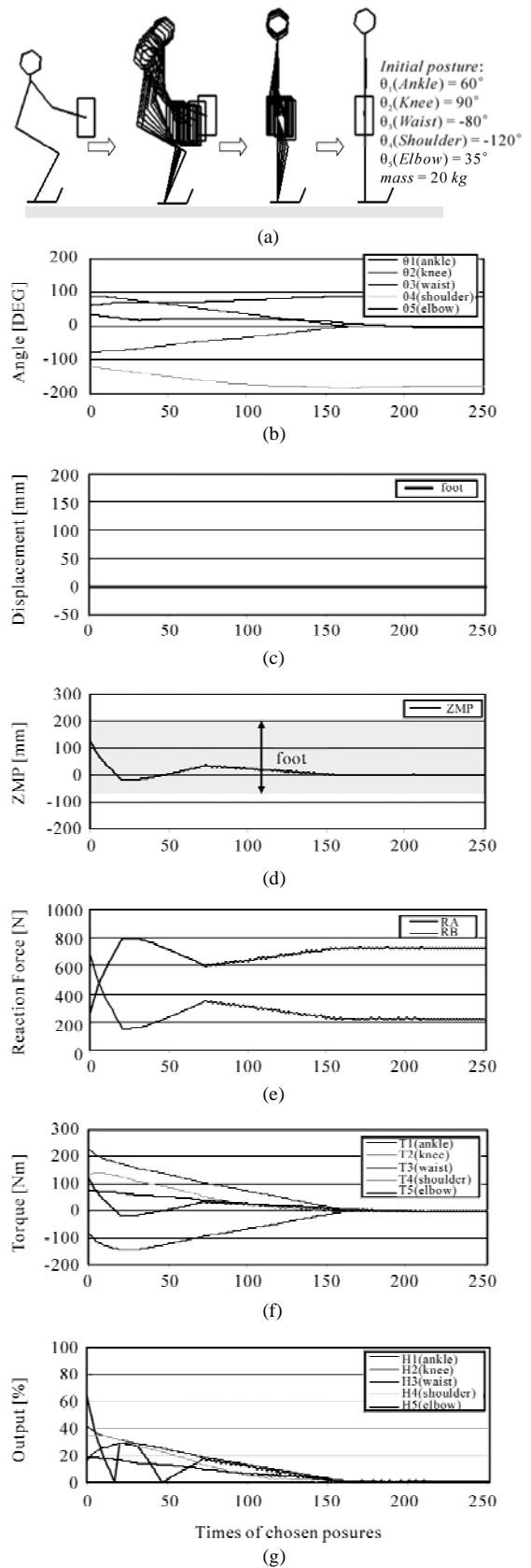


Figure 5. Simulation 4 of weightlifting.

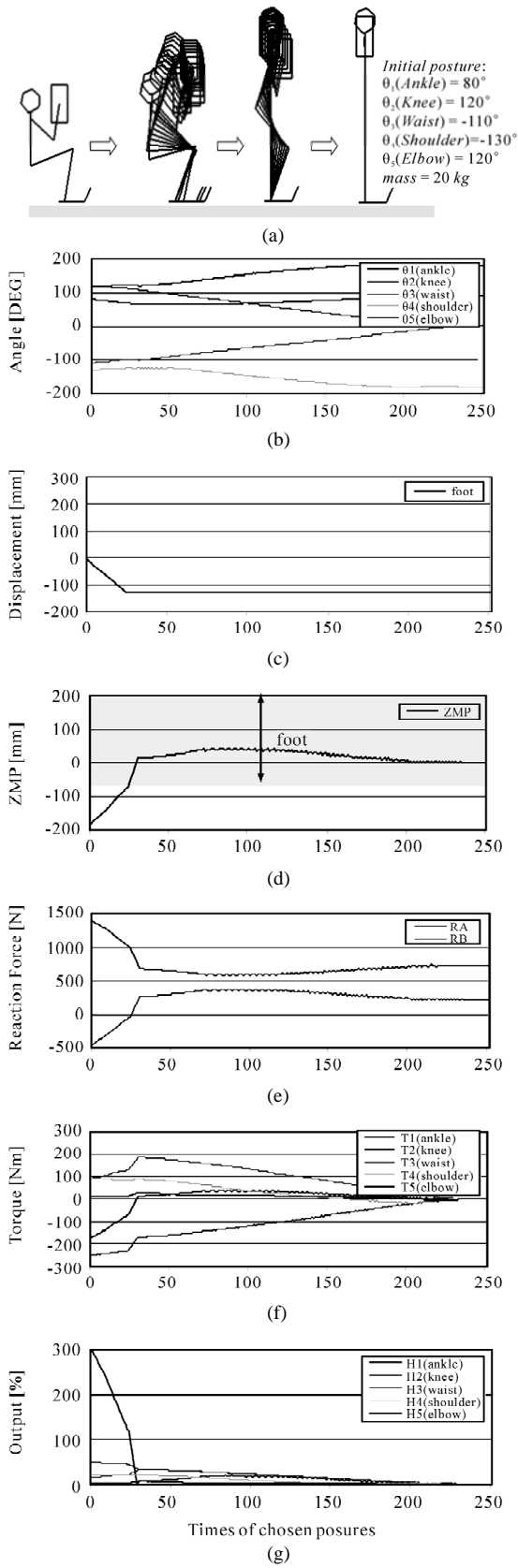


Figure 6. Simulation 5 of weightlifting.

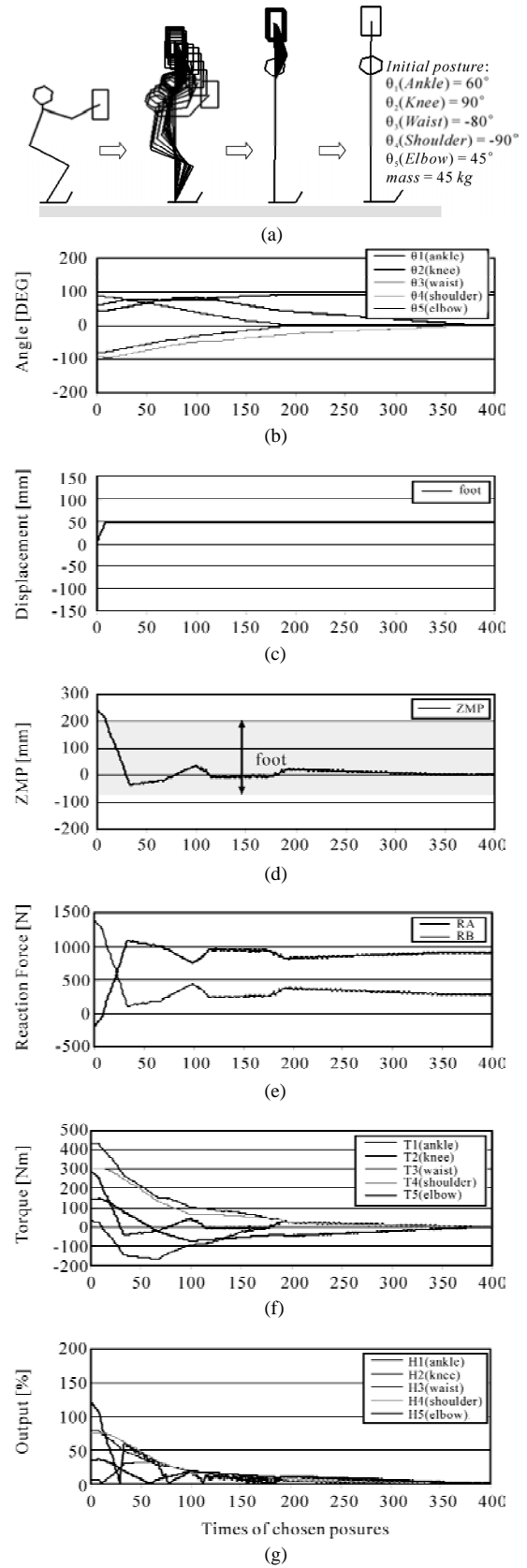


Figure 7. Simulation 6 of weightlifting.

The graph (b) shows the change of the joint angle with the posture. According to graph (b), we can obtain that when the object is lifted to the top, the robot has stood up completely and stretched its arm, where the angle of the ankle joint approximates to  $90^\circ$ , the ones of other joints approximate to  $0^\circ$ , just like human being. The reaction forces are always positive in the graph (e) indicates that the robot is stable without no displacement in each direction, just as shown in the graph (c), which is satisfying the balance constraint. The graph (f) shows the change of the joint torque with the posture. We can see in the graph (g) that the outputs of all joints are within the limits, meaning that it never reaches saturation when lifting the object. Here, we want to explain that the output of the ankle joint is calculated for the balance limitation, when it is bigger than the load limitation. Finally, the weightlifting motion is finished successfully.

Simulation 2 has a same initial posture with the Simulation 1, but the mass of the object is different, 45 kg. Because of the initial condition, as shown in the graph (d) of **Figure 3**, in the beginning stage, the ZMP is in front of the tiptoe (200 mm). So the robot moves forward (in the graph (c)) to avoid tumbling until the position of the ZMP enters into the stability region. At this time, the value of the reaction force  $R_A$  changes from negative to positive in the graph (e). The graph (f) shows the change of the joint torque with the posture. In the graph (g), we can see that the output of the ankle joint is more than 1 at the beginning, meaning that the robot will tumble down. After ZMP entering into the stable area, the weightlifting motion is finished.

Simulation 3 has a different initial posture from the Simulation 1, but the mass of the object is same. Because of the initial condition, as shown in the graph (d) of **Figure 3**, in the beginning stage, the ZMP is behind the heel (-60 mm), meaning that the ZMP moves out of the predefined stability region. So the robot moves backward (in the graph (c)) to avoiding tumbling backward until the position of the ZMP enters into the stability region. Meanwhile, the value of the reaction force  $R_B$  changes from negative to positive in the graph (e). The graph (f) shows the change of the joint torque with the posture. In the graph (g), we can see that the output of the ankle joint is more than 1 at the beginning, meaning that the load torque that the ankle joint withstands has exceeded the balance torque limitation. After ZMP entering into the stable area, the weightlifting motion is finished.

With the same algorithm, the Simulation 4~6 are provided that we choose the shoulder joint as the datum to evaluate the whole weightlifting motion, where the rise of the shoulder must be first considered. In these simulations, we still take the load constraint and balance constraint into account to implement the weightlifting motion.

**Figure 5** shows Simulation 4 in the case that the mass of the 20 kg's object is held. The robot has no motion in

the x-direction, because the ZMP moves within the predefined stability region. Finally, the trajectory of the motion is generated where the object is held around the waist joint, like a person lifting up a water bucket. Although Simulation 5 and Simulation 3 are implemented under a same initial condition, the trajectory generations are different because of the different datum. And the end position of the object is not always located on the top. Simulation 6 and Simulation 2 are implemented under a same initial condition, even though the trajectory generations are different, we still realize the weightlifting motion to hold the object at the highest spot.

It is similar with human being that the robot cannot always lift up any object, if the object is too heavy for the robot. For example, in the Simulation 1, the robot can lift up 20 kg's object easily. But in the Simulation 2, the robot has to move forward not to tumble with 45 kg's object, and if the mass of the object is more than 50 kg, the robot cannot implement the weightlifting motion. At this time, the load torque of the knee joint exceeds the torque limitation showed in **Table 1**, so the robot cannot stand up with the object as usual, unless the torque limitation of the knee joint is enlarged.

All these results show that our proposed algorithm of weightlifting motion is effective.

## 5. Conclusions

In this paper, we realized the weightlifting motion successfully with the multi-joint robot model under some predefined conditions. The trajectory of a lift-up motion for a stance robot is also generated by RDK method. We proposed the algorithm with considering the output of the joint to reduce the load on the joint to protect the relatively frailest joint. According to simulations, we verified the rationality and the effectiveness of the proposed algorithm. We also hope that this paper can contribute the research about the configuration of humanoid robot or human being and helping the aged and the handicapped in daily.

This method based on RDK method is used to obtain a continuous trajectory generation, which is under the static environment. In the future, the dynamic influence will be considered.

## 6. References

- [1] Japan Industrial Safety and Health Association, "Investigation Research on Development of the Evaluation Criteria of the Work Load Considering Advanced Age Labourers' Safety and Health-The Heisei 13 fiscal year report," Japanese, 2001.
- [2] N. Miyata, "Individual Human Motion Performance Index to Generate Lift-up Motion," *Proceedings of the 19th Annual Conference of the Robotics Society of Japan*

- (RSJ2001), Tokyo, 2001, pp. 721-742.
- [3] E. Bayo and B. Paden, "On Trajectory Generation for Flexible Robots," *Journal of Robotic Systems*, Vol. 4, No. 2, 1987, pp. 229-235.
- [4] L. Song, Y. Kamiya, H. Seki, S. M. Hikizu and Q. Zhang, "Solutions of Inverse Kinematics of Articulated Robot by Using Repeatedly Direct Kinematics," *Journal of the Japan Society for Precision Engineering*, Vol. 67, No. 6, 2001, pp. 971-976.
- [5] R. Kamnik: "Standing-Up Robot," *Journal of Medical Engineering & Technology*, Vol. 28, No. 2, 2004, pp. 74-80.
- [6] T. Matsumaru, S. Fukuyama and T. Sato, "Model for Analysis of Weight Lifting Motion Considering the Abdominal Pressure Increased by Valsalva Maneuver," *Transactions of the Japan Society of Mechanical Engineers (Series C)*, Vol. 72, No. 724, 2006, pp. 169-176.
- [7] Y. Kamiya, T. Kubo, S. Aoyagi and S. Okabe, "Control of Robotic Manipulators Using the Solutions of Repeated Direct Kinematics," *Transactions of the Japan Society of Mechanical Engineers (Series C)*, Vol. 59, No. 564, 1993, pp. 125-130.

# A Nonmonotone Line Search Method for Symmetric Nonlinear Equations\*

Gonglin Yuan<sup>1</sup>, Laisheng Yu<sup>2</sup>

<sup>1</sup>College of Mathematics and Information Science, Guangxi University, Nanning, China

<sup>2</sup>Student Affairs Office, Guangxi University, Nanning, China

E-mail: glyuan@gxu.edu.cn

Received February 7, 2010; revised March 21, 2010; accepted July 7, 2010

## Abstract

In this paper, we propose a new method which based on the nonmonotone line search technique for solving symmetric nonlinear equations. The method can ensure that the search direction is descent for the norm function. Under suitable conditions, the global convergence of the method is proved. Numerical results show that the presented method is practicable for the test problems.

**Keywords:** Nonmonotone Line Search, Symmetric Equations, Global Convergence

## 1. Introduction

Consider the following nonlinear equations:

$$g(x) = 0, x \in R^n \quad (1)$$

where  $g: R^n \rightarrow R^n$  be continuously differentiable and its Jacobian  $\nabla g(x)$  is symmetric for all  $x \in R^n$ . This problem can come from unconstrained optimization problems, a saddle point problem, and equality constrained problems [the detail see [1]]. Let  $\phi(x)$  be the norm function defined by  $\phi(x) = \frac{1}{2} \|g(x)\|^2$ . Then the nonlinear equation problem (1) is equivalent to the following global optimization problem

$$\min \phi(x), x \in R^n \quad (2)$$

The following iterative formula is often used to solve (1) and (2):

$$x_{k+1} = x_k + \alpha_k d_k$$

where  $\alpha_k$  is a steplength, and  $d_k$  is one search direction. To begin with, we briefly review some methods for (1) and (2) by line search technique. First, we give some techniques for  $\alpha_k$ . Li and Fukushima [1] proposed an approximate monotone line search technique to obtain the step-size  $\alpha_k$  satisfying:

$$\begin{aligned} & \varphi(x_k + \alpha_k d_k) - \varphi(x_k) \\ & \leq -\delta_1 \|\alpha_k d_k\|^2 - \delta_2 \|\alpha_k g_k\|^2 + \varepsilon_k \|g_k\|^2 \end{aligned} \quad (3)$$

where  $\delta_1 > 0$  and  $\delta_2 > 0$  are positive constants,  $\alpha_k = r^{i_k}$ ,  $r \in (0, 1)$ ,  $i_k$  is the smallest nonnegative integer  $i$  such that (3), and  $\varepsilon_k$  satisfies  $\sum_{k=0}^{\infty} \varepsilon_k < \infty$ . Combining the line search (3) with one special BFGS update formula, they got some better results (see [1]). Inspired by their idea, Wei [2] and Yuan [3] made a further study. Brown and Saad [4] proposed the following line search method to obtain the stepsize

$$\varphi(x_k + \alpha_k d_k) - \varphi(x_k) \leq \sigma \alpha_k \nabla \varphi(x_k)^T d_k \quad (4)$$

where  $\sigma \in (0, 1)$ . Based on this technique, Zhu [5] gave the nonmonotone line search technique:

$$\varphi(x_k + \alpha_k d_k) - \varphi(x_{l(k)}) \leq \sigma \alpha_k \nabla \varphi(x_k)^T d_k \quad (5)$$

where  $\varphi_{l(k)} = \max_{0 \leq j \leq n(k)} \{\varphi_{k-j}\}$ ,  $k = 0, 1, 2, \dots$ ,  $n(k) = \min\{M, k\}$ , and  $M \geq 0$  is an integer constant. From these two techniques (4) and (5), it is easy to see that the Jacobian matrix  $\nabla g(x)$  must be computed at every iteration, which will increase the workload especially for large-scale problems or this matrix is expensive. Considering these points, we [6] presented a new backtracking inexact technique to obtain the stepsize  $\alpha_k$

\*This work is supported by China NSF grants 10761001, the Scientific Research Foundation of Guangxi University (Grant No. X081082), and Guangxi SF grants 0991028.

$$\|g(x_k + \alpha_k d_k)\|^2 - \|g(x_k)\|^2 \leq \delta \alpha_k^2 g(x_k)^T d_k \quad (6)$$

where  $\delta \in (0,1)$ . Second, we present some techniques for  $d_k$ . One of the most effective methods is Newton method. It normally requires a fewest number of function evaluations, and it is very good at handling ill-conditioning. However, its efficiency largely depends on the possibility to efficiently solve a linear system which arises when computing the search  $d_k$  at each iteration

$$\nabla g(x_k) d_k = -g(x_k) \quad (7)$$

Moreover, the exact solution of the system (7) could be too burdensome, or it is not necessary when  $d_k$  is far from a solution [7]. Inexact Newton methods [5,7] represent the basic approach underlying most of the Newton-type large-scale algorithms. At each iteration, the current estimate of the solution is updated by approximately solving the linear system (7) using an iterative algorithm. The inner iteration is typically "truncated" before the solution to the linear system is obtained. Griewank [8] firstly proposed the Broyden's rank one method for nonlinear equations and obtained the global convergence. At present, a lot of algorithms have been proposed for solving these two problems (1) and (2) (see [9-15]). The famous BFGS formula is one of the most effective quasi-Newton methods, where the  $d_k$  is the solution of the system of linear equations

$$B_k d_k + g_k = 0 \quad (8)$$

where  $B_k$  is generated by the following BFGS update formula

$$B_{k+1} = B_k - \frac{B_k s_k s_k^T B_k}{s_k^T B_k s_k} + \frac{y_k y_k^T}{s_k^T y_k} \quad (9)$$

where  $s_k = x_{k+1} - x_k$  and  $y_k = g(x_{k+1}) - g(x_k)$ . Recently, there are some results on nonlinear equations can be found at [6,17-20].

Zhang and Hager [21] present a nonmonotone line search technique for unconstrained optimization problem  $\min_{x \in R^n} f(x)$ , where the nonmonotone line search technique is defined by

$$\begin{aligned} f(x_k + \alpha_k d_k) &\leq C_k + \delta \alpha_k \nabla f(x_k)^T d_k, \\ \nabla f(x_k + \alpha_k d_k)^T d_k &\geq \sigma \nabla f(x_k)^T d_k \end{aligned}$$

where

$$\begin{aligned} 0 < \delta < \sigma < 1, \quad C_0 &= f(x_0), \quad Q_0 = 1, \\ Q_{k+1} &= \eta_k Q_k + 1, \quad C_{k+1} = \frac{\eta_k Q_k C_k + f(x_k + \alpha_k d_k)}{Q_{k+1}} \end{aligned}$$

$\eta_k \in [\eta_{\min}, \eta_{\max}]$ , and  $0 \leq \eta_{\min} \leq \eta_{\max} \leq 1$ . They proved the global convergence for nonconvex, smooth functions, and R-linear convergence for strongly convex functions. Numerical results show that this method is more effective than other similar methods. Motivated by their technique, we propose a new nonmonotone line search technique which can ensure the descent search direction on the norm function for solving symmetric nonlinear Equations (1) and prove the global convergence of our method. The numerical results are reported too. Here and throughout this paper,  $\|\cdot\|$  denote the Euclidian norm of vectors or its induced matrix norm.

This paper is organized as follows. In the next section, we will give our algorithm for (2). The global convergence and the numerical result are established in Section 3 and in Section 4, respectively.

## 2. The Algorithm

Precisely, our algorithm is stated as follows.

### Algorithm 1.

Step 0: Choose an initial point  $x_0 \in R^n$ , an initial symmetric positive definite matrix  $B_0 \in R^{n \times n}$ , and constants  $r \in (0,1)$ ,  $0 \leq \rho_1 \leq \rho_2 \leq 1$ ,  $0 < \delta_1 < 1$ ,  $J_0 = \|g_0\|^2$ ,  $E_0 = 1$ , and  $k = 0$ ;

Step 1: If  $g_k = 0$ ; then stop; Otherwise, solving the following linear Equations (10) to obtain  $d_k$  and go to step 2;

$$B_k d_k + g_k = 0 \quad (10)$$

Step 2: Let  $i_k$  be the smallest nonnegative integer  $i$  such that

$$\|g(x_k + \lambda_k d_k)\|^2 - \|g(x_k)\|^2 \leq \delta \lambda_k^2 g(x_k)^T d_k \quad (11)$$

holds for  $\lambda = r^i$ . Let  $\lambda_k = r^{i_k}$ ;

Step 3: Let  $x_{k+1} = x_k + \alpha_k d_k$ ,  $s_k = x_{k+1} - x_k$  and  $y_k = g(x_{k+1}) - g(x_k)$ . If  $y_k^T s_k > 0$ , update  $B_k$  to generate  $B_{k+1}$  by the BFGS Formula (9). Otherwise, let  $B_{k+1} = B_k$ ;

Step 4: Choose  $\rho_k \in [0,1]$ , and set

$$E_{k+1} = \rho_k E_k + 1, \quad J_{k+1} = \frac{\rho_k E_k J_k + \|g(x_{k+1})\|^2}{E_{k+1}} \quad (12)$$

Step 5: Let  $k = k + 1$ , go to Step 1.

**Remark 1:** 1) By the technique of the step 3 in the algorithm [see [1]], we deduce that  $B_{k+1}$  can inherit the positive and symmetric properties of  $B_k$ . Then, it is not difficult to get  $d_k^T g_k < 0$ .

2) It is easy to know that  $J_{k+1}$  is a convex combination of  $J_k$  and  $\|g(x_{k+1})\|^2$ . By  $J_0 = \|g_0\|^2$ , it follows that  $J_k$  is a convex combination of function values  $\|g_0\|^2, \|g_1\|^2, \dots, \|g_k\|^2$ . The choice of  $\rho_k$  controls the degree of nonmonotonicity. If  $\rho_k = 0$  for each  $k$ , then the line search is the usual monotone line search. If  $\rho_k = 1$  for each  $k$ , then  $V_k = \frac{1}{k+1} \sum_{i=0}^k \|g_i\|^2$ ,  $J_k = V_k$ , where is the average function value.

3) By (9), we have  $B_{k+1}s_k = y_k = g_{k+1} - g_k \approx \nabla g_{k+1}s_k = \nabla g_{k+1}^T s_k$ , this means that  $B_{k+1}$  approximate to  $\nabla g_{k+1}$  along  $s_k$ .

### 3. The Global Convergence Analysis of Algorithm 1

In this section, we establish global convergence for Algorithm 1. The level set  $\Omega$  is defined by

$$\Omega = \{x \in R^n \mid \|g(x)\| \leq \|g(x_0)\|\}.$$

**Assumption A.** The Jacobian of  $g$  is symmetric and there exists a constant  $M > 0$  holds

$$\|g(x) - g(x_k)\| \leq M \|x - x_k\| \quad (13)$$

for  $x \in \Omega$ .

Since  $B_k$  approximates  $\nabla g_k$  along direction  $s_k$ , we can give the following assumption.

**Assumption B.**  $B_k$  is a good approximation to  $\nabla g_k$ , i.e.,

$$\|(\nabla g(x_k) - B_k)d_k\| \leq \varepsilon \|g_k\| \quad (14)$$

where  $\varepsilon \in (0,1)$  is a small quantity.

**Assumption C.** There exist positive constants  $b_1$  and  $b_2$  satisfy

$$g_k^T d_k \leq -b_1 \|g_k\|^2 \quad (15)$$

and

$$\|d_k\| \leq b_2 \|g_k\| \quad (16)$$

for all sufficiently large  $k$ .

By (10) and Assumption C, we have

$$b_1 \|g_k\| \leq \|d_k\| \leq b_2 \|g_k\| \quad (17)$$

**Lemma 3.1.** Let Assumption B hold and  $\{\alpha_k, d_k, x_{k+1}, g_{k+1}\}$  be generated by Algorithm 1. Then  $d_k$  is descent direction for  $\varphi(x)$  at  $x_k$ , i.e.,

$$\nabla \varphi(x_k)^T d_k < 0 \quad (18)$$

**Proof.** By (10), we have

$$\begin{aligned} \nabla \varphi(x_k)^T d_k &= g_k^T \nabla g_k d_k = g_k^T [(\nabla g_k d_k - B_k)d_k - g_k] \\ &= g_k^T (\nabla g_k d_k - B_k)d_k - g_k^T g_k \end{aligned} \quad (19)$$

Using (14) and taking the norm in the right-hand-side of (19), we get

$$\begin{aligned} \nabla \varphi(x_k)^T d_k &\leq \|g_k^T (\nabla g_k d_k - B_k)d_k\| - \|g_k\|^2 \\ &\leq -(1-\varepsilon)\|g_k\|^2 \end{aligned} \quad (20)$$

Therefore, for  $\varepsilon \in (0,1)$ , we get the lemma.

By the above lemma, we know that the norm function  $\varphi(x)$  is descent along  $d_k$ , then  $\|g_{k+1}\| \leq \|g_k\|$  holds.

**Lemma 3.2.** Let Assumption B hold and  $\{\alpha_k, d_k, x_{k+1}, g_{k+1}\}$  be generated by Algorithm 1. Then  $\{x_k\} \subset \Omega$ . Moreover,  $\{\|g_k\|\}$  converges.

**Proof.** By Lemma 3.1, we get  $\|g_{k+1}\| \leq \|g_k\|$ . Then, we conclude that  $\{\|g_k\|\}$  converges. Moreover, we have for all  $k$

$$\|g_{k+1}\| \leq \|g_k\| \leq \dots \leq \|g_0\|.$$

Which means that  $\{x_k\} \subset \Omega$ .

The next lemma will show that for any choice of  $\rho_k \in [0,1]$ ,  $J_k$  lies between  $\|g_k\|^2$  and  $V_k$ .

**Lemma 3.3.** Let  $\{\alpha_k, d_k, x_{k+1}, g_{k+1}\}$  be generated by Algorithm 1, we have  $\|g_k\|^2 \leq J_k \leq V_k, J_{k+1} \leq J_k$  for each  $k$ .

**Proof.** We will prove the lower bound for  $J_k$  by induction. For  $k=0$ , by the initialization  $J_0 = \|g_0\|^2$ , this holds. Now we assume that  $J_i \geq \|g_i\|^2$  holds for all  $0 \leq i \leq k$ . By (2.3) and  $\|g_{i+1}\|^2 \leq \|g_i\|^2$ , we have

$$\begin{aligned} J_{i+1} &= \frac{\rho_i E_i J_i + \|g_{i+1}\|^2}{E_{i+1}} \geq \frac{\rho_i E_i \|g_i\|^2 + \|g_{i+1}\|^2}{E_{i+1}} \\ &\geq \frac{\rho_i E_i \|g_{i+1}\|^2 + \|g_{i+1}\|^2}{E_{i+1}} = \|g_{i+1}\|^2 \end{aligned} \quad (21)$$

where  $E_{i+1} = \rho_i E_i + 1$ . Now we prove that  $J_{k+1} \leq J_k$  is true. By (12) again, and using  $\|g_k\|^2 \geq \|g_{k+1}\|^2$ , we obtain

$$J_{k+1} = \frac{\rho_k E_k J_k + \|g_{k+1}\|^2}{E_{k+1}} \leq \frac{\rho_k E_k J_k + J_{k+1}}{E_{k+1}}.$$

Which means that  $J_{k+1} \leq J_k$  for all  $k$  is satisfied. Then we have

$$\|g_k\|^2 \leq J_k \leq J_{k-1} \quad (22)$$

Let  $L_k : R \rightarrow R$  be defined by

$$L_k(t) = \frac{tJ_{k-1} + \|g_k\|^2}{t+1},$$

we can get

$$L_k'(t) = \frac{J_{k-1} + \|g_k\|^2}{(t+1)^2}.$$

By  $J_{k-1} \leq \|g_k\|^2$ , we obtain  $L_k'(t) \geq 0$  for all  $t \geq 0$ . Then,  $L_k$  is nondecreasing, and  $\|g_k\|^2 = L_k(0) \leq L_k(t)$  for all  $t \geq 0$ . Now we prove the upper bound  $J_k \leq V_k$  by induction. For  $k = 0$ , by the initialization  $J_0 = \|g_0\|^2$ , this holds. Now assume that  $J_j \leq V_j$  hold for all  $0 \leq j \leq k$ . By using  $E_0 = 1$ , (12), and  $\rho_k \in [0, 1]$ , we obtain

$$E_{j+1} = 1 + \sum_{i=0}^j \prod_{p=0}^i \rho_{j-p} \leq j+2 \quad (23)$$

Denote that  $L_k$  is monotone nondecreasing, (23) implies that

$$J_k = L_k(\rho_{k-1}E_{k-1}) = L(E_k - 1) \leq L_k(k) \quad (24)$$

Using the induction step, we have

$$L_k(k) = \frac{kJ_{k-1} + \|g_k\|^2}{k+1} \leq \frac{kV_{k-1} + \|g_k\|^2}{k+1} = V_k \quad (25)$$

Combining (24) and (25) implies the upper bound of  $J_k$  in this lemma. Therefore, we get the result of this lemma.

The following lemma implies that the line search technique is well-defined.

**Lemma 3.4.** Let Assumption A, B and C hold. Then Algorithm 1 will produce an iterate  $x_{k+1} = x_k + \alpha_k d_k$  in a finite number of backtracking steps.

**Proof.** From Lemma 3.8 in [4] we have that in a finite number of backtracking steps,  $\alpha_k$  must satisfy

$$\|g(x_k + \alpha_k d_k)\|^2 - \|g(x_k)\|^2 \leq \sigma \alpha_k g(x_k)^T \nabla g_k d_k \quad (26)$$

where  $\sigma \in (0, 1)$ . By (20) and (15), we get

$$\begin{aligned} \alpha_k g(x_k)^T \nabla g_k d_k &\leq -\alpha_k (1-\varepsilon) \|g_k\|^2 \\ &= -\alpha_k (1-\varepsilon) \frac{g_k^T d_k}{g_k^T d_k} \|g_k\|^2 \leq \alpha_k (1-\varepsilon) \frac{1}{b_1} g_k^T d_k \end{aligned} \quad (27)$$

Using  $\alpha_k \in (0, 1)$ , we obtain

$$\begin{aligned} \alpha_k g(x_k)^T \nabla g_k d_k &\leq \alpha_k (1-\varepsilon) \frac{1}{b_1} g_k^T d_k \\ &\leq \alpha_k^2 (1-\varepsilon) \frac{1}{b_1} g_k^T d_k \end{aligned} \quad (28)$$

So let  $\delta_1 \in \left(0, \min\left(1, \sigma(1-\varepsilon)\frac{1}{b_1}\right)\right)$ . By Lemma 3.3,

we know  $\|g_k\|^2 \leq J_k$ . Therefore, we get the line search (11). The proof is complete.

**Lemma 3.5.** Let Assumption A, B and C hold. Then we have the following estimate for  $\alpha_k$ , when  $k$  sufficiently large:

$$\alpha_k \geq b_0 > 0 \quad (29)$$

**Proof.** Assuming the step-size  $\alpha_k$  such that (11).

Then  $\alpha_k' = \alpha_k / 1$  does not satisfy (11), i.e.,

$$\|g(x_k + \alpha_k' d_k)\|^2 - J_k > \delta_1 \alpha_k'^2 g(x_k)^T d_k$$

By  $\|g_k\|^2 \leq J_k$ , we get

$$\begin{aligned} \|g(x_k + \alpha_k' d_k)\|^2 - \|g_k\|^2 \\ \geq \|g(x_k + \alpha_k' d_k)\|^2 - J_k > \delta_1 \alpha_k'^2 g(x_k)^T d_k \end{aligned}$$

Which implies that

$$-\delta_1 \alpha_k'^2 g(x_k)^T d_k > \|g(x_k + \alpha_k' d_k)\|^2 - \|g_k\|^2 \quad (30)$$

By Taylor formula, (19), (20), and (17), we get

$$\begin{aligned} \|g(x_k + \alpha_k' d_k)\|^2 - \|g_k\|^2 &= -2\alpha_k' g_k^T \nabla g_k d_k \\ &+ O(\alpha_k'^2 \|d_k\|^2) \geq \alpha_k' (1-\varepsilon) \|g_k\|^2 + O(\alpha_k'^2 \|d_k\|^2) \\ &\geq \alpha_k' (1-\varepsilon) \frac{1}{b_2} \|d_k\|^2 + O(\alpha_k'^2 \|d_k\|^2) \end{aligned} \quad (31)$$

Using (15), (17), (30), and (31) we obtain

$$\begin{aligned} \alpha_k'^2 \left(2(1-\varepsilon) \frac{1}{b_2} + \delta_1 \frac{1}{b_1}\right) \|d_k\|^2 \\ = 2\alpha_k'^2 (1-\varepsilon) \frac{1}{b_2} \|d_k\|^2 + \alpha_k'^2 \delta_1 \frac{1}{b_1} \|d_k\|^2 \\ \geq 2\alpha_k'^2 (1-\varepsilon) \frac{1}{b_2} \|d_k\|^2 - \delta_1 \alpha_k'^2 g_k^T d_k \\ > \|g(x_k + \alpha_k' d_k)\|^2 - \|g_k\|^2 \\ \geq \alpha_k' (1-\varepsilon) \frac{1}{b_2} \|d_k\|^2 + O(\alpha_k'^2 \|d_k\|^2) \end{aligned} \quad (32)$$

which implies when  $k$  sufficiently large,

$$\alpha_k' \geq \frac{b_1(1-\varepsilon)}{2(1-\varepsilon)b_1 + b_2^2\delta_1}.$$

Let

$$b_0 \in \left(0, \frac{b_1(1-\varepsilon)}{2(1-\varepsilon)b_1 + b_2^2\delta_1}\right). \text{ The proof is complete.}$$

In the following, we give the global convergence theorem.

**Theorem 3.1.** Let  $\{\alpha_k, d_k, x_{k+1}, g_{k+1}\}$  be generated by Algorithm 1, Assumption A, B, and C hold, and  $\|g_k\|^2$  be bounded from below. Then

$$\liminf_{k \rightarrow \infty} \|g_k\| = 0 \quad (33)$$

Moreover, if  $\rho_2 < 1$ , then

$$\lim_{k \rightarrow \infty} \|g_k\| = 0 \quad (34)$$

Therefore, every convergent subsequence approaches to a point  $x^*$ , where  $g(x^*) = 0$ .

**Proof.** By (11), (15), (16), and (19), we have

$$\begin{aligned} \|g_{k+1}\|^2 &\leq J_k + \delta_1 \alpha_k d_k^T g_k \leq J_k - \alpha_k \delta_1 b_1 \|g_k\|^2 \\ &\leq J_k - b_0 \delta_1 b_1 \|g_k\|^2 \end{aligned} \quad (35)$$

Let  $\varsigma = \delta_1 b_0 b_1$ . Combining (12) and the upper bound of (35), we get

$$\begin{aligned} J_{k+1} &= \frac{\rho_k E_k J_k + \|g_{k+1}\|^2}{E_{k+1}} \leq \frac{\rho_k E_k J_k + J_k - \varsigma \|g_k\|^2}{E_{k+1}} \\ &\leq J_k - \frac{\varsigma \|g_{k+1}\|^2}{E_{k+1}} \end{aligned} \quad (36)$$

Since  $\|g_k\|^2$  is bounded from below and  $\|g_k\|^2 \leq J_k$  for all  $k$ , we can conclude that  $J_k$  is bounded from below. Then, using (36), we obtain

$$\sum_{k=0}^{\infty} \frac{\|g_k\|^2}{E_{k+1}} < \infty \quad (37)$$

By (23), we get

$$E_{k+1} < k + 2 \quad (38)$$

If  $\|g_k\|^2$  were bounded away from 0, then (37) would violate (38). Hence, (33) holds. If  $\rho_2 < 1$ , by (23), we have

$$\begin{aligned} E_{k+1} &= 1 + \sum_{j=0}^k \prod_{i=0}^j \rho_{k-i} \leq 1 + \sum_{j=0}^k \rho_2^{j+1} \\ &\leq \sum_{j=0}^k \rho_2 = \frac{1}{1-\rho_2} \end{aligned} \quad (39)$$

Then, (37) implies (34). The proof is complete.

## 4. Numerical Results

In this section, we report the results of some numerical experiments with the proposed method.

**Problem 1.** The discretized two-point boundary value problem is the same to the problem in [22]

$$g(x) = Ax + \frac{1}{(n+1)^2} F(x),$$

where  $A$  is the  $n \times n$  tridiagonal matrix given by

$$A = \begin{bmatrix} 4 & -1 & & & \\ -1 & 4 & -1 & & \\ & \ddots & \ddots & \ddots & \\ & & \ddots & \ddots & -1 \\ & & & -1 & 4 \end{bmatrix}$$

and  $F(x) = (F_1(x), F_2(x), \dots, F_n(x))^T$ , with  $F_i(x) = \sin x_i - 1$ ,  $i = 1, 2, \dots, n$ .

**Problem 2.** Unconstrained optimization problem  $\min f(x), x \in R^n$ , with Engval function [23] defined by

$$f(x) = \sum_{i=2}^n \left[ (x_{i-1}^2 + x_i^2)^2 - 4x_{i-1} + 3 \right]$$

The related symmetric nonlinear equation is

$$g(x) = \frac{1}{4} \nabla f(x)$$

where  $g(x) = (g_1(x), g_2(x), \dots, g_n(x))^T$  with

$$g_1(x) = x_1(x_1^2 + x_2^2) - 1$$

$$g_i(x) = x_i(x_{i-1}^2 + 2x_i^2 + x_{i+1}^2) - 1, i = 2, 3, \dots, n-1$$

$$g_n(x) = x_n(x_{n-1}^2 + x_n^2)$$

In the experiments, the parameters in Algorithm 1 were chosen as  $r = 0.1, \delta_1 = 0.001, \rho_k = 0.8, B_0$  is unit matrix. The program was coded in MATLAB 6.1. We stopped the iteration when the condition  $\|g(x)\|^2 \leq 10^{-6}$  was satisfied. **Tables 1** and **2** show the performance of the method need to solve the Problem 1. **Tables 3** and **4** show the performance of the method need to solve the Problem 2. The columns of the tables have the following meaning:

Dim: the dimension of the problem.

NI: the total number of iterations.

NG: the number of the function evaluations.

GG: the function evaluations.

From the above tabulars, we can see that the numerical

**Test Result for the Problem 1****Table 1. Small-scale.**

| $x_0$   | (4, ..., 4)       | (20, ..., 20)     | (100, ..., 100)   | (-4, ..., -4)     | (-20, ..., -20)   | (-100, ..., -100) |
|---------|-------------------|-------------------|-------------------|-------------------|-------------------|-------------------|
| Dim     | NI/NG/GG          | NI/NG/GG          | NI/NG/GG          | NI/NG/GG          | NI/NG/GG          | NI/NG/GG          |
| n = 10  | 16/22/3.714814e-7 | 16/20/2.650667e-7 | 16/20/4.014933e-7 | 16/22/3.723721e-7 | 16/20/2.643713e-7 | 16/20/4.013770e-7 |
| n = 50  | 44/47/1.388672e-7 | 44/47/6.929395e   | 46/49/3.713174e-8 | 44/47/1.388793e-7 | 44/47/6.929516e-7 | 46/49/3.726373e-8 |
| n = 100 | 68/71/5.905592e-7 | 70/73/8.759459e   | 72/75/3.125373e-7 | 68/71/5.905724e-7 | 70/73/8.759500e-7 | 72/75/3.125382e-7 |
| $x_0$   | (4, .0, ...)      | (20, 0, ..., 20)  | (100, .0, ...)    | (-4, .0, ...)     | (-20, .0, ...)    | (-100, .0, ...)   |
| Dim     | NI/NG/GG          | NI/NG/GG          | NI/NG/GG          | NI/NG/GG          | NI/NG/GG          | NI/NG/GG          |
| n = 10  | 21/23/1.297275e-9 | 21/23/5.577021e-9 | 1/23/9.029402e-9  | 1/23/1.208563e-9  | 1/23/4.707707e-9  | 21/23/1.061736e-8 |
| n = 50  | 63/65/8.204623e-7 | 67/69/9.997988e-7 | 9/71/4.511023e-7  | 3/65/8.204744e-7  | 7/69/9.997996e-7  | 69/71/4.511007e-7 |
| n = 100 | 65/67/6.046233e-7 | 69/71/7.845951e-7 | 1/73/6.996085e-7  | 65/67/6.046254e-7 | 9/71/7.845962e-7  | 71/73/6.996092e-7 |

**Table 2. Large-scale.**

| $x_0$   | (4, ..., 4)       | (20, ..., 20)     | (30, ..., 30)    | (-4, ..., -4)     | (-20, ..., -20)   | (-30, ..., -30)   |
|---------|-------------------|-------------------|------------------|-------------------|-------------------|-------------------|
| Dim     | NI/NG/GG          | NI/NG/GG          | NI/NG/GG         | NI/NG/GG          | NI/NG/GG          | NI/NG/GG          |
| n = 300 | 70/73/7.844778e-7 | 76/79/7.741702e-7 | 8/81/6.759628e-7 | 0/73/7.844800e-7  | 6/79/7.741706e-7  | 78/81/6.759631e-7 |
| n = 500 | 70/73/8.547195e-7 | 76/79/8.435874e-7 | 8/81/7.366072e-7 | 0/73/8.547204e-7  | 6/79/8.435876e-7  | 78/81/7.366073e-7 |
| n = 800 | 68/70/6.505423e-7 | 74/76/6.414077e-7 | 4/76/9.621120e-7 | 8/70/6.505425e-7  | 4/76/6.414078e-7  | 74/76/9.621120e-7 |
| $x_0$   | (4, .0, ...)      | (20, 0, ..., 20)  | (30, .0, ...)    | (-4, .0, ...)     | (-20, .0, ...)    | (-30, .0, ...)    |
| Dim     | NI/NG/GG          | NI/NG/GG          | NI/NG/GG         | NI/NG/GG          | NI/NG/GG          | NI/NG/GG          |
| n = 300 | 67/69/5.896038e-7 | 71/73/9.997625e-7 | 3/75/8.731533e-7 | 67/69/5.896038e-7 | 71/73/9.997625e-7 | 73/75/8.731533e-7 |
| n = 500 | 67/69/7.145027e-7 | 73/75/7.057076e-7 | 5/77/6.163480e-7 | 7/69/7.145024e-7  | 73/75/7.057075e-7 | 75/77/6.163479e-7 |
| n = 800 | 69/71/6.188110e-7 | 75/77/6.115054e-7 | 5/77/9.172559e-7 | 9/71/6.188106e-7  | 5/77/6.115053e-7  | 75/77/9.172558e-7 |

**Test Result for the Problem 2****Table 3. Small-scale.**

| $x_0$   | (1, ..., 1)       | (3, ..., 3)       | (4, ..., 4)        | (1, 0, ...)      | (3, 0, , ...)    | (4, 0, ...)       |
|---------|-------------------|-------------------|--------------------|------------------|------------------|-------------------|
| Dim     | NI/NG/GG          | NI/NG/GG          | NI/NG/GG           | NI/NG/GG         | NI/NG/GG         | NI/NG/GG          |
| n = 10  | 20/22/3.007469e-7 | 38/47/6.088293e-7 | 44/48/4.898591e-7  | 0/23/3.452856e-7 | 5/41/5.833715e-7 | 29/34/4.338894e-7 |
| n = 50  | 36/38/6.966974e-7 | 76/88/6.845101e-7 | 99/114/8.556270e-7 | 6/39/7.812438e-7 | 9/77/4.466497e-7 | 67/75/4.681269e-7 |
| n = 100 | 36/38/7.207203e-7 | 6/109/4.173166e-7 | 0/87/7.911692e-7   | 6/39/8.220367e-7 | 9/92/8.640158e-7 | 69/76/8.515673e-7 |

Table 4. Large-scale.

| $x_0$   | (1, ..., 1)       | (3, ..., 3)       | (4, ..., 4)        | (1, 0, ...)      | (3, 0, ...)      | (4, 0, ...)        |
|---------|-------------------|-------------------|--------------------|------------------|------------------|--------------------|
| Dim     | NI/NG/GG          | NI/NG/GG          | NI/NG/GG           | NI/NG/GG         | NI/NG/GG         | NI/NG/GG           |
| n = 300 | 40/42/4.452904e-7 | 4/106/6.146797e-7 | 63/68/4.232021e-7  | 0/43/9.348673e-7 | 6/72/7.638011e-7 | 92/106/9.095927e-7 |
| n = 500 | 44/46/9.611950e-7 | 9/171/4.445314e-7 | 18/133/7.054347e-7 | 2/45/8.280486e-7 | 3/79/7.159029e-7 | 85/98/4.229872e-7  |
| n = 800 | 41/43/4.510999e-7 | 7/185/5.274922e-7 | 74/198/4.239839e-7 | 1/44/9.502624e-7 | 2/77/6.117626e-7 | 93/106/8.797380e-7 |

results are quite well for the test Problems with the proposed method. The initial points and the dimension don't influence the performance of the algorithm 1 very much. However, we find the started points will influence the result for the problem 2 a little in our experiment. In one word, the numerical are attractively. The method can be used to the system of nonlinear equations whose Jacobian is not symmetric.

## 5. Conclusions

In this paper, we propose a new nonmonotone line search method for symmetric nonlinear equations. The global convergence is proved and the numerical results show that this technique is interesting. The reason is that the new nonmonotone line search algorithm used fewer function and gradient evaluations, on average, than either the monotone or the traditional nonmonotone scheme. We hope the method will be a further topic for symmetric nonlinear equations.

## 6. Acknowledgements

We would like to thank these referees for giving us many valuable suggestions and comments that improve this paper greatly.

## 7. References

- [1] D. Li and M. Fukushima, "A Global And Superlinear Convergent Gauss-Newton-based BFGS Method for Symmetric Nonlinear Equations," *SIAM Journal on Numerical Analysis*, Vol. 37, No. 1, 1999, pp. 152-172.
- [2] Z. Wei, G. Yuan and Z. Lian, "An Approximate Gauss-Newton-Based BFGS Method for Solving Symmetric Nonlinear Equations," *Guangxi Sciences*, Vol. 11, No. 2, 2004, pp. 91-99.
- [3] G. Yuan and X. Li, "An Approximate Gauss-Newton-based BFGS Method with Descent Directions for Solving Symmetric Nonlinear Equations," *OR Transactions*, Vol. 8, No. 4, 2004, pp. 10-26.
- [4] P. N. Brown and Y. Saad, "Convergence Theory of Nonlinear Newton-Krylov Algorithms," *SIAM Journal on Optimization*, Vol. 4, 1994, pp. 297-330.
- [5] D. Zhu, "Nonmonotone Backtracking Inexact Quasi-Newton Algorithms for Solving Smooth Nonlinear Equations," *Applied Mathematics and Computation*, Vol. 161, No. 3, 2005, pp. 875-895.
- [6] G. Yuan and X. Lu, "A New Backtracking Inexact BFGS Method for Symmetric Nonlinear Equations," *Computers and Mathematics with Applications*, Vol. 55, No. 1, 2008, pp. 116-129.
- [7] S. G. Nash, "A Survey of Truncated-Newton Methods," *Journal of Computational and Applied Mathematics*, Vol. 124, No. 1-2, 2000, pp. 45-59.
- [8] A. Griewank, "The 'Global' Convergence of Broyden-Like Methods with a Suitable Line Search," *Journal of the Australian Mathematical Society Series B*, Vol. 28, No. 1, 1986, pp. 75-92.
- [9] A. R. Conn, N. I. M. Gould and P. L. Toint, "Trust Region Method," Society for Industrial and Applied Mathematics, Philadelphia, 2000.
- [10] J. E. Dennis and R. B. Schnabel, "Numerical Methods for Unconstrained Optimization and Nonlinear Equations," Englewood Cliffs, Prentice-Hall, 1983.
- [11] K. Levenberg, "A Method for The Solution of Certain Nonlinear Problem in Least Squares," *Quarterly of Applied Mathematics*, Vol. 2, 1944, pp. 164-166.
- [12] D. W. Marquardt, An algorithm for least-squares estimation of nonlinear inequalities, *SIAM Journal on Applied Mathematics*, Vol. 11, 1963, pp. 431-441.
- [13] J. Nocedal and S. J. Wright, "Numerical Optimization," Springer, New York, 1999.
- [14] N. Yamashita and M. Fukushima, "On the Rate of Convergence of the Levenberg-Marquardt Method," *Computing*, Vol. 15, No. Suppl, 2001, pp. 239-249.
- [15] Y. Yuan and W. Sun, "Optimization Theory and Algorithm," Scientific Publisher House, Beijing, 1997.
- [16] G. Yuan and X. Li, "A Rank-One Fitting Method for Solving Symmetric Nonlinear Equations," *Journal of Applied Functional Analysis*, Vol. 5, No. 4, 2010, pp. 389-407.
- [17] G. Yuan, X. Lu and Z. Wei, "BFGS Trust-Region Method for Symmetric Nonlinear Equations," *Journal of Computational and Applied Mathematics*, Vol. 230, No. 1, 2009, pp. 44-58.

- [18] G. Yuan, S. Meng and Z. Wei, "A Trust-Region-Based BFGS Method with Line Search Technique for Symmetric Nonlinear Equations," *Advances in Operations Research*, Vol. 2009, 2009, pp. 1-20.
- [19] G. Yuan, Z. Wang and Z. Wei, "A Rank-One Fitting Method with Descent Direction for Solving Symmetric Nonlinear Equations," *International Journal of Communications, Network and System Sciences*, Vol. 2, No. 6, 2009, pp. 555-561.
- [20] G. Yuan, Z. Wei and X. Lu, "A Nonmonotone Trust Region Method for Solving Symmetric Nonlinear Equations," *Chinese Quarterly Journal of Mathematics*, Vol. 24, No. 4, 2009, pp. 574-584.
- [21] H. Zhang and W. Hager, "A Nonmonotone Line Search Technique and Its Application to Unconstrained Optimization," *SIAM Journal on Optimization*, Vol. 14, No. 4, 2004, pp. 1043-1056.
- [22] J. M. Ortega and W. C. Rheinboldt, "Iterative Solution of Nonlinear Equations in Several Variables," Academic Press, New York, 1970.
- [23] E. Yamakawa and M. Fukushima, "Testing Parallel Bariable Transformation," *Computational Optimization and Applications*, Vol. 13, 1999, pp. 253-274.

# Stability Analysis and Hadamard Synergic Control for a Class of Dynamical Networks\*

Xinjin Liu, Yun Zou

*School of Automation, Nanjing University of Science and Technology, Nanjing, China*

*E-mail: liuxinjin2006@163.com, zouyun@vip.163.com*

*Received February 9, 2010; revised March 21, 2010; accepted June 28, 2010*

## Abstract

Hadamard synergic control is a new kind of control problem which is achieved via a composite strategy of the state feedback control and the direct regulation of the part of connection coefficients of system state variables. Such a control is actually used very often in the practical areas. In this paper, we discuss Hadamard synergic stabilization problem for a class of dynamical networks. We analyze three cases: 1) Synergic stabilization problem for the general two-node-network. 2) Synergic stabilization problem for a special kind of networks. 3) Synergic stabilization problem for special kind of networks with communication time-delays. The mechanism of the synergic action between two control strategies: feedback control and the connection coefficients regulations are presented.

**Keywords:** Hadamard Synergic Control, Algebraically Graph Theory, Decentralized Feedback Control, Connection Coefficient Gain Matrix

## 1. Introduction

Complex networks of dynamic agents have attracted great interesting in recently years. This is partly due to broad applications of multiagent systems in many areas including physicists, biologists, social scientists and control scientists [1-3], distributed sensor networks [4], and congestion control in communication networks [5] and so on. In fact, a complex dynamical network can be viewed as a large-scale system with special interconnections among its dynamical nodes from a system-theoretic point of view and when we solved the control problems of electric power systems, socioeconomic systems, etc., large-scale interconnected systems with many state variables often appear. In order to stabilize large-scale interconnected systems via the local feedback, the traditional methods usually ignore or try to reduce the influence of interconnections under the condition that the subsystems are controllable. The interconnections among subsystems in large-scale systems are thought to be one of the most important roots to produce complexity recently [6]. To enhance the effects of stabilization, the strategy of coupling two decoupled subsystems via designing a suitable combined feedback are considered in [7,8], which is

called the harmonic control.

Along the development of society, interconnections play more and more important roles in social systems, economic systems, power systems, etc. The connections of the system states are a type of the most important structures of a system. In fact, in many fields and even in our daily life, besides the usual feedback controls, it is also very useful for us to control our business by regulating the connections among the subsystems directly. For examples, the damages in power and transportation ties is one of the main facts to result in the huge loss in the freeze disaster in several provinces in southern China in 2008, and reflects the effects of the connections of the subsystems for the social large-scale system; the strict and active quarantine and isolation measures among regions in the SARS and H1N1 is also an example. In fact, in our daily life, we always deal with the interpersonal relationship between ourselves and those around us and the inter-relations between ourselves and the collective around us. Therefore, we can say that the human world is a complex network system through these relationships, and the handling of these relationships is actually the regulation of the connection among persons.

The consideration of the connection problem were mainly seen in the power system research early times, including the transient stability analysis [9] and splitting control [10-12]. The interconnection coefficients of the

\*This work was supported in part by the National Natural Science Foundation of P. R. China under Grant 60874007 and the Research Fund for the Doctoral Program of Higher Education 200802550024.

state variables of the subsystems are considered as the control variables that are regulated directly in the splitting control for power system. Furthermore, the isolation treatment strategy is further discussed in the emergency control [13-15]. The studies give a theoretical interpretation for the practical experiences that the early quarantine and isolation strategies are critically important to control the outbreaks of epidemics. Finally, a new kind of concept called Hadamard synergic control is introduced based on the Hadamard matrix product [16]. It is achieved via a composite strategy of the state feedback control and the direct regulation of the part of connection coefficients of system state variables. Such a control improves the limitations of the traditional feedback control [17-19] and may be of some potential applications in the emergency treatment such as isolation and obstruction control. For clear, we give this model again here.

Consider the following linear time-invariant system:

$$\dot{x}(t) = Ax(t) + Bu(t) \quad (1)$$

Here,  $A = [a_{ij}]_{n \times n}$ ,  $B = [b_i]^T$ ,  $b_i \in R^m$ ,  $i = 1, 2, \dots, n$

Obviously, the element  $a_{ij}$  is the interconnection coefficient between the  $i$ -th state and the  $j$ -th state, for convenience, we call the system matrix  $A$  as system interconnection matrix. In many practical cases, such as the switches and circuit breakers in the power systems, firewall in the Internet etc., the system interconnection matrix  $A$  can be directly regulated, of course, can be pre-designed in some extent. Thus, the system interconnection matrix  $A$  can be divided into two parts:  $A_1 + A_2$ .  $A_1$  is the fixed part of  $A$  which is not able to be regulated directly and  $A_2$  is the flexible part of  $A$  which can be regulated directly in some extent. By using the Hadamard matrix product, this direct regulation of the interconnection matrix  $A$  can be written as follows:

$$A_K = A_1 + A_2 \circ K \quad (2)$$

Here, for convenience, we call  $K = [k_{ij}]_{n \times n}$  as the connection coefficient gain matrix. It may be need to satisfy some constraints such as  $0 \leq k_{ij} \leq 1$  etc. Of course, the control strategy above is different from the feedback control.  $A_2 \circ K$  is the Hadamard matrix product defined as [20]:

$$A_2 \circ K = [\tilde{a}_{ij} k_{ij}]_{n \times n}, A_2 = [\tilde{a}_{ij}]_{n \times n}$$

Then, the general feedback control problem formulation can be extended as follows: find direct connection coefficient gain matrix  $K$  and feedback gain matrix  $F$  such that the generalized closed loop system

$$\dot{x} = (A_1 + A_2 \circ K + BF)x \quad (3)$$

is stable, robust stable, or some other specific perform-

ances. For convenience, we call this kind of control strategy as Hadamard synergic control.

In order to illustrate the idea of isolation and obstruction of the connections among subsystems, we give the following examples [21].

**Example 1.** Replacing the scalars  $a_{ij}, b_i, f_j, k_{ij}$  by matrices  $A_{ij}, B_i, F_j, k_{ij} E_{ij}$  with appropriate dimensions and the self-loops are not allowed, the general Hadamard synergic control model (3) can be rewritten as:

$$\begin{aligned} \dot{x}_1 &= A_{11}x_1 + k_{12}A_{12}x_2 + \dots + k_{1n}A_{1n}x_n + B_{11}u_1 \\ \dot{x}_2 &= A_{22}x_2 + k_{21}A_{21}x_1 + \dots + k_{2n}A_{2n}x_n + B_{22}u_2 \\ &\dots\dots\dots \\ \dot{x}_n &= A_{nn}x_n + k_{n1}A_{n1}x_1 + \dots + k_{n,m-1}A_{n,m-1}x_{n-1} + B_{nn}u_n \end{aligned}$$

where  $x_i \in R^{n_i}$ ,  $i = 1, 2, \dots, n$  is the local state of the  $i$ -th subsystem.  $k_{ij}$  are the control variables. System model above can be rewritten as:

$$\dot{x} = (A_1 + A_2 \circ K)x + Bu \quad (4)$$

Here,

$$A_1 = \begin{bmatrix} A_{11} & & & \\ & \ddots & & \\ & & A_{mm} & \\ & & & \end{bmatrix}, A_2 = \begin{bmatrix} 0 & A_{12} & \dots & A_{1n} \\ A_{21} & 0 & \dots & A_{2n} \\ \vdots & \vdots & \ddots & \vdots \\ A_{n1} & A_{n2} & \dots & 0 \end{bmatrix}$$

$$B = \begin{bmatrix} B_{11} & & & \\ & \ddots & & \\ & & B_{mm} & \\ & & & \end{bmatrix}, K = \begin{bmatrix} 0 & k_{12}E_{12} & \dots & k_{1n}E_{1n} \\ k_{21}E_{21} & 0 & \dots & k_{2n}E_{2n} \\ \vdots & \vdots & \ddots & \vdots \\ k_{n1}E_{n1} & k_{n2}E_{n2} & \dots & 0 \end{bmatrix}$$

$$E_{ij} = [1]_{n_i \times n_j}$$

In power systems, the model (4) can be used to describe the frequency control in multi-areas loads with the balance of active powers among the networks of different areas.

**Example 2.** Consider the network model researched in [1,3], in fact, the system interconnection matrix  $A$  is divided into two parts. By the Kronecker product, this network model can be written as [22]:

$$\dot{x} = (I_n \otimes A_O + C \otimes A_C)x + (I_n \otimes B_1)u \quad (5)$$

where  $x = (x_1^T, x_2^T, \dots, x_n^T)^T$ ,  $u = (u_1^T, u_2^T, \dots, u_n^T)^T$ ,  $C \in R^{n \times n}$  is called as the outer coupling matrix,  $A_C$  is the inner coupling matrix describing the interconnections.

Obviously, the network model (5) is a special case of the model (4). From the definition of the matrix Kronecker product we know, the connection matrix of the system has very symmetrically consistency structure if we describe the system by using the corresponding Hadamard product, this is: any two subsystems have the same basic

connection structure except the coupling coefficient, *i.e.*

$$A_{ij} = \begin{cases} A_O & i = j = 1, 2, \dots, n \\ A_C & 1 \leq i \neq j \leq n \end{cases}$$

$$B_{11} = B_{22} = \dots = B_{nn}$$

Network model (5) has very specific project background such as in the consensus and formation control problem. This also illustrates the rationality and generality of the abstract model (4).

**Example 3.** The host population consists of six sub populations: namely susceptible individuals  $x_1(t)$ , asymptomatic individuals  $x_2(t)$ , quarantined individuals  $x_3(t)$ , symptomatic individuals  $x_4(t)$ , isolated individuals  $x_5(t)$ , recovered individuals  $x_6(t)$ . The total population size is  $N = \sum_{i=1}^6 x_i(t)$ . The detailed descriptions of other parameters see [23]. The SARS transmission model with quarantine and isolation controls  $u$  and  $v$  is given by the following nonlinear system of differential equations:

$$\begin{aligned} \dot{x}_1 &= \Pi - \frac{\beta x_4 + \xi_E \beta x_2 + \xi_Q \beta x_3 + \xi_I \beta x_5}{N} - \mu x_1 \\ \dot{x}_2 &= p + \frac{\beta x_4 + \xi_E \beta x_2 + \xi_Q \beta x_3 + \xi_I \beta x_5}{N} - (k_1 + \mu - u)x_2 \\ \dot{x}_3 &= ux_2 - (k_2 + \mu)x_3 \\ \dot{x}_4 &= k_1 x_2 - (d_1 + \delta_1 + \mu)x_4 - vx_4 \\ \dot{x}_5 &= vx_4 - k_2 x_3 - (d_2 + \delta_2 + \mu)x_5 \\ \dot{x}_6 &= \delta_1 x_4 + \delta_2 x_5 - \mu x_6 \end{aligned}$$

Obviously, the model above is a typical interconnection-regulation control of a nonlinear system with the control variables  $u$  and  $v$  (see **Figure 1**).

Hadamard product is a classical matrix product. It has many applications in some areas especially in mathematics and physics. It also has some applications in signal processing [24]. In the existing literatures, almost all the results about the eigenvalue estimations on Hadamard products were obtained under the presupposition that the involved matrices are special ones such as M-matrices, Hermitian (or the form of  $A^*A$ ), diagonal matrices, etc. See [25-29] and the other corresponding references. Also, the discussions on the mixture products like  $A(B \circ C)$  are scarcely reported. Hence, the basic properties and expressions on Hadamard product still remain to be extensively studied.

Although almost all the existing control theory and applications are implemented by feedback controls, the feedback is, in a general sense, only one of the specific measures to implement the regulations of the connections of system states.

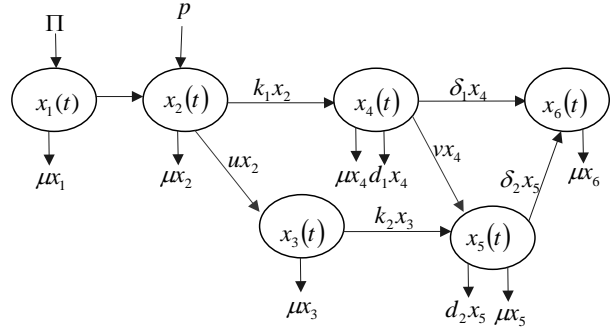


**Figure 1.** A schematic representation of the populations flow.

Let the feedback law be  $u = Fx$ ,  $F = [f_j] \in R^{m \times n}$ ,  $f_j \in R^m$ ,  $j = 1, 2, \dots, n$ . Then the system matrix of the closed loop is of the form:  $A = [a_{ij} + b_i^T f_j]_{n \times n}$ . The actual functions of the feedback are the compensations of  $a_{ij}$ , *i.e.*, regulating the interconnection coefficients from  $a_{ij}$  to  $a_{ij} + b_i^T f_j$  via the input information channel. Hence, in an open-loop viewpoint, the feedback control is just a special indirect regulation of interconnections of system states.

The observation above show that the feedback control strategy is only one of the specific measures to implement the regulations of the connections of system states via the input information channel, rather than the direct physical regulation of the system interconnection matrix  $A$ .

In this paper, we mainly discuss the Hadamard synergic stabilization problem for the general two-node-network (4), and then Hadamard synergic stabilization problem for the special model (5) is studied. Matrix algebra and algebraic graph theory are proved useful tools in modeling the communication network and relating its topology to the discussion of the network stability.

The rest of this paper is organized as follows. System models and problem formulation discussed in this paper are given in Section 2. Hadamard synergic stabilization problem for the general two-node-network (4) is studied in Section 3. In Section 4, Hadamard synergic stabilization problem for the special network model (5) is discussed. Furthermore, networks with communication time-delays are investigated. The last section concludes the paper.

## 2. System Models and Problem Formulation

In this section, we give the system models and problem formulation discussed in this paper.

Because of the existence of the Hadamard product,

this makes that the stability analysis of the general network model (4) become difficult. Therefore, we mainly consider the Hadamard synergic control problem for the special model (5). Furthermore, Hadamard synergic control for the two-node-network model of the general network system (4) is investigated simply. For convenience, the network model (5) can be rewritten as:

$$\dot{x} = (I_n \otimes A_O + K \otimes A_C)x + (I_n \otimes B_1)u \quad (6)$$

$K = [k_{ij}]_{n \times n}$  is the connection coefficient gain matrix.

In the general case, the control variables  $k_{ij}$  often need to satisfy some constraints. There exist the following cases being researched.

**Case 1:**  $k_{ij}$  is discrete. For example  $k_{ij} = 0, 1$ . When  $k_{ij} = 0$ , it means that we cut off the connections from the  $j$ -th subsystem to the  $i$ -th subsystem; When  $k_{ij} = 1$ , it means that we keep the corresponding connections. In this case, the control is called the isolation treatment strategy. In fact, this kind of control strategy has been researched in many literatures [15] especially in the power electrical engineering [10-12].

**Case 2:**  $k_{ij}$  is continuous. It often needs to meet some constraints. For example,  $0 \leq k_{ij} \leq 1$  in the epidemic control [13,14,25];  $k_{ii} = -\sum_{j \neq i}^n k_{ij}$  in the consensus or formation control problem [30,31], etc.

Although the control variables  $k_{ij}$  often need to satisfy some constraints, as the stability research in the classical feedback control of the system (1) required to unconstrained control  $u(t)$  we also suppose that the connection coefficient  $k_{ij} \in R$  in this paper.

We present the formulations of the Hadamard synergic stabilization problems as follows:

**Hadamard synergic stabilization problem (HSSP) [21]:** Given system (1), and let  $A + A_1 + A_2$ . Find connection coefficient gain matrix  $K \subseteq R^{n \times n}$  and feedback control  $u = Fx$  such that the corresponding Hadamard synergic closed loop (3) is stable, *i.e.*

$$\lambda(A_1 + A_2 \circ K + BF) \subset C^-$$

where  $\lambda(\cdot)$  represents the set of eigenvalues of the corresponding matrix,  $C^-$  means the left-half complex plane. For convenience, we call the matrix pair  $(K, F)$  as the synergic control matrix pair.

**Remark 1.** Obviously, the HSSP is equivalent to the problem that is to find connection coefficient gain matrix  $K$  such that  $(A_1 + A_2 \circ K, B)$  is stabilizable. One of the stronger conditions of it is to find a matrix  $K$  such that  $(A_1 + A_2 \circ K, B)$  is completely controllable. Also, for

convenience, we call these two problems as Hadamard synergic stabilization and Hadamard synergic Controllability problems respectively.

In this paper, we mainly consider the Hadamard synergic stabilization problem for the two cases:

**Case 1:** The two-node-network model of the general network system (4).

**Case 2:** The special network model (6).

### 3. Hadamard Synergic Stabilization for the General Two-Node-Network

In this section, we consider the Hadamard synergic Stabilization problem for the general dynamical network model (4). We mainly consider the two-node-network described as:

$$\begin{aligned} \dot{x}_1 &= A_{11}x_1 + \alpha_{12}A_{12}x_2 + B_{11}u_1 \\ \dot{x}_2 &= A_{22}x_2 + \alpha_{21}A_{21}x_1 + B_{22}u_2 \end{aligned} \quad (7)$$

Then, the Hadamard synergic stabilization problem for the network model (7) can be presented as: find connection coefficients  $\alpha_{12}, \alpha_{21} \in R$  and decentralized feedback control  $u_1 = F_1x_1, u_2 = F_2x_2$  such that the closed loop matrix

$$A_{loop}(2) = \begin{bmatrix} A_{11} + B_{11}F_1 & \alpha_{12}A_{12} \\ \alpha_{21}A_{21} & A_{22} + B_{22}F_2 \end{bmatrix}$$

is stable.

When  $\alpha_{12} = 0$  or  $\alpha_{21} = 0$ , the stability of  $A_{loop}(2)$  is equal to the stability of the two subsystems, so we do not consider this condition. In the following, we suppose that  $\alpha_{12} \neq 0, \alpha_{21} \neq 0$ .

#### 3.1. Case of $\text{rank}(A_{12}) = \text{rank}(A_{21}) = 1$

In this section, we discuss the Hadamard synergic stabilization problem of the network model (7) with the special case  $\text{rank}(A_{12}) = \text{rank}(A_{21}) = 1$ .

Based on the theorem of the Linear Algebra, let  $A_{12} = a_1b_2^T, A_{21} = a_2b_1^T, a_1, b_1, a_2, b_2 \in R^n$ . Then, the system (7) without local input can be rewritten as:

$$\begin{aligned} \dot{x}_1 &= A_{11}x_1 + \alpha_{12}a_1b_2^T x_2 \\ \dot{x}_2 &= A_{22}x_2 + \alpha_{21}a_2b_1^T x_1 \end{aligned} \quad (8)$$

Note that system above is equivalent to the following system:

$$\begin{aligned} \dot{x}_1 &= A_{11}x_1 + \alpha_{12}a_1y_2 & y_1 &= b_1^T x_1 \\ \dot{x}_2 &= A_{22}x_2 + \alpha_{21}a_2y_1 & y_2 &= b_2^T x_2 \end{aligned}$$

Let  $\tilde{u}_1 = y_2, \tilde{u}_2 = y_1$  are the inputs of the intercon-

nected control;  $y_1, y_2$  are the outputs of the first and second subsystem respectively. Then  $\alpha_{12}a_1, \alpha_{21}a_2$  can be viewed as the matrix of the first and second subsystem accepting the interconnected control respectively. Hence, let

$$H_1(s) = \alpha_{12}b_1^T (sI - A_{11})^{-1} a_1$$

$$H_2(s) = \alpha_{12}b_2^T (sI - A_{22})^{-1} a_2$$

Then, the matrix  $A(2) = \begin{bmatrix} A_{11} & \alpha_{12}A_{12} \\ \alpha_{21}A_{21} & A_{22} \end{bmatrix}$  can be viewed as the state matrix of the closed-loop feedback system as shown in **Figure 2**.

**Theorem 1.** There exist  $\alpha_{12}, \alpha_{21} \in R$  such that the matrix  $A(2)$  is stable if and only if there exist  $\alpha_{12}, \alpha_{21} \in R$  such that the polynomial  $f(s) = d_1(s)d_2(s) - \alpha_{12}\alpha_{21}f_1(s)f_2(s)$  is stable. In this case, the matrices  $A_{12}, A_{21}$  must satisfy that  $\text{tr}(A_{12}) + \text{tr}(A_{21}) < 0$ .

Here,

$$d_1(s) = \det(sI - A_{11}), \quad f_1(s) = b_1^T (sI - A_{11})^* a_1$$

$$d_2(s) = \det(sI - A_{22}), \quad f_2(s) = b_2^T (sI - A_{22})^* a_2$$

$\text{tr}(\cdot), (\cdot)^*$  denote the trace and adjoints of the corresponding matrix respectively.

**Proof.** From the analysis above we know that  $A(2)$  is stable if and only if the feedback system shown in **Figure 2** is stable, where the closed loop transfer function in **Figure 2** is

$$H(s) = \frac{H_1(s)}{1 - H_1(s)H_2(s)}$$

$$= \frac{\det(sI - A_{11})b_2^T (sI - A_{22})^* a_2}{d_1(s)d_2(s) - \alpha_{12}\alpha_{21}f_1(s)f_2(s)}$$

Therefore,  $A(2)$  is stable if and only if the polynomial  $d(s)$  is stable. Let  $A_{11} \in R^{n_1 \times n_1}, A_{22} \in R^{n_2 \times n_2}$ . Then, note that  $d(s)$  and  $f_1(s)f_2(s)$  are the polynomials with degree  $n_1 + n_2$  and  $n_1 + n_2 - 2$  respectively. Hence, if we let  $d(s) = s^{n_1+n_2} - cs^{n_1+n_2-1} + d_0(s)$ , then we have that  $c = \text{tr}(A_{12}) + \text{tr}(A_{21}) < 0$ . This completes the proof.

**Remark 2.** When  $\text{rank}(M) = 1$ , there exist vectors  $a, b \in R^n$  such that  $M = ab^T$  and the different decompositions are unique up to a constant, so the result above is independent of the decompositions of the coupled matrices  $A_{12}, A_{21}$ . The results above can be generalized to cases of multiple subsystems simply.

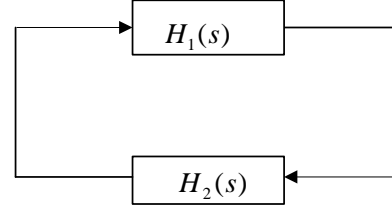


**Figure 2.** The closed loop of the system (8).

### 3.2. Case of $\text{rank}(A_{12}) \geq 1, \text{rank}(A_{21}) \geq 1$

In this section, we discuss the Hadamard synergic stabilization problem of the network model (7) with the general case  $\text{rank}(A_{12}) \geq 1, \text{rank}(A_{21}) \geq 1$  by using the small gain theorem.

Decompose  $A_{12} = B_1C_2, A_{21} = B_2C_1$ , then  $\alpha_{12}A_{12} = (\alpha_{12}B_1)C_2, \alpha_{21}A_{21} = (\alpha_{21}B_2)C_1$ . Let

$$H_1(s) = C_1 (sI - A_{11})^{-1} (\alpha_{12}B_1)$$

$$H_2(s) = C_2 (sI - A_{22})^{-1} (\alpha_{21}B_2)$$

Similarly as in the section 3.1, the matrix  $A(2)$  can be viewed as the state matrix of the closed-loop feedback system as shown in **Figure 2**. In this way,  $A_{loop}(2)$  can be viewed as an interconnected system composing of two subsystems  $(A_{11}, \alpha_{12}B_1, C_1), (A_{22}, \alpha_{21}B_2, C_2)$  under the local feedback.

Using the small gain theorem, we can get the following result.

**Proposition 1.** If there exist  $\alpha_{12}, \alpha_{21}, F_1, F_2$  such that

$$\left\| C_1 (sI - A_{11} - B_{11}F_1)^{-1} (\alpha_{12}B_1) \right\|_{\infty}$$

$$\times \left\| C_2 (sI - A_{22} - B_{22}F_2)^{-1} (\alpha_{21}B_2) \right\|_{\infty} < 1 \quad (9)$$

then the system (7) can be stabilized by the synergic control.

In the following, we suppose that

$$\alpha_{12} \in [\beta_1, \gamma_1], \quad \alpha_{21} \in [\beta_2, \gamma_2],$$

$$\gamma_1 > \beta_1 > 0, \quad \gamma_2 > \beta_2 > 0 \quad (10)$$

**Remark 3.** Based on the Proposition 1, we know that if there exist  $\alpha_{12}, \alpha_{21}$  such that

$$\left\| C_1 (sI - A_{11})^{-1} (\alpha_{12}B_1) \right\|_{\infty}$$

$$\times \left\| C_2 (sI - A_{22})^{-1} (\alpha_{21}B_2) \right\|_{\infty} < 1 \quad (11)$$

then  $A(2)$  is stable. Obviously, there exist  $\alpha_{12}, \alpha_{21}$  as in (10) such that (11) holds if and only if

$$\begin{aligned} & \left\| C_1 (sI - A_{11})^{-1} (B_1) \right\|_{\infty} \\ & \times \left\| C_2 (sI - A_{22})^{-1} (B_2) \right\|_{\infty} < \frac{1}{\beta_1 \beta_2} \end{aligned} \quad (12)$$

But the decompositions of  $A_{12}, A_{21}$  are general not unique.

In the following, we give the suitable decompositions and the explain (12) by LMI method by using the result in [32].

**Theorem 2.** For any fixed full rank decompositions  $A_{12} = B_1^0 C_2^0, A_{21} = B_2^0 C_1^0$ , there exist connection coefficients  $\alpha_{12}, \alpha_{21}$  as in (10) and decompositions  $A_{12} = B_1 C_2, A_{21} = B_2 C_1$  such that (11) holds if and only if there exist positive matrices  $P_1, P_2, X, Y$  such that

$$\begin{aligned} & \begin{bmatrix} P_1 A_{11} + A_{11}^T P_1 + B_1^0 X B_1^{0T} & P_1 C_1^{0T} \\ C_1^0 P_1 & -\frac{1}{\beta_2^2} Y \end{bmatrix} < 0 \\ & \begin{bmatrix} P_2 A_{22} + A_{22}^T P_2 + B_2^0 Y B_2^{0T} & P_2 C_2^{0T} \\ C_2^0 P_2 & -\frac{1}{\beta_1^2} X \end{bmatrix} < 0 \end{aligned} \quad (13)$$

**Proof.** Based on the result in [32], we know for any fixed full rank decompositions  $A_{12} = B_1^0 C_2^0, A_{21} = B_2^0 C_1^0$ , there exist connection coefficients  $\alpha_{12}, \alpha_{21}$  and decompositions  $A_{12} = B_1 C_2, A_{21} = B_2 C_1$  such that (11) holds if and only if there exist positive matrices  $P_1, P_2, \tilde{X}, \tilde{Y}$  such that

$$\begin{aligned} & \begin{bmatrix} P_1 A_{11} + A_{11}^T P_1 + \alpha_{12}^2 B_1^0 X B_1^{0T} & P_1 C_1^{0T} \\ C_1^0 P_1 & -\tilde{Y} \end{bmatrix} < 0 \\ & \begin{bmatrix} P_2 A_{22} + A_{22}^T P_2 + \alpha_{21}^2 B_2^0 Y B_2^{0T} & P_2 C_2^{0T} \\ C_2^0 P_2 & -\tilde{X} \end{bmatrix} < 0 \end{aligned}$$

Let  $X = \alpha_{12}^2 \tilde{X}, Y = \alpha_{21}^2 \tilde{Y}$ , then the inequalities above can translate into

$$\begin{aligned} & \begin{bmatrix} P_1 A_{11} + A_{11}^T P_1 + B_1^0 X B_1^{0T} & P_1 C_1^{0T} \\ C_1^0 P_1 & -\frac{1}{\alpha_{21}^2} Y \end{bmatrix} < 0 \\ & \begin{bmatrix} P_2 A_{22} + A_{22}^T P_2 + B_2^0 Y B_2^{0T} & P_2 C_2^{0T} \\ C_2^0 P_2 & -\frac{1}{\alpha_{12}^2} X \end{bmatrix} < 0 \end{aligned}$$

If there exist positive matrices  $P_1, P_2, X, Y$  such that (13) holds, and we can choose connection coefficient  $\alpha_{12} = \beta_1, \alpha_{21} = \beta_2$  such that (11) holds.

Conversely, if there exist connection coefficients  $\alpha_{12}, \alpha_{21}$  as in (10) such that (11) holds, then we can get:

$$\begin{aligned} & \begin{bmatrix} P_1 A_{11} + A_{11}^T P_1 + B_1^0 X B_1^{0T} & P_1 C_1^{0T} \\ C_1^0 P_1 & -\frac{1}{\alpha_{21}^2} Y \end{bmatrix} < 0 \\ & \begin{bmatrix} P_2 A_{22} + A_{22}^T P_2 + B_2^0 Y B_2^{0T} & P_2 C_2^{0T} \\ C_2^0 P_2 & -\frac{1}{\alpha_{12}^2} X \end{bmatrix} < 0 \end{aligned}$$

By using Schur complement, we know that the inequalities above are equal to:

$$\begin{cases} Y > 0 \\ P_1 A_{11} + A_{11}^T P_1 + B_1^0 X B_1^{0T} + \alpha_{12}^2 C_1^0 P_1 Y^{-1} P_1 C_1^{0T} < 0 \\ X > 0 \\ P_2 A_{22} + A_{22}^T P_2 + B_2^0 Y B_2^{0T} + \alpha_{21}^2 C_2^0 P_2 X^{-1} P_2 C_2^{0T} < 0 \end{cases}$$

Since  $0 < \beta_1 \leq \alpha_{12}, 0 < \beta_2 \leq \alpha_{21}$ , thus  $0 < \beta_1^2 \leq \alpha_{12}^2, 0 < \beta_2^2 \leq \alpha_{21}^2$ , so we have

$$\begin{aligned} & P_1 A_{11} + A_{11}^T P_1 + B_1^0 X B_1^{0T} + \beta_1^2 C_1^0 P_1 Y^{-1} P_1 C_1^{0T} < 0 \\ & P_2 A_{22} + A_{22}^T P_2 + B_2^0 Y B_2^{0T} + \beta_2^2 C_2^0 P_2 X^{-1} P_2 C_2^{0T} < 0 \end{aligned}$$

use Schur complement, then (13) holds. This completes the proof.

**Remark 4.** From the Theorem above, we know that we only need to consider full rank decompositions among the different decompositions of  $A_{12}, A_{21}$  under the minimal connection coefficients. From the proof of the Theorem 1 in [32], we know that  $\left\| C_1 (sI - A_{11})^{-1} B_1 \right\|_{\infty} \times \left\| C_2 (sI - A_{22})^{-1} B_2 \right\|_{\infty}$  can be minimized among different decompositions of  $A_{12}, A_{21}$  by LMI method, if we let

$$\min \left( \left\| C_1 (sI - A_{11})^{-1} B_1 \right\|_{\infty} \times \left\| C_2 (sI - A_{22})^{-1} B_2 \right\|_{\infty} \right) = \eta_0$$

we can get  $\max |\alpha_{12} \alpha_{21}| = \eta_0^{-1}$ .

From the proof above, we can give the following algorithm to get the estimation of  $\max \alpha_{12}, \max \alpha_{21}$  for any fixed full rank decompositions.

**Step 1.** For any fixed full rank decompositions  $A_{12} = B_1^0 C_2^0, A_{21} = B_2^0 C_1^0$ , solve the LMI (13) if it holds, go to step 2; otherwise, stop.

**Step 2.** Solving the following LMIs:

$$\begin{aligned} & \begin{bmatrix} P_1 A_{11}^T + A_{11} P_1 + B_1^0 X B_1^{0T} & P_1 C_1^{0T} \\ C_1^0 P_1 & -\frac{1}{\gamma_2^2} Y \end{bmatrix} < 0 \\ & \begin{bmatrix} P_2 A_{22}^T + A_{22} P_2 + B_2^0 Y B_2^{0T} & P_2 C_2^{0T} \\ C_2^0 P_2 & -\frac{1}{\gamma_1^2} X \end{bmatrix} < 0 \end{aligned}$$

If it holds, then, we can get:

$$\max \alpha_{12} = \gamma_1, \max \alpha_{21} = \gamma_2$$

Otherwise, go to step 3.

**Step 3.** Choose the appropriate step size  $\Delta\beta_1, \Delta\beta_2$  and move one step size for the LIM (13), *i.e.*, solve the following inequalities:

$$\begin{bmatrix} P_1 A_{11}^T + A_{11} P_1 + B_1^0 X B_1^{0T} & P_1 C_1^{0T} \\ C_1^0 P_1 & -\frac{1}{(\beta_2 + \Delta\beta_2)^2} Y \end{bmatrix} < 0$$

$$\begin{bmatrix} P_2 A_{22}^T + A_{22} P_2 + B_2^0 Y B_2^{0T} & P_2 C_2^{0T} \\ C_2^0 P_2 & -\frac{1}{(\beta_1 + \Delta\beta_1)^2} X \end{bmatrix} < 0 \quad (14)$$

If it does not hold, stop and get

$$\max \alpha_{12} \in (\beta_1, \beta_1 + \Delta\beta_1), \max \alpha_{21} \in (\beta_2, \beta_2 + \Delta\beta_2)$$

Otherwise, keep on moving one step size for the LIM (14) and solve the corresponding inequalities and continue the following process in step 3. If it moves the  $n$  step size, we can get:

$$\max \alpha_{12} \in (\beta_1 + (n-1)\Delta\beta_1, \beta_1 + n\Delta\beta_1)$$

$$\max \alpha_{21} \in (\beta_2 + (n-1)\Delta\beta_2, \beta_2 + n\Delta\beta_2)$$

Obviously, (13) is only a sufficient condition, but it is easy to establish an LMI algorithm for designing decentralized control  $F_1, F_2$ .

**Theorem 3.** For any fixed full rank decompositions  $A_{12} = B_1^0 C_2^0, A_{21} = B_2^0 C_1^0$ , there exist  $F_1, F_2$  and  $\alpha_{12}, \alpha_{21}$  as in (10) and decomposition  $A_{12} = B_1 C_2, A_{21} = B_2 C_1$  such that (9) holds, if and only if there exist positive  $P_1, P_2, X_1, X_2$  and any matrices  $Y_1, Y_2$  such that

$$\begin{bmatrix} P_1 A_{11}^T + A_{11} P_1 + B_{11} Y_1 + Y_1^T B_{11}^T + B_1^0 X_1 B_1^{0T} & P_1 C_1^{0T} \\ C_1^0 P_1 & -\frac{1}{\beta_2^2} X_2 \end{bmatrix} < 0$$

$$\begin{bmatrix} P_2 A_{22}^T + A_{22} P_2 + B_{22} Y_2 + Y_2^T B_{22}^T + B_2^0 X_2 B_2^{0T} & P_2 C_2^{0T} \\ C_2^0 P_2 & -\frac{1}{\beta_1^2} X_1 \end{bmatrix} < 0$$

and decentralized controllers gain are given by  $F_1 = Y_1 P_1^{-1}$ ,  $F_2 = Y_2 P_2^{-1}$ .

**Remark 5.** LMIs can be solved easily by using the toolbox [33]. Compare to the result in the Subsection 3.1, result in this section is only sufficient condition, but it is easier to establish an LMI algorithm for designing decentralized control and more simple to compute.

## 4. Synergic Stabilization for the Special Dynamical Network

In this section, we discuss the HSSP for the special model

(6).

### 4.1. Nyquist Criterion Method

For stability analysis of network (6), we show the following to be true.

**Theorem 4.** There exist connection coefficient gain matrix  $K = [k_{ij}], k_{ij} \in R$  such that  $I_n \otimes A_O + K \otimes A_C$  is stable if and only if there exist  $\lambda_i \in R$  such that  $A_O + \lambda_i A_C$  are stable simultaneously for  $i = 1, 2, \dots, n$ .

**Proof.** Let  $P \in R^{n \times n}$  be a nonsingular matrix such that  $P^{-1} K P = J$  and  $J$  is the Jordan standard form of  $K$ . Then, based on the Properties of the matrix Kronecker product, we can get:

$$\begin{aligned} & (P \otimes I_{n_1})(I_n \otimes A_O + K \otimes A_C)(P^{-1} \otimes I_{n_1}) \\ &= I_n \otimes A_O + J \otimes A_C \end{aligned}$$

Since the Jordan form matrix  $J$  is block upper-triangular, the stability of this system is equivalent to the stability of the  $n$  systems defined in the diagonal blocks. For  $J \otimes A_C$ , the diagonal blocks are each  $\lambda_i A_C$ , and then we can get the conclusion. This completes the proof.

**Remark 6.** If  $k_{ij}$  need to meet some constraints, then,  $\lambda_i$  also should satisfy some constraints correspondingly. For example in the consensus or formation control problem:

$$k_{ij} = \begin{cases} -\sum_{q=1, q \neq i}^n k_{iq} & j = i \\ k_{ij} \in R & j \neq i \end{cases} \quad (15)$$

Then, we need that there must exist  $\lambda_{i_0} = 0$  such that  $A_O + \lambda_{i_0} A_C$  is stable, *i.e.*,  $A_O$  is stable, and the associated eigenvector of  $\lambda_{i_0}$  is  $(1 \dots 1)^T$ .

In the following discussion, we suppose that  $A_C = B_1 C_1$ ,  $C_1 \in R_m^{m \times n}$ . We can get the following result.

**Theorem 5.** There exists Hadamard synergic control matrix pair  $(K = [k_{ij}], k_{ij} \in R, F)$  such that the network (6) is stable if and only if there exist  $\lambda_i \in R, i = 1, 2, \dots, n$  such that the controller  $u_i = F y_i + z_i$  simultaneously stabilizes the set of the following  $n$  systems:

$$\begin{aligned} \dot{x}_i &= A_O x_i + B_1 u_i \\ y_i &= x_i \\ z_i &= \lambda_i C_1 x_i \end{aligned} \quad (16)$$

**Proof.** Using the same transform method as in the Theorem 4, we can get that the network (6) is stable if and only if the following  $n$  systems is stable simulta-

neously if  $A_c = B_1 C_1$ .

$$\dot{\bar{x}}_i = (A_o + \lambda_i B_1 I C_1 + B_1 I F) \bar{x}_i$$

where  $\bar{x} = (P^{-1} \otimes I_{n_i}) x$ .

This is equivalent to the controller  $u_i = F y_i + z_i$  stabilizes the set of the  $n$  systems as in (16). This completes the proof.

**Remark 7.** Theorem 5 reveals that the special network (6) can be analyzed for stability by analyzing the stability of a single system with the same dynamics, modified by only a scalar, representing the interconnection, that take values according to the eigenvalues of the connection coefficient gain matrix  $K$ .

Hereafter, we refer to the transfer function from  $u_i$  to  $y_i$  as  $G(s)$ ; the closed loop system can be shown as **Figure 3** in this case. If  $G(s)$  is single-input-single-output (SISO), we can state a second version of Theorem 5 which is useful for stability analysis.

**Theorem 6.** Suppose  $G(s)$  is SISO and  $p$  is the number of right-half plant poles of  $P(s)$ . Then, the closed loop system as in **Figure 3** is stable if and only if

- 1) If  $\lambda_i \neq 0, i=1, 2, \dots, n$ , then, the counterclockwise net encirclement of  $(-\lambda_i^{-1}, j0)$  by the Nyquist plot of  $-C_1 P(s)$  is equal to  $p$  for  $i=1, 2, \dots, n$ .
- 2) Otherwise,  $p=0$  and this net encirclement is equal to zero.

**Proof.** The Nyquist criterion states that the stability of the closed loop system in **Figure 3** is equivalent to the number of counterclockwise encirclements of  $(-1, j0)$  by the forward loop  $\lambda_i C_1 P(j\omega)$  being equal to the number of the right-half plant poles of  $P(s)$ , which is assumed to be  $p$ . This criterion is equivalent to the number of encirclements of  $(-\lambda_i^{-1}, j0)$  by the Nyquist plot of  $-C_1 P(s)$  being  $p$ . This completes the proof.

Similarly, if  $G(s)$  is MIMO, we can give the following result.

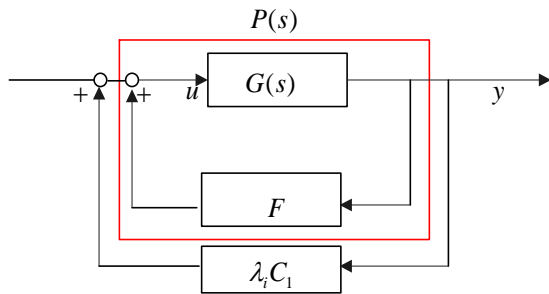


**Figure 3.** The closed loop of the system (16).

**Corollary 1.** Suppose  $G(s)$  is MIMO and  $p$  is the number of right-half plant poles of  $P(s)$ . Then, the closed loop system as in **Figure 3** is stable if and only if

- 1) If  $\lambda_i \neq 0, i=1, 2, \dots, n$ , then, the counterclockwise net encirclement of the origin by the Nyquist plot of  $\det(I + \lambda_i C_1 P(s))$  is equal to  $p$  for  $i=1, 2, \dots, n$ .
- 2) Otherwise,  $p=0$  and this net encirclement is equal to zero.

**Remark 8.** The zero eigenvalue of  $K$  can be interpreted as the unobservability of absolute motion in the measurements  $z_i$ . The design strategy in the Theorem 6 can be interpreted as follows: firstly, close the inner loop around  $y_i$  such that the internal closed loop system  $P(s)$  has  $p$  right-half plant poles which is equal to the number of uncontrollable poles of the system (16); secondly, close the outer loop around  $z_i$  such that the whole network system is stable. This can be seen as the synergic action between the feedback control and the connection gain regulation.

## 4.2 Algebraic condition

In this section, we consider the Hadamard synergic stability problem by using the algebraic method. First, we give the following Lemma.

**Lemma 1.** For any matrix  $K$ ,

$$(I_n \otimes A_o)(K \otimes A_c) = (K \otimes A_c)(I_n \otimes A_o)$$

if and only if  $A_o A_c = A_c A_o$ .

**Proof.** Based on the fact

$$\begin{cases} (I_n \otimes A_o)(K \otimes A_c) = K \otimes (A_o A_c) \\ (K \otimes A_c)(I_n \otimes A_o) = K \otimes (A_c A_o) \end{cases}$$

We can get the conclusion directly. This completes the proof.

**Lemma 2.** [20] Let  $S, T \in C^{n \times n}$  and  $ST = TS$ ,  $\lambda_1, \dots, \lambda_n, \mu_1, \dots, \mu_n$  are their eigenvalues respectively. Then, there exists a permutation  $i_1, \dots, i_n$  of  $1, 2, \dots, n$  such that  $\lambda_1 + \mu_{i_1}, \dots, \lambda_n + \mu_{i_n}$  are eigenvalues of  $S + T$ .

**Remark 9.** Lemma 2 implies that if  $ST = TS$ , then  $\lambda(S + T) \subset \lambda(S) + \lambda(T)$ , i.e.

$$\begin{aligned} \max(\operatorname{Re} \lambda(S + T)) &\leq \max(\operatorname{Re} \lambda(S)) + \max(\operatorname{Re} \lambda(T)) \\ \min(\operatorname{Re} \lambda(S + T)) &\geq \min(\operatorname{Re} \lambda(S)) + \min(\operatorname{Re} \lambda(T)) \end{aligned}$$

Here,  $\lambda(X)$  denotes the eigenvalue of matrix  $X$ .

**Theorem 7.** Suppose  $A_o A_c = A_c A_o$  and satisfied

- 1) If  $\max(\operatorname{Re} \lambda(A_c)) \leq 0$ , then,

$$\operatorname{Re} \lambda(K) > \max \left\{ \frac{-\max(\operatorname{Re} \lambda(A_o))}{\max(\operatorname{Re} \lambda(A_c))}, 0 \right\} \text{ or}$$

$$\frac{-\max(\operatorname{Re} \lambda(A_o))}{\min(\operatorname{Re} \lambda(A_c))} < \operatorname{Re} \lambda(K) < 0$$

2) If  $\min(\operatorname{Re} \lambda(A_c)) \geq 0$ , then,

$$\operatorname{Re} \lambda(K) < \min \left\{ \frac{-\max(\operatorname{Re} \lambda(A_o))}{\min(\operatorname{Re} \lambda(A_c))}, 0 \right\} \text{ or}$$

$$0 < \operatorname{Re} \lambda(K) < \frac{-\max(\operatorname{Re} \lambda(A_o))}{\max(\operatorname{Re} \lambda(A_c))}$$

3) If  $\max(\operatorname{Re} \lambda(A_c)) > 0$ , then,

$$\min(\operatorname{Re} \lambda(A_c)) < 0, 0 < \operatorname{Re} \lambda(K) < \frac{-\max(\operatorname{Re} \lambda(A_o))}{\min(\operatorname{Re} \lambda(A_c))}$$

$$\min(\operatorname{Re} \lambda(A_c)) > 0, 0 < \operatorname{Re} \lambda(K) < \frac{-\max(\operatorname{Re} \lambda(A_o))}{\min(\operatorname{Re} \lambda(A_c))}$$

**Proof.** Based on the Lemma 1 and Lemma 2, we have that

$$\begin{aligned} & \max(\operatorname{Re} \lambda(I_n \otimes A_o + K \otimes A_c)) \\ & \leq \max(\operatorname{Re} \lambda(I_n \otimes A_o)) + \max(\operatorname{Re} \lambda(K \otimes A_c)) \\ & = \max(\operatorname{Re} \lambda(A_o)) + \max(\operatorname{Re} \lambda(K) \operatorname{Re} \lambda(A_c)) \end{aligned}$$

then, we can get the conclusion directly. This completes the proof.

**Corollary 2.** Suppose that the connection gain matrix  $K = [k_{ij}]$  meet constraint (15),  $A_o A_c = A_c A_o$  and  $A_o$  is stable.

1) If  $\max(\operatorname{Re} \lambda(A_c)) \leq 0$ , then,  $I_n \otimes A_o + K \otimes A_c$  is stable for any  $K$  satisfied  $k_{ij} \leq 0$ .

2) If  $\min(\operatorname{Re} \lambda(A_c)) \geq 0$ , then,  $I_n \otimes A_o + K \otimes A_c$  is stable for any  $K$  satisfied  $k_{ij} \geq 0$ .

**Proof.** Based on the Gerschgorin disk theorem, we know that all the eigenvalues of  $K = [k_{ij}]$  are located in the union of the  $n$  disk:

$$G_i = \left( z \in \mathbb{R} \mid |z - k_{ii}| \leq \sum_{j=1}^n |k_{ij}| \right)$$

thus, we can get that all the eigenvalues of  $K = [k_{ij}]$  are positive except zero when  $k_{ij} \leq 0$  and are negative except zero when  $k_{ij} \geq 0$ . Then based on the Theorem 7, we can get the conclusion directly. This completes the proof.

When we consider the common decentralized controller  $u_i = Fx_i$ , if we want to use the conclusions above, we must require that  $(A_o + B_1 F)A_c = A_c(A_o + B_1 F)$ , this is difficult to solve. Thus, we consider the special case that  $A_c = aI_n, a \neq 0$  and can get the following result.

**Corollary 3.** If  $(A_o, B_1)$  is controllable, then for any  $K$  there must exist common decentralized controller  $u_i = Fx_i$  such that  $I_n \otimes (A_o + B_1 F) + K \otimes (aI_n)$  is stable; otherwise, suppose  $TA_o T^{-1} = \begin{bmatrix} A_1 & A_2 \\ 0 & A_3 \end{bmatrix}$ , then, there exist common decentralized controller  $u_i = Fx_i$  such that  $I_n \otimes (A_o + B_1 F) + K \otimes (aI_n)$  is stable if and only if  $\lambda(K) \leq \frac{\max(\operatorname{Re} \lambda(A_3))}{a}$  for  $a > 0$  or  $\lambda(K) \geq \frac{\max(\operatorname{Re} \lambda(A_3))}{a}$  for  $a < 0$ .

**Proof.** From the fact that for any matrix  $K, F$

$$\begin{aligned} & (I_n \otimes (A_o + B_1 F))(K \otimes (aI_n)) \\ & = (K \otimes (aI_n))(I_n \otimes (A_o + B_1 F)) \end{aligned}$$

and based on the Lemma 2 we can get the conclusion directly.

**Remark 10.** Based on the analysis in the Corollary 3 for this special case, synergic action between the decentralized feedback control and the connection gain regulations can be interpret as follows, that is: designing the common decentralized controller  $u_i = Fx_i$  to stabilize the controllable part firstly, and designing connection coefficient gain matrix  $K$  to stabilize the uncontrollable part secondly.

### 4.3. Network with Communication Time-Delays

In this section, we consider a network of continuous-time integrators in which the  $i$ -th subsystem state  $x_i$  passes through a communication channel  $e_{ij}$  with time-delay  $\tau_{ij} > 0$  before getting to  $j$ -th subsystem. The transfer function associated with the edge  $e_{ij}$  can be expressed as:  $h_{ij}(s) = e^{-\tau_{ij}s}$  in the Laplace domain. As the discussion in [34], to gain further insight in the relation between the connection gain matrix  $K$  and the maximum time-delays, we focus on the simplest possible case where the time-delays in all channels are equal to  $\tau > 0$  and  $h_{ij}(s) = h(s) = e^{-\tau s}$ . Then the network system can be written as:

$$\dot{x}_i(t) = A_o x_i(t - \tau) + \sum_{j=1}^n k_{ij} A_c(x_j(t - \tau)) + B_1 u_i$$

After taking the Laplace transform of both sides, we

can get

$$sX_i(s) - x_i(0) = h(s)A_oX_i(s) + \sum_{j=1}^n h(s)k_{ij}A_c(X_j(s))$$

The set of equations above can be rewritten in a compact form as:

$$X(s) = (sI - h(s)(I_n \otimes A_o + K \otimes A_c))^{-1} x(0) \quad (17)$$

The convergence analysis for a network of integrator nodes with communication time-delays reduces to stability analysis for a multiple-input-multiple-output (MIMO) transfer function:

$$G(s) = (sI - h(s)(I_n \otimes A_o + K \otimes A_c))^{-1}$$

In the following, we give the stability result of the model (17).

**Theorem 8.** Consider a network of integrator nodes with equal communication time-delay  $\tau > 0$  in all links. Assume the matrix  $I_n \otimes A_o + K \otimes A_c$  has no eigenvalue of zero or the algebraic multiplicity of the zero eigenvalue is 1. Then the model (17) is stable if and only if either of the following equivalent conditions are satisfied:

- 1)  $\tau \in (0, \tau_0)$  with  $\tau_0 = \min(\alpha_i)$ , where

$$\alpha_i = \begin{cases} \frac{\arcsin \frac{\operatorname{Re}(\lambda_i)}{\sqrt{\operatorname{Re}(\lambda_i)^2 + \operatorname{Im}(\lambda_i)^2}}}{\sqrt{\operatorname{Re}(\lambda_i)^2 + \operatorname{Im}(\lambda_i)^2}} & \operatorname{Re}(\lambda_i) > 0 \\ 2\pi + \frac{\arcsin \frac{\operatorname{Re}(\lambda_i)}{\sqrt{\operatorname{Re}(\lambda_i)^2 + \operatorname{Im}(\lambda_i)^2}}}{\sqrt{\operatorname{Re}(\lambda_i)^2 + \operatorname{Im}(\lambda_i)^2}} & \operatorname{Re}(\lambda_i) \leq 0 \end{cases} \quad (18)$$

$\lambda_i$  is the eigenvalue of the matrix  $I_n \otimes A_o + K \otimes A_c$ .

- 2) The Nyquist plot of  $\Gamma(s) = \frac{e^{-\tau s}}{s}$  has a zero encirclement around  $\frac{1}{\lambda_i}$  for  $\lambda_i \neq 0$ .

**Proof.** To establish the stability of (17), we use frequency domain analysis. We have  $X(s) = G(s)x(0)$ . Define  $H(s) = G^{-1}(s) = sI + h(s)(I_n \otimes A_o + K \otimes A_c)$ . Then, we require that all the zeros of  $\det(H(s))$  are on the Left Hand Plane (LHP) or  $s = 0$ . Let  $\omega_i$  be the normalized eigenvector of  $I_n \otimes A_o + K \otimes A_c$  associated with the eigenvalue  $\lambda_i$ . If the matrix  $I_n \otimes A_o + K \otimes A_c$  has zero eigenvalue and suppose  $\lambda_1 = 0$ , then  $s = 0$  in the direction  $\omega_1$  is a zero of  $\det(H(s))$  since

$H(0)\omega_1 = (I_n \otimes A_o + K \otimes A_c)\omega_1 = 0$ ; otherwise  $s = 0$  is not a zero of  $\det(H(s))$ .

Furthermore, we can get that any eigenvector of  $H(s)$  is an eigenvector of  $I_n \otimes A_o + K \otimes A_c$  and vice versa. Then, we can get that for any  $s$  of the zero of  $\det(H(s))$ , we must have  $H(s)\omega_i = 0$  for some one  $i$ , i.e.,

$$\begin{aligned} H(s)\omega_i &= (sI + h(s)(I_n \otimes A_o + K \otimes A_c))\omega_i \\ &= (s + \lambda_i e^{-\tau s})\omega_i = 0 \end{aligned}$$

But  $\omega_i \neq 0$ , thus,  $s \neq 0$  satisfies the following equation:

$$\frac{1}{\lambda_i} + \frac{e^{-\tau s}}{s} = 0 \quad (19)$$

Thus, if the net encirclement of the Nyquist plot of  $\Gamma(s) = \frac{e^{-\tau s}}{s}$  around  $-\frac{1}{\lambda_i}$  for  $\lambda_i \neq 0$  is zero, then all the poles of  $G(s)$  except  $s = 0$  are stable.

We calculate the upper bound on time-delay  $\tau$  as follows. We want to find the smallest value of the time-delay  $\tau > 0$  such that  $\det(H(s))$  has a zero on the imaginary axis. Set  $s = \pm j\omega$  in (19), we can get

$$\begin{aligned} j\omega + e^{-j\omega\tau} \lambda_i &= 0 \\ -j\omega + e^{j\omega\tau} \lambda_i &= 0 \end{aligned}$$

multiplying both sides of the two equations above, we get  $\omega^2 + \lambda_i^2 - 2\omega\lambda_i \sin(\omega\tau) = 0$ .

Let  $\lambda_i = \operatorname{Re}(\lambda_i) + j\operatorname{Im}(\lambda_i)$ , then, we have

$$\begin{aligned} (\omega - \operatorname{Re}(\lambda_i)) + 2\omega\operatorname{Re}(\lambda_i)(1 - \sin(\omega\tau)) - \operatorname{Im}(\lambda_i) \\ + 2j\omega(\operatorname{Re}(\lambda_i)\operatorname{Im}(\lambda_i) - \operatorname{Im}(\lambda_i)\sin(\omega\tau)) = 0 \end{aligned}$$

Assume  $\omega > 0$  (due to  $s \neq 0$ ), then from the equation above, we can get:

$$\omega = \sqrt{(\operatorname{Re} \lambda_i)^2 + (\operatorname{Im} \lambda_i)^2}, \quad \operatorname{Re}(\lambda_i) = \omega \sin(\omega\tau)$$

This implies

$$\tau \left( \sqrt{(\operatorname{Re} \lambda_i)^2 + (\operatorname{Im} \lambda_i)^2} \right) = 2k\pi + \arcsin \frac{\operatorname{Re}(\lambda_i)}{\sqrt{\operatorname{Re}(\lambda_i)^2 + \operatorname{Im}(\lambda_i)^2}},$$

i.e.

$$\tau = \frac{2k\pi + \arcsin \frac{\operatorname{Re}(\lambda_i)}{\sqrt{\operatorname{Re}(\lambda_i)^2 + \operatorname{Im}(\lambda_i)^2}}}{\sqrt{\operatorname{Re}(\lambda_i)^2 + \operatorname{Im}(\lambda_i)^2}}$$

thus, the smallest  $\tau > 0$  satisfied that  $\tau_0 = \min(\alpha_i)$  and  $\alpha_i$  are given in (18).

Due to the continuous dependence of the roots of (19) in  $\tau$  and the fact that all the zeros of this equation except  $s = 0$  for  $\tau = 0$  are located on the open LHP, for all  $\tau \in (0, \tau_0)$ , the roots of (19) are on the open LHP, and therefore the poles of  $G(s)$  are all stable except  $s = 0$ , but the algebraic multiplicity of the zero eigenvalue is 1. We can repeat a similar argument for the assumption that  $\omega < 0$ . This completes the proof.

**Remark 11.** From the condition (1) of the Theorem above, we can see that the upper bound on time-delay  $\tau_0$  is determined by the eigenvalues  $I_n \otimes A_o + K \otimes A_c$ . Thus, if  $A_o A_c = A_c A_o$ , then based on the Lemma 2, we can design the desired connection gain matrix  $K$  in order to obtain expected upper bound on time-delay.

## 5. Conclusions

In this paper, Hadamard synergic stabilization problem is investigated. Synergic stabilization problem for a special kind of networks are studied by using the Nyquist criterion. The mechanism of the synergic action between two control strategies: feedback control and the connection coefficients regulations are presented. Networks with communication time-delays are also discussed. Furthermore, synergic stabilization problem for the general dynamical network composed of two subsystems are investigated. The regulations of the interconnections can be exploited to improve the stability of the closed-loop system. It should be noted that only some special network models have been investigated in this paper, many more general network models remain to be challenging subjects for future research. Although Hadamard synergic control problem has not received much attention, we suggest that it will probably turn out to be widespread in power electrical engineering and the epidemic control system. We hope that our work will stimulate further studies of this new kind of control problem.

## 6. References

- [1] X. F. Wang, "Complex Networks: Topology, Dynamics, and Synchronization," *International Journal of Bifurcation and Chaos*, Vol. 5, No. 12, 2002, pp. 885-916.
- [2] D. J. Watts and S. H. Strogatz, "Collective Dynamics of 'Small-World' Networks," *Nature*, Vol. 393, No. 6684, 1998, pp. 440-442.
- [3] X. Li, X. F. Wang and G. R. Chen., "Pinning a Complex Dynamical Network to its Equilibrium," *IEEE Transactions on Circuits and Systems-I*, Vol. 51, No. 10, 2004, pp. 2074-2085.
- [4] V. Lesser, C. L. Ortiz and M. Tamb, "Distributed Sensor Networks: A Multiagent Perspective," Kluwer Academic Publishers, Boston, 2003.
- [5] S. S. Mascolo, "Congestion Control in High-Speed Communication Networks Using the Smith Principle," *Automatica*, Vol. 35, No. 11, 1999, pp. 1921-1935.
- [6] L. Huang and Z. S. Duan, "Complexity in Control Science," *Acta Automatica Sinica*, Vol. 29, No. 5, 2003, pp. 748-753.
- [7] Z. S. Duan, L. Huang, J. Z. Wang and L. Wang, "Harmonic Control between Two Systems," *Acta Automatica Sinica*, Vol. 129, No. 1, 2003, pp. 14-21.
- [8] Z. S. Duan, J. Z. Wang and L. Huang, "Special Decentralized Control Problems and Effectiveness of Parameter-Depend Lyapunov Function Method," *Proceedings of the American Control Conference*, Boston, 2005, pp. 1697-1702.
- [9] Y. Zou, M. H. Yin and H. D. Chiang, "Theoretical Foundation of Controlling U.E.P Method in Network Structure Preserving Power System Model," *IEEE Transactions on Circuits and Systems I*, Vol. 50, No. 10, 2003, pp. 1324-1336.
- [10] K. Sun, D. Z. Zheng and Q. Lu, "A Simulation Study of OBDD-Based Proper Splitting Strategies for Power Systems, under Consideration of Transient Stability," *IEEE Transaction on Power Systems*, Vol. 120, No. 1, 2005, pp. 389-399.
- [11] K. Sun, D. Z. Zheng and Q. Lu, "Splitting Strategies for Islanding Operation of Large-Scale Power Systems Using OBDD-Based Methods," *IEEE Transactions on Power Systems*, Vol. 18, No. 2, 2003, pp. 912-923.
- [12] Q. C. Zhao, K. Sun, D. Z. Zheng, J. Ma and Q. Lu, "A Study of System Splitting Strategies for Island Operation of Power System: A Two-Phase Method Based on OBDDs," *IEEE Transactions on Power Systems*, Vol. 18, No. 4, 2003, pp. 1556-1565.
- [13] X. F. Yan, Y. Zou and J. Li, "Optimal Quarantine and Isolation Strategies in Epidemics Control," *World Journal of Modeling and Simulation*, Vol. 3, No. 3, 2007, pp. 202-211.
- [14] X. F. Yan and Y. Zou, "Optimal Control for Internet Worm," *ETRI Journal*, Vol. 30, No. 1, 2008, pp. 81-88.
- [15] X. F. Yan and Y. Zou, "Isolation Treatment Strategy for Emergency Control," *Journal of systems Engineering*, Vol. 24, No. 2, 2009, pp. 129-135.
- [16] Y. Zou, "Investigation on Mechanism and Extension of Feedback: An Extended Closed-loop Coordinate Control of Interconnection-regulation and Feedback," *Journal of Nanjing University of Science and Technology*, Vol. 34, No. 1, 2010, pp. 1-7.
- [17] K. J. Astrom, "Limitations on Control System Performance," *European Journal of Control*, Vol. 4, No. 1, 2000, pp. 2-20.
- [18] R. M. Murray, K. J. Astrom, S. P. Boyd, et al., "Future Directions in Control in an Information-Rich World," *IEEE Control Systems Magazine*, Vol. 23, No. 2, 2003, pp. 20-33.

- [19] L. Guo, "Exploring the Maximum Capability of Adaptive Feedback," *International Journal of Adaptive Control and Signal Processing*, Vol. 16, No. 1, 2002, pp. 341-354.
- [20] J. L. Chen and X. H. Chen, "Special Matrices," Tsinghua Publisher, Beijing, 2001.
- [21] X. J. Liu and Y. Zou, "On the Hadamard Synergic Stabilization Problem: The Stabilization Via a Composite Strategy of Connection-Regulation and Feedback Control: Matrix Inequality Approach," *International Journal of Innovative Computing, Information and Control*, Vol. 6, No. 5, 2010, pp. 2383-2392.
- [22] Z. S. Duan, J. Z. Wang, G. R. Chen and L. Huang, "Stability Analysis and Decentralized Control of a Class of Complex Dynamical Networks," *Automatica*, Vol. 44, No. 4, 2008, pp. 1028-1035.
- [23] A. B. Gumel, S. Ruan, T. Day, *et al.*, "Modeling Strategies for Controlling SARS Outbreaks," *Proceedings of the Royal Society*, Vol. 49, No. 9, 2004, pp. 1465-1476.
- [24] X. Zhang, X. Hu and Z. Bao, "Blind Source Separation Based on Grading Learning," *Science in China-Series E*, Vol. 32, No. 5, 2002, pp. 693-793.
- [25] S. Chen, "A Lower Bound for the Minimum Eigenvalue of the Hadamard Product of Matrices," *Linear Algebra and its Applications*, Vol. 37, No. 8, 2004, pp. 159-166.
- [26] H. Li, T. Huang, S. Shen, *et al.*, "Lower Bounds for the Minimum Eigenvalue of Hadamard Product of an M-matrix and its Inverse," *Linear Algebra and its Applications*, Vol. 4, No. 20, 2007, pp. 235-247.
- [27] G. Visick, "A Quantitative Version of the Observation that the Hadamard Product is a Principal Submatrix of the Kronecker Product," *Linear Algebra and its Applications*, Vol. 30, No. 4, 2000, pp. 45-68.
- [28] M. Neumann, "A Conjecture Concerning the Hadamard Product of Inverses of  $M$ -matrices," *Linear Algebra and its Applications*, Vol. 28, No. 5, 1998, pp. 277-290.
- [29] L. Qiu and X. Zhan, "On the Span of Hadamard Products of Vectors," *Linear Algebra and its Applications*, Vol. 422, No. 1, 2006, pp. 304-307.
- [30] J. A. Fax and R. M. Murray, "Information Flow and Cooperative Control of Vehicle Formations," *IEEE Transactions on Automatic Control*, Vol. 49, No. 9, 2004, pp. 1465-1476.
- [31] R. O. Saber and M. Murray, "Consensus Protocols for Networks of Dynamic Agents," *Proceedings of the American Control Conference*, Denver, 2003, pp. 951-956.
- [32] Z. S. Duan, L. Huang, L. Wang and J. Z. Wang, "Some Applications of Small Gain Theorem to Interconnected Systems," *Systems and Control Letters*, Vol. 52, No. 3-4, 2004, pp. 263-273.
- [33] P. Gahinet, A. Nemirovski and A. J. Laub, "LMI Control Toolbox," TheMath Works, Inc., Natick, 1995.
- [34] R. O. Saber and M. Murray, "Consensus Problems in Networks of Agents with Switching Topology and Time-Delays," *IEEE Transactions on Automatic Control*, Vol. 49, No. 9, 2004, pp. 1520-1533.

# Maximizing of Asymptomatic Stage of Fast Progressive HIV Infected Patient Using Embedding Method

Hassan Zarei, Ali Vahidian Kamyad, Sohrab Effati

*Department of Applied Mathematics, Ferdowsi University of Mashhad, Mashhad, Iran*

*E-mail: zarei2003@yahoo.com*

*Received July 7, 2010; revised July 15, 2010; accepted July 23, 2010*

## Abstract

A system of ordinary differential equations, which describe various aspects of the interaction of HIV with healthy cells in fast progressive patient, is utilized, and an optimal control problem is constructed to prolong survival and delay the progression to AIDS as far as possible, subject to drug costs. Optimal control problem is approximated by linear programming model using measure theoretical approach and suboptimal combinations of reverse transcriptase inhibitor (RTI) and protease inhibitor (PI) drug efficacies are proposed. The Comparison of healthy CD4+ T-cells counts, virus particles and immune response, before and after the treatment is introduced.

**Keywords:** HIV Model, Optimal Control, Measure Theory, Linear Programming

## 1. Introduction

Human Immunodeficiency Virus infects CD4+ T-cells, which are an important part of the human immune system, and other target cells. The infected cells produce a large number of viruses. Medical treatments for HIV have greatly improved during the last two decades. Highly active antiretroviral therapy (HAART) allows for the effective suppression of HIV-infected individuals and prolongs the time before the onset of Acquired Immune Deficiency Syndrome (AIDS) for years or even decades and increase life expectancy and quality to the patient but antiretroviral therapy cannot eradicate HIV from infected patients because of long-lived infected cells and sites within the body where drugs may not achieve effective levels [1-3]. HAART contain two major types of anti-HIV drugs, reverse transcriptase inhibitors (RTI) and protease inhibitors (PI). Reverse transcriptase inhibitors prevent HIV from infecting cells by blocking the integration of the HIV viral code into the host cell genome. Protease inhibitors prevent infected cells from replication of infectious virus particles, and can reduce and maintain viral load below the limit of detection in many patients. Moreover, treatment with either type of drug can also increase the CD4+ T-cell count that are target cells for HIV.

Many of the host-pathogen interaction mechanisms during HIV infection and progression to AIDS are still unknown. Mathematical modeling of HIV infection is of

interest to the medical community as no adequate animal models exist in which to test efficacy of drug regimes. These models can test different assumptions and provide new insights into questions that is difficult to answer by clinical or experimental studies. A number of mathematical models have been formulated to describe various aspects of the interaction of HIV with healthy cells, See [4]. The basic model of HIV infection is presented by Perelson *et al.* [5] that contain three state variables healthy CD4+ T-cells, infected CD4+ T-cells and concentration of free virus. Another model is presented in [6] that although maintaining a simple structure, the model offers important theoretical insights into immune control of the virus based on treatment strategies Furthermore this modified model is developed to describe the natural evolution of HIV infection, as qualitatively described in several clinical studies [7].

Some authors use mathematical model for HIV infection in conjunction with control theory to achieve appropriate goals, by incorporating the effects of therapy on an HIV-infected individuals. For example, these goals may be maximizing the level of healthy CD4+ T-cells and minimizing the cost of treatment [8-12], maximizing immune response and minimizing both the cost of treatment and viral load [13,14], maximizing both the level of healthy CD4+ T-cells and immune response and minimizing the cost of treatment [15], Maximizing the level of healthy CD4+ T-cells while minimizing both the side effects and drug resistance [16] and maximizing survival

time of patient subject to drug cost [17] and etc.

The papers [18-21] consider only RTI medication while the papers [22,23] consider only PIs. In [24-27] all effects of a HAART medication are combined to one control variable in the model. In [13,28-31] dynamical multidrug therapies based on RTIs and PIs are designed.

In this paper, we consider a mathematical model of HIV dynamics that includes the effect of antiretroviral therapy, and perform an analysis of optimal control regarding appropriate goal.

The paper is organized as follows. In Section 2, the underlying HIV mathematical model is described. Our formulation of the control problem which attempts to delay appearance of AIDS as far as possible is described in Section 3. Formulated optimal control problem is approximated by linear programming (LP) problem. Related procedure is described in Section 4. Numerical results obtained from using LP model are presented in Section 5. Finally Section 6 is assigned to concluding remarks.

## 2. Presentation of a Working Model

In this paper, the pathogenesis of HIV is modeled with a system of ordinary differential equations (ODEs) described in [7]. This model can be viewed as an extension of basic HIV Models of Perelson *et al.* [5].

$$\dot{x} = \lambda - dx - rxv \tag{1}$$

$$\dot{y} = rxv - ay - \rho yz \tag{2}$$

$$\dot{w} = cxyw - qyw - bw \tag{3}$$

$$\dot{z} = qyw - hz \tag{4}$$

$$\dot{v} = k(1 - u_p)y - \tau v \tag{5}$$

$$\dot{r} = r_0 - u_r \tag{6}$$

Most of the terms in the model have straightforward interpretations as following:

The first equation represents the dynamics of the concentration of healthy CD4+ T-cells ( $x$ ). The healthy CD4+ T-cells are produced from a source, such as the thymus, at a constant rate  $\lambda$ , and die at a rate  $dx$ . The cells are infected by the virus at a rate  $rxv$ . The second equation describes the dynamics of the concentration of infected CD4+ T-cells ( $y$ ). The infected CD4+ T-cells result from the infection of healthy CD4+ T-cells and die at a rate  $ay$  and killed by cytotoxic T-lymphocyte effectors CTL $e(z)$  at a rate  $\rho yz$ . The population of CTLs is subdivided into precursors or CTL $p(w)$ , and effectors or CTL $e(z)$ . Equations (3)-(4) describe the dynamics of these compartments. In accordance with experimental findings [32] establishment of a lasting CTL response depends on CD4+ T-cell help, and that HIV impairs T helper cell function. Thus, proliferation of the CTL $p$

population is given by  $cxyw$  and is proportional to both virus load ( $y$ ) and the number of uninfected T helper cells ( $x$ ). CTL $p$  differentiation into effectors occurs at a rate  $cqyw$ . Finally, CTL $e$  die at a rate  $hz$ . Equation (5) describes the dynamics of the free-virus particles ( $v$ ). These free-virus particles are produced from infected CD4+ T-cells at a rate  $ky$  and are cleared at a rate  $\tau v$ . Model also contain an index of the intrinsic virulence or aggressiveness of the virus ( $r$ ). This index increases linearly in the case of an untreated HIV-infected individual, with a growth rate that depends on the constant  $r_0$  Finally Equation (6) describes the dynamic of this index. In model variables  $u_p$  and  $u_r$  denotes protease inhibitors (PI) and reverse transcriptase inhibitors (RTI), respectively.  $u_r$  reduces infection rate of healthy CD4+ T-cells by reducing the growth rate of the aggressiveness of the virus ( $r$ ) and  $u_p$  prevents virus production by reducing the production rate from infected CD4+ T-cells.

The model has several parameters that must be assigned for numerical simulations. The descriptions, numerical values and units of the parameters are summarized in **Table 1**. These descriptions and values were taken from [7]. We note that Equations (1)-(6) with these parameters, model dynamics of fast progressive patients (FPP).

## 3. Optimal Control Formulation

In clinical practice, Anti-retroviral therapy is initiated at  $t_0$ , the time at which CD4+ T-cell counts reach 350 cells/ $\mu$ l. The transition from HIV to AIDS occurred when patients CD4+ T-cell count falls below  $CD4^+_{AIDS}$  around 200 cells/ $\mu$ l. Our aim is to propose drug regimen

**Table 1. Parameter Values for the HIV model.**

| Parameters | Value/Unit  | Description             |
|------------|---|-------------------------|
| $\lambda$  | 7 cells/ $\mu$ l $day^{-1}$                         | Healthy CD4+ Production |
| $d$        | $7 \times 10^{-3} day^{-1}$                         | Healthy CD4+ clearance  |
| $a$        | 0.0999 $day^{-1}$                                   | Infected CD4+ clearance |
| $\rho$     | 2 $\mu$ cells $^{-1} day^{-1}$                      | Infected CD4+ kill      |
| $c$        | $5 \times 10^{-6} \mu$ l $^2$ cells $^{-2}day^{-1}$ | CTL $p$ proliferation   |
| $q$        | $6 \times 10^{-4} \mu$ cells $^{-1}day^{-1}$        | CTL $p$ differentiation |
| $b$        | 0.017 $day^{-1}$                                    | CTL $p$ clearance       |
| $h$        | 0.06 $day^{-1}$                                     | CTL $e$ clearance       |
| $k$        | 300 copies $ml^{-1}cells^{-1} \mu$ l $day^{-1}$     | Virus production        |
| $\tau$     | 0.2 $day^{-1}$                                      | Virus clearance         |
| $r_0$      | $10^9$ copies $^{-1}ml day^{-2}$                    | Virulence growth        |

to maximize asymptomatic stage time or equivalently prolong survival and delays the progression to AIDS as far as possible, subject to drug costs. This can be modeled as follows:

Assume that the onset of AIDS occurs after time  $t_f$ . Hence we should have:

$$x(t_f) = CD4^+_{AIDS}, x(t) \geq CD4^+_{AIDS}, \forall t \in [t_0, t_f] \quad (7)$$

We follow [8] and [22] in assuming systemic costs of the PI and RTI drugs treatment is proportional to  $u_p^2(t)$  and  $u_r^2(t)$  at time  $t$  respectively. Therefore Overall cost of the PI and RTI drugs treatment is  $\int_{t_0}^{t_f} u_p^2(t)dt$  and  $\int_{t_0}^{t_f} u_r^2(t)dt$  respectively and overall cost of treatment is given by  $\int_{t_0}^{t_f} u_p^2(t)dt + \sigma \int_{t_0}^{t_f} u_r^2(t)dt$ . Because symmetric costs for two types of drugs are in different scale, coefficient  $\sigma$  is set to balance them. Administration of drugs in high dose, are toxic to the human body. Moreover emergence of drug resistant strains is one of the basic complications in drug treatments. Many authors have ignored drug resistance issues, since fixing a maximum cost for a drug regime is equivalent to only administering a limited amount of chemotherapeutic agent. If that limited amount is chosen to be sufficiently small positive  $\gamma$ , the risk of drug resistance can be largely ignored. Therefore we impose following constraint on drug cost:

$$\int_{t_0}^{t_f} (u_p^2(t) + \sigma u_r^2(t)) dt \leq \gamma \quad (8)$$

Setting,  $\xi = (x, y, w, z, v, r)$  and  $u(t) = (u_p, u_r)$  the differential Equations (1)–(6) can be represented in a generalized form as:

$$\dot{\xi}(t) = g(t, \xi(t), u(t)) = \begin{pmatrix} \lambda - d\xi_1 - \xi_1\xi_3\xi_6 \\ \xi_1\xi_5\xi_6 - a\xi_2 - \rho\xi_2\xi_4 \\ c\xi_1\xi_2\xi_3 - q\xi_2\xi_3 - b\xi_3 \\ q\xi_2\xi_3 - h\xi_4 \\ k(1 - u_p)\xi_2 - \tau\xi_5 \\ r_0 - u_r \end{pmatrix} \quad (9)$$

Now with respect to above descriptions and (7) and (8) the optimal drug regime problem can be stated as follows:

$$\max_{u, t_f} \int_{t_0}^{t_f} dt \quad (10)$$

subject to

$$\dot{\xi} = g(t, \xi, u) \quad (11)$$

$$\int_{t_0}^{t_f} (u_p^2(t) + \sigma u_r^2(t)) dt \leq \gamma \quad (12)$$

$$\xi_1(t_0) = \xi_0, \xi_1(t_f) = CD4^+_{AIDS} \quad (13)$$

$$\xi_1(t) \geq CD4^+_{AIDS}, t \in [t_0, t_f] \quad (14)$$

We refer to this time optimal control problem as TOCP. Some problems may arise in the quest for the optimal solution. For example, may not exist control function  $u(\cdot)$  and corresponding state  $\xi(\cdot)$  and final time  $t_f$  that satisfy in (11)–(14). In order to overcome these difficulties in the next section we transfer the TOCP into a modified problem in measure space.

## 4. Approximation of TOCP by Linear Programming Model

Using the measure theory for solving optimal control problems based on the idea of Young [33], which was applied for the first time by Wilson and Rubio [34], has been theoretically established by Rubio in [35]. Then the method has been extended and improved by Mehne et al. [36] for solving time optimal control problems that leads to approximation of problem by linear programming (LP) model. We shall follow their approach here.

### 4.1. Transformation to Functional Space

We assume that state variable  $\xi(\cdot)$  and control input  $u(\cdot)$ , get their values in the compact sets  $A = A_1 \times \dots \times A_6 \subset \mathfrak{R}^6$  and  $U = U_1 \times U_2 \subset \mathfrak{R}^2$ , respectively. Set  $J = [t_0, t_f]$ .

**Definition 4.1.1.** We define a triple  $p = [t_f, \xi, u]$  to be admissible if the following conditions hold:

- 1) The vector function  $\xi(\cdot)$  be absolutely continuous and belongs to  $A$  for all  $t \in J$ .
- 2) The function  $u(\cdot)$  takes its value in the set  $U$  and is Lebesgue measurable on  $J$ .
- 3)  $p$  satisfies in the system (11)–(14), i.e. on  $J^0$ , the interior set of  $J$ .

We assume that the set of all admissible triples is non-empty and denote it by  $W$ . Let  $p$  be an admissible triple and  $B$  be an open ball in  $\mathfrak{R}^6$  containing  $J \times A$  and  $C'(B)$  be the space of all real-valued continuous differentiable functions on it. Let  $\varphi \in C'(B)$  and define  $\varphi^g$  as follows:

$$\begin{aligned} \varphi^g(t, \xi(t), u(t)) &= \frac{d\varphi(t, \xi(t))}{dt} \\ &= \sum_{j=1}^6 \frac{\partial \varphi(t, \xi(t))}{\partial \xi_j} g_j(t, \xi(t), u(t)) + \frac{\partial \varphi(t, \xi(t))}{\partial t} \end{aligned} \quad (15)$$

for each  $[t, \xi(t), u(t)] \in \Omega$ , where  $\Omega = J \times A \times U$ . The function  $\varphi^g$  is in the space  $C(\Omega)$ , the set of all continuous functions on the compact set  $\Omega$ . Since  $p = [t_f, \xi, u]$  is an admissible triple, we have

$$\begin{aligned} &\int_{t_0}^{t_f} \varphi^g(t, \xi(t), u(t)) dt \\ &= \varphi(t_f, \xi(t_f)) - \varphi(t_0, \xi(t_0)) = \Delta\varphi \end{aligned} \quad (16)$$

for all  $\varphi \in C'(B)$ . Let  $D(J^0)$  be the space of infinitely differentiable all real-valued function with compact support in  $J^0$ . Define:

$$\begin{aligned} \psi^j(t, \xi(t), u(t)) &= \xi_j(t)\psi'(t) + g_j(t, \xi(t), u(t))\psi(t), \\ j &= 1, \dots, 6 \quad \forall \psi \in D(J^0) \end{aligned} \quad (17)$$

Then if  $p = [t_f, \xi, u]$  be an admissible triple for  $j = 1, \dots, 6$ , and  $\forall \psi \in D(J^0)$ , from (17) we have

$$\begin{aligned} &\int_{t_0}^{t_f} \psi^j(t, \xi(t), u(t)) dt = \int_{t_0}^{t_f} \xi_j(t)\psi'(t) dt \\ &+ \int_{t_0}^{t_f} g_j(t, \xi(t), u(t))\psi(t) dt = \xi_j(t)\psi(t) \Big|_{t_0}^{t_f} \\ &+ \int_{t_0}^{t_f} \left\{ g_j(t, \xi(t), u(t)) - \dot{\xi}_j(t) \right\} \psi(t) dt \end{aligned}$$

since the function  $\psi(\cdot)$  has compact support in  $J^0$ , so  $\psi(t_0) = \psi(t_f) = 0$  and  $\dot{\xi}_j = g_j$  so

$$\int_{t_0}^{t_f} \psi^j(t, \xi(t), u(t)) dt = 0 \quad (18)$$

Also by choosing the functions which are dependent only on time, we have:

$$\int_{t_0}^{t_f} \mathcal{G}(t, \xi(t), u(t)) dt = a_g, \quad \forall \mathcal{G} \in C^1(\Omega) \quad (19)$$

where  $C^1(\Omega)$  is the space of all functions in  $C(\Omega)$  that depend only on time and  $a_g$  is the integral of  $\mathcal{G}$  on  $J$ . Equations (16), (18) and (19) are really weak form of (11), (13) and (14). We note that, the role of constraint (13) is considered on the right side of equation (16) by considering functions  $\varphi \in C'(B)$  which are monomials of  $\xi_1$ . Furthermore, the constraint (14) is

considered, by choosing appropriate set  $A$ . Now we consider the following positive linear functional on  $C(\Omega)$ .

$$\Gamma_p : F \rightarrow \int_J F(t, \xi(t), u(t)) dt, \quad \forall F \in C(\Omega) \quad (20)$$

**Proposition 4.1.1.** Transformation  $p \rightarrow \Gamma_p$  of admissible triples in  $W$  into the linear mappings  $\Gamma_p$  defined in (20) is an injection.

**Proof.** We must show that if  $p_1 \neq p_2$ , then  $\Gamma_{p_1} \neq \Gamma_{p_2}$ .

Let  $p_j = [t_{f_j}, \xi_j, u_j]$ ,  $j = 1, 2$  be different admissible triples. If  $t_{f_1} = t_{f_2}$ , then there is a subinterval of  $[t_0, t_{f_1}]$ , say  $J_1$ , where  $\xi_1(t) \neq \xi_2(t)$  for each  $t \in J_1$ . A continuous function  $F$  can be constructed on  $\Omega$  so that the right-hand side of (20) corresponding to  $p_1$  and  $p_2$  are not equal. For instance, assume  $F$  is independent of  $u$  such that for all  $t \in J_1$ , this function is positive on the appropriate portion of the graph of  $\xi_1(t)$ , and zero on  $\xi_2(t)$ , then the linear functionals are not equal. In other words if  $t_{f_1} \neq t_{f_2}$ , then  $\Gamma_{p_1}$  and  $\Gamma_{p_2}$  have different domains and are not equal.

Thus, the TOCP (10)-(14) is converted to following optimization problem in functional space:

$$\text{Maximize}_{\Gamma_p} \Gamma_p(1) \quad (\text{from (10)}) \quad (21)$$

Subject to

$$\Gamma_p(\phi^g) = \Delta\phi, \quad \phi \in C'(B) \quad (\text{from (16)}) \quad (22)$$

$$\Gamma_p(\psi^j) = 0, \quad j = 1, \dots, 6, \quad \psi \in D(J^0) \quad (\text{from (18)}) \quad (23)$$

$$\Gamma_p(\mathcal{G}) = a_g, \quad \mathcal{G} \in C^1(\Omega) \quad (\text{from (19)}) \quad (24)$$

$$\Gamma_p(H) \leq \gamma \quad (\text{from (12)}) \quad (25)$$

where  $H(t, \xi(t), u(t)) = u_p^2(t) + \sigma u_r^2(t)$ .

## 4.2. Transformation to Measure Space

Let  $M^+(\Omega)$  denotes the space of all positive Radon measures on  $\Omega$ . By the Riesz representation theorem, there exists a unique positive Radon measure  $\mu$  on  $\Omega$  such that:

$$\begin{aligned} \Gamma_p(F) &= \int_J F(t, \xi(t), u(t)) dt \\ &= \int_{\Omega} F(t, \xi, u) d\mu \equiv \mu(F), \quad F \in C(\Omega) \end{aligned} \quad (26)$$

So, we may change the space of optimization problem

to measure spaces. In other words, the optimization problem in functional space (21)-(25) can be replaced by the following new problem in measure space:

$$\text{Maximize } \mu(1) \quad (27)$$

$$\mu \in M^+(\Omega)$$

Subject to

$$\mu(\varphi^s) = \Delta\varphi, \quad \varphi \in C'(B) \quad (28)$$

$$\mu(\psi^j) = 0, \quad j = 1, \dots, 6, \psi \in D(J^0) \quad (29)$$

$$\mu(\mathcal{G}) = a_g, \quad \mathcal{G} \in C^1(\Omega) \quad (30)$$

$$\mu(H) \leq \gamma \quad (31)$$

We shall consider the maximization of (27) over the set  $Q$  of all positive Radon measures on  $\Omega$  satisfying (28)-(31). The main advantages of considering this measure theoretic form of the problem is the existence of an optimal measure in the set  $Q$  which this point can be studied in a straightforward manner without having to impose conditions such as convexity which may be artificial.

**Theorem 4.2.1.** The measure theoretical problem of maximizing (27) with equality and inequality constraints (28)-(31) has an optimal solution  $\mu^*$ .

**Proof.** As we will show in the next, (29) and (30) are special version of (28). Therefore, the set  $Q$  can be written as  $Q = Q_1 \cap Q_2$  where

$$Q_1 = \bigcap_{\varphi \in C'(B)} \left\{ \mu \in M^+(\Omega) : \mu(\varphi^s) = \Delta\varphi \right\}$$

and

$$Q_2 = \left\{ \mu \in M^+(\Omega) : \mu(H) \leq \gamma \right\}.$$

Assume that  $p = [t_f, \xi, u]$  is an admissible triple. It is well known that, the set  $\left\{ \mu \in M^+(\Omega) : \mu(1) = t_f - t_0 \right\}$  is compact in weak\*-topology. Furthermore,  $Q_1$  as intersection of inverse image of closed singleton sets  $\{ \Delta\varphi \}$  under continuous functions  $\mu \rightarrow \mu(\varphi^s)$  is also closed. It can be shown in a similar way that  $Q_2$  is closed. Thus,  $Q$  is a closed subset of a compact set. This proves the compactness of the set  $Q$ . Since the functional  $\mu \rightarrow \mu(1)$  mapping the compact set  $Q$  on the real line, is continuous and so has a maximum on the compact set  $Q$ .

Next, based on analysis in [35], the problem (27)-(31) is approximated by a LP problem and a triple  $p^*$  which approximate the action of  $\mu^* \in Q$  is achieved.

### 4.3. Approximation

Problem (27)-(31) is an infinite dimensional linear programming problem and all the functions in (28)-(31) are linear with respect to measure  $\mu$ . Of course, it is an infinite dimensional LP problem, because  $M^+(\Omega)$  is infinite dimensional space. It is possible to approximate the solution of this problem by the solution of a finite-dimensional LP of sufficiently large dimension. Also, from the solution of this new finite dimensional LP we induce an approximated admissible triple in a suitable manner. We shall first develop an intermediate problem, still infinite-dimensional by considering the maximization (27), not over the set  $Q$  but over a subset of  $M^+(\Omega)$  with only a finite numbers of the constraints in (28)-(31) being satisfied. This will be achieved by choosing countable sets of functions whose linear combinations are dense in the sets  $C'(B)$ ,  $C^1(\Omega)$  and  $D(J^0)$ , and then selecting a finite number of them. Assume the set  $\{\varphi_i : i = 1, 2, \dots\}$  be such that the linear combinations of the functions  $\varphi_i \in C'(B)$  are uniformly dense in  $C'(B)$ . For instance, these functions can be taken to be monomials in  $t$  and the components of the vector  $\xi$ . As we will show in the next, some of these monomials are suitable for our problem and are as follows:

$$t^i \xi_j \text{ and } \xi_i^j \xi_h^i, \quad i \in \{0, 1\}, j \in \{1, 2, \dots\}, \quad (32)$$

$$h \in \{2, 3, 4, 5, 6\}$$

Let set  $\{\psi_i : i = 1, 2, \dots\}$  be such that linear combinations of the functions  $\psi_i \in D(J^0)$  are uniformly dense in  $D(J^0)$ . For  $r = 1, 2, \dots$  some of these functions can be taken as follows [36]:

$$\psi_{2r-1}(t) = \begin{cases} \sin\left(\frac{2\pi r(t-t_0)}{\Delta T}\right) & t \leq t_l \\ 0 & \text{otherwise} \end{cases}$$

and

$$\psi_{2r}(t) = \begin{cases} 1 - \cos\left(\frac{2\pi r(t-t_0)}{\Delta T}\right) & t \leq t_l \\ 0 & \text{otherwise} \end{cases} \quad (33)$$

where  $\Delta T = t_l - t_0$  and  $t_l$  is a lower bound for optimal time which can be obtained using controllability.

Finally, let set  $\{\mathcal{G}_i : i = 1, 2, \dots\}$  be such that linear combinations of the functions  $\mathcal{G}_i \in C^1(\Omega)$  are uni-

formly dense in  $C^1(\Omega)$ . These functions can be considered monomials in  $t$  as follows:

$$\mathcal{G}_s(t) = t^s, \quad s = 0, 1, 2, \dots \quad (34)$$

**Remark 1.** With respect to (15) and (17) it can be seen that (29) and (30) are also achieved from (28) by setting  $\varphi(t, \xi(t)) = \xi_j(t)\psi(t)$  and  $\varphi(t, \xi(t)) = \int_0^t \mathcal{G}(\tau) d\tau$  respectively.

The first approximation will be completed by using above subjects and the following propositions.

**Proposition 4.3.1.** Consider the linear program consisting of the maximizing function  $\mu \rightarrow \mu(1)$  over the set  $Q_M$  of measures in  $M^+(\Omega)$  satisfying:

$$\begin{aligned} \mu(\varphi_i^g) &= \Delta\varphi_i, \quad i = 1, \dots, M \\ \mu(H) &\leq \gamma \end{aligned}$$

Then  $\lambda_M \equiv \max_{Q_M} \mu(1)$  tends to  $\lambda \equiv \max_Q \mu(1)$  as  $M \rightarrow \infty$ .

**Proof.** We have  $Q_1 \supseteq Q_2 \supseteq \dots \supseteq Q_M \supseteq \dots \supseteq Q$ ; hence,  $\lambda_1 \geq \lambda_2 \geq \dots \geq \lambda_M \geq \dots \geq \lambda$ . Therefore,  $\{\lambda_n\}$  is non increasing and bounded sequence then converges to a number  $\zeta$  such that  $\zeta \geq \lambda$ . We show that,  $\zeta = \lambda$ .

Set  $R \equiv \bigcap_{M=1}^{\infty} Q_M$ . Then,  $R \supseteq Q$  and  $\zeta \equiv \max_R \mu(1)$ . It is sufficient to show  $R \subseteq Q$ . Assume  $\mu \in R$  and  $\varphi \in C'(B)$ . Since Linear combinations of the functions  $\{\varphi_j, j = 1, 2, \dots\}$  are uniformly dense in  $C'(B)$ , there is the Sequence  $\{\tilde{\varphi}_k\} \in \text{span}\{\varphi_j, j = 1, 2, \dots\}$  such that  $\tilde{\varphi}_k$  tends to  $\varphi$  uniformly as  $k \rightarrow \infty$ . Hence,  $S_1, S_2$  and  $S_3$  tend to zero as  $k \rightarrow \infty$  where  $S_1 = \sup|\varphi_\xi - \tilde{\varphi}_{k\xi}|$ ,  $S_2 = \sup|\varphi_t - \tilde{\varphi}_{kt}|$  and  $S_3 = \sup|\varphi - \tilde{\varphi}_k|$ . We have  $\mu \in R$ , and functional  $f \rightarrow \mu(f)$  is linear. Therefore,  $\mu(\tilde{\varphi}_k^g) = \Delta\tilde{\varphi}_k$  and

$$\begin{aligned} |\mu(\varphi^g) - \Delta\varphi| &= |\mu(\varphi^g) - \Delta\varphi - \mu(\tilde{\varphi}_k^g) + \Delta\tilde{\varphi}_k| \\ &= \left| \int_{\Omega} \left\{ \left[ \varphi_\xi(t, \xi) - \tilde{\varphi}_{k\xi}(t, \xi) \right] g(t, \xi, u) \right. \right. \\ &\quad \left. \left. + \left[ \varphi_t(t, \xi) - \tilde{\varphi}_{kt}(t, \xi) \right] \right\} d\mu - (\Delta\varphi - \Delta\tilde{\varphi}_k) \right| \\ &\leq S_1 \int_{\Omega} |g(t, \xi, u)| d\mu + S_2 \int_{\Omega} d\mu + 2S_3 \end{aligned}$$

Since the right-hand side of the above inequality tends to zero as  $k \rightarrow \infty$ , while left-hand side is independent of  $k$ , therefore  $\mu(\varphi^g) = \Delta\varphi$ . Thus  $R \subseteq Q$  and  $\zeta \leq \lambda$

which implies  $\zeta = \lambda$ .

**Proposition 4.3.2.** The measure  $\mu^*$  in the set  $Q_M$  at which the functional  $\mu \rightarrow \mu(1)$  attains its maximum has the form

$$\mu^* = \sum_{j=1}^{M+1} \alpha_j^* \delta(z_j^*) \quad (35)$$

where  $\alpha_j^* \geq 0, z_j^* \in \Omega$  and  $\delta(z)$  is unitary atomic measure with the support being the singleton set  $\{z_j^*\}$ , characterized by  $\delta(z)(F) = F(z), z \in \Omega$ .

**Proof.** See appendix of [35].

Therefore, with respect to above descriptions we restrict our attention to finding measure in form  $\mu = \sum_{j=1}^{M+1} \alpha_j \delta(z_j)$ , which maximizes functional  $\mu = \mu \rightarrow \mu(1)$  and satisfies in (31) and  $M$  number of constraints in the form of (28)-(30). Clearly,  $\mu(F) = \sum_{j=1}^{M+1} \alpha_j F(z_j), \forall F \in C(\Omega)$ . Therefore, by choosing  $M_1$  number of functions in the form of (32),  $S$  number of functions in the form of (34) and  $M'_2$  number of functions in the form of (33), which leads to  $M_2 = 6M'_2$  number of functions of the type (17) where are numbered sequentially as  $\theta_h, h = 1, \dots, M_2$ , infinite dimensional problem (27)-(31) is approximated with following finite dimensional nonlinear programming (NLP) problem:

$$\begin{aligned} &\text{Maximize} && \sum_{j=1}^{M+1} \alpha_j \\ &\alpha_j \geq 0, z_j \in M^+(\Omega) \end{aligned} \quad (36)$$

Subject to

$$\sum_{j=1}^{M+1} \alpha_j \varphi_i^g(z_j) = \Delta\varphi_i, \quad i = 1, \dots, M_1 \quad (37)$$

$$\sum_{j=1}^{M+1} \alpha_j \theta_h(z_j) = 0, \quad h = 1, \dots, M_2 \quad (38)$$

$$\sum_{j=1}^{M+1} \alpha_j \mathcal{G}_s(z_j) = a_g, \quad s = 1, \dots, S \quad (39)$$

$$\sum_{j=1}^{M+1} \alpha_j H(z_j) \leq \gamma \quad (40)$$

where,  $M = M_1 + M_2 + S$ . We confront with NLP with more than  $2(M+1)$  unknowns  $\alpha_j, z_j, j = 1, \dots, M+1$ . Finally, the following proposition enables us to approximate the problem via the finite dimensional linear programming problem.

**Proposition 4.3.3.** Let  $\Omega_N = \{y_1, y_2, \dots, y_N\}$  be a countable dense subset of  $\Omega$ , for any  $N$  sufficiently large number. Given  $\varepsilon > 0$ , a measure  $\nu \in M^+(\Omega)$  can be

found such that:

$$\left|v(\varphi_i^s) - \mu^*(\varphi_i^s)\right| \leq \varepsilon \quad i = 1, \dots, M_1 \quad (41)$$

$$\left|v(\theta_h) - \mu^*(\theta_h)\right| \leq \varepsilon \quad h = 1, \dots, M_2 \quad (42)$$

$$\left|v(\mathcal{G}_s) - \mu^*(\mathcal{G}_s)\right| \leq \varepsilon \quad s = 1, \dots, S \quad (43)$$

$$\left|v(H) - \mu^*(H)\right| \leq \varepsilon \quad (44)$$

where measure  $v$  has the form

$$v = \sum_{j=1}^{M+1} \alpha_j^* \delta(z_j) \quad (45)$$

where the coefficients  $\alpha_j^*$ ,  $j = 1, \dots, M+1$  are the same as optimal measure (35), and  $z_j \in \mathcal{Q}_N$ ,  $j = 1, \dots, M+1$ .

**Proof.** We rename functions  $\varphi_i^s$ 's,  $\theta_h$ 's,  $v_s$ 's and  $H$  sequentially as  $f_j$ ,  $j = 1, 2, \dots, M+1$ . Then, for  $j = 1, \dots, M+1$ ,

$$\begin{aligned} \left|(\mu^* - v)f_j\right| &= \left|\sum_{i=1}^{M+1} \alpha_i^* [f_j(z_i^*) - f_j(z_i)]\right| \\ &\leq \left(\sum_{i=1}^{M+1} \alpha_i^*\right) \max_{i,j} |f_j(z_i^*) - f_j(z_i)| \end{aligned}$$

$f_j$ 's are continues. Therefore,  $\max_{i,j}$  can be made less than  $\frac{\varepsilon}{\sum_{j=1}^{M+1} \alpha_j^*}$  by choosing  $z_i$ ,  $i = 1, 2, \dots, M+1$ , sufficiently near to  $z_i^*$ .

For construction of dense subset  $\Omega_N$ ,  $J$  is divided to  $S$  subintervals as follows:

$$J_s = \left[ t_0 + \frac{(s-1)\Delta T}{S-1}, t_0 + \frac{s\Delta T}{S-1} \right), \quad s = 1, 2, \dots, S-1$$

and

$$J_s = [t_l, t_f) \quad (46)$$

Furthermore, intervals  $A_i$ 's and  $U_j$ 's are divided into  $n_i$  and  $m_j$  subintervals respectively, then the set  $\Omega$  is divided into  $N = S n_1 n_2 n_3 n_4 n_5 m_1 m_2$  cells. One point is chosen from each cell. In this way we will have a grid of points, which are numbered sequentially as  $y_j = (t_j, \xi_{1j}, \dots, \xi_{6j}, u_{P_j}, u_{R_j})$ ,  $j = 1, \dots, N$ .

**Remark 2.** It is well known that each function type (34) can be approximated in a nice way by a linear combination of characteristic function of subintervals of  $J$ . In practice we consider  $\mathcal{G}_s(t) = \chi_{J_s}(t)$ ,  $s = 1, \dots, S$  instead of functions of the type (34), where  $J_s$ 's are given by (46)

and  $\chi_{J_s}$  denotes the characteristic function of  $J_s$ . The main reason for this choice of  $\mathcal{G}_s$ 's is related to their essential role in construction of control functions. For more details see [35,36].

Considering (45) the NLP (36)-(40) is converted to the following LP:

$$\text{Maximize } \sum_{j=1}^N \alpha_j \quad (47)$$

subject to

$$\sum_{j=1}^N \alpha_j \varphi_i^s(y_j) = \Delta \varphi_i, \quad i = 1, \dots, M_1 \quad (48)$$

$$\sum_{j=1}^N \alpha_j \theta_h(y_j) = 0, \quad h = 1, \dots, M_2 \quad (49)$$

$$\sum_{j=1}^N \alpha_j H(y_j) \leq \gamma \quad (50)$$

$$\sum_{j=1}^l \alpha_j = \frac{\Delta T}{S-1}$$

⋮

$$\sum_{j=(S-2)l+1}^{(S-1)l} \alpha_j = \frac{\Delta T}{S-1} \quad (51)$$

$$\sum_{j=(S-1)l+1}^{Sl} \alpha_j = t_f - t_l$$

$$\xi_i(t_f) \in A_i, \quad i = 2, 3, 4, 5, 6 \quad (52)$$

where  $l = \frac{N}{S}$ . Of course, we need only to construct the function  $u(\cdot)$ , since the  $\xi(\cdot)$  is simply the corresponding solution of differential Equations (1)-(6) which can be estimated numerically. Using simplex method, nonzero optimal solution  $\alpha_{i_1}^*, \alpha_{i_2}^*, \dots, \alpha_{i_p}^*$ ,  $i_1 < i_2 < \dots < i_p$  of LP (47)-(52) can be found where  $p$  cannot exceed the number of constraints *i.e.*,  $p \leq M_1 + M_2 + S + 1$ .

Setting  $\alpha_{i_0}^* = t_0$ , piecewise control pair  $u(t) = (u_p(t), u_R(t))$  which approximate the action of the optimal control, is constructed based on these nonzero coefficients as follows [35,36]:

$$u(t) = \begin{cases} (u_{P_j}, u_{R_j}) & t \in \left[ \sum_{h=0}^{j-1} \alpha_{i_h}^*, \sum_{h=0}^j \alpha_{i_h}^* \right), \quad j = 1, 2, \dots, p \\ 0 & \text{otherwise} \end{cases}$$

It should be remembered,  $u_{P_j}$  and  $u_{R_j}$  are respectively 7th and 8th components of  $y_{i_j}$ .

### 5. Numerical Results

In our implementation, we set  $M_1 = 14$  and chosen functions  $\varphi$  from  $C'(B)$  are as follows:

$$\xi_1, \xi_2, \xi_3, \xi_4, \xi_5, \xi_6, t_{\xi_1}, \xi_1 \xi_2, \xi_1 \xi_3, \xi_1 \xi_4, \xi_1 \xi_5, \xi_1 \xi_6, \xi_1^2, t_{\xi_1}^2$$

Furthermore, we set  $M'_2 = 2$ . Hence, we have  $M_2 = 12$  number of functions in the form of (17). Parameter  $S$  is set to 11 and desired lower bound for optimal time is set to  $t_l = 2007.5$  (5.5 years). Setting  $u = (0, 0)$ , and solving ODE (1)-(6) using 4th order Runge-Kutta method, shows that at  $t_0 = 620$ ,  $\xi(t_0) = (350, 12.40, 1.26, 0.16, 18454)$ . Starting points of our simulation runs are:

$$x(0) = 10^3 \text{ cells}\mu\text{l}^{-1}, v(0) = 104 \text{ copies}\text{ml}^{-1}, y(0) = 0 \text{ cells}\mu\text{l}^{-1}, w(0) = 10^{-3} \text{ cells}\text{ml}^{-1}, z(0) = 10^{-7} \text{ cells}\mu\text{l}^{-1} \text{ and } r(0) = 2 \times 10^7 \text{ mlcopies}^{-1}\text{day}^{-1}.$$

Maximum values for  $u_p$  and  $u_r$ , are 0.7 and  $9 \times 10^{-10}$  respectively [7]. Therefore, the coefficient  $\sigma$  for balancing both PI and RTI costs in (8) is set to  $\sigma = \left(\frac{0.7}{9 \times 10^{-10}}\right)^2$ . Furthermore, the total costs are bounded above by  $\gamma = 480$ . By using controllability, considered ranges for states and controls and corresponding partitions for construction of  $y_j, j=1, \dots, N$  are summarized in **Table 2**. Note that, selected values from the set  $U_1$  for construction of  $y_j$ 's are 0, 0.4 and 0.7. These values indicate off, moderate and strong PI-therapy. Similarly, corresponding values for RTI control are 0,  $5 \times 10^{-10}$  and  $9 \times 10^{-10}$  [7]. Therefore, we have linear programming with  $M = 33$  constraints and  $N = 59405$  unknowns, that is solved using simplex method and environment of MATLAB. Implementing the corresponding LP model, the suboptimal time has been found  $t_f^* = 2133.2$  (71.11 Months).

**Figure 1** shows the resulting suboptimal control pair. The response of the system to the control functions is depicted in **Figure 2**. **Figure 2(a)** shows that condition

(14) violates in a subinterval of  $J$ , which is due to approximate nature of control pair and can be ignored. Because, the length of this subinterval is very small as compared to the length of  $J$ . We found  $\xi_1(t_f^*) = 199.28$ , which is close to exact value *i.e.*, 200. From **Figures 2(a)** and **2(b)**, we see drop in the number of CD4+ T-cells, and a rise in viral load following the initial infection until about the third month. After this time, CD4+ T-cells start recovering and virus starts decreasing due to the immune response, but can never eradicate virus completely. Then CD4+ T-cells level decreases and viral load increases due to destruction of immune system in absence of treatment. **Figures 2(b)** and **2(c)** show a clear correlation between the CTLe and virus population. As the virus increases upon initial infection, CTLe increases in order to decrease the virus. Once this is accomplished, virus decreases. Then virus grows back slowly, and this triggers an increase in the CTLe population. CTLe, further increases in an attempt to keep the virus at constant levels but lose the battle because of virus-induced impairment of CD4+ T-cell function, in absence of treatment (dotted line). Memory CTL responses depend on the

**Table 2. Considered ranges for states and controls and corresponding number of partitions.**

| State   | Range                          | Number of partitions |
|---------|--------------------------------|----------------------|
| $\xi_1$ | $A_1 = [200, 1000]$            | $n_1 = 5$            |
| $\xi_2$ | $A_2 = [5, 30]$                | $n_2 = 3$            |
| $\xi_3$ | $A_3 = [0, 1.6]$               | $n_3 = 2$            |
| $\xi_4$ | $A_4 = [0, 1.3]$               | $n_4 = 2$            |
| $\xi_5$ | $A_5 = [500, 35000]$           | $n_5 = 10$           |
| $\xi_6$ | $A_6 = [0, 2 \times 10^7]$     | $n_6 = 1$            |
| $u_p$   | $U_1 = [0, 0.7]$               | $m_1 = 3$            |
| $u_r$   | $U_2 = [0, 9 \times 10^{-10}]$ | $m_2 = 3$            |

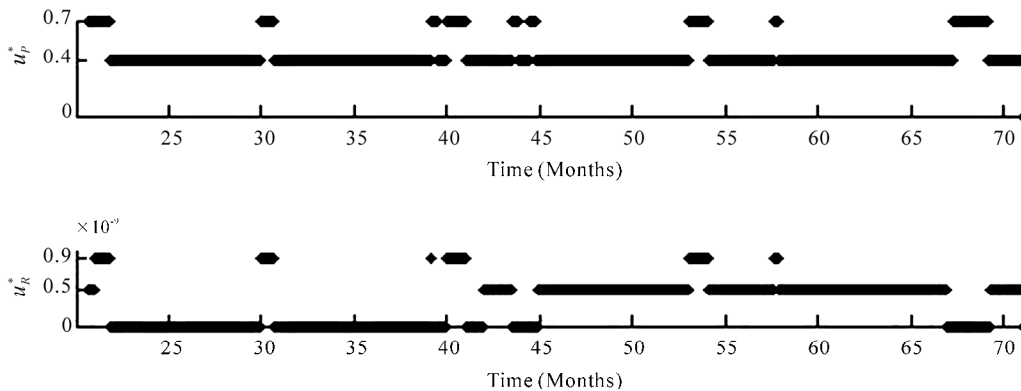


**Figure 1. The suboptimal piecewise constant control pair  $u_p^*(\cdot)$  and  $u_r^*(\cdot)$ .**

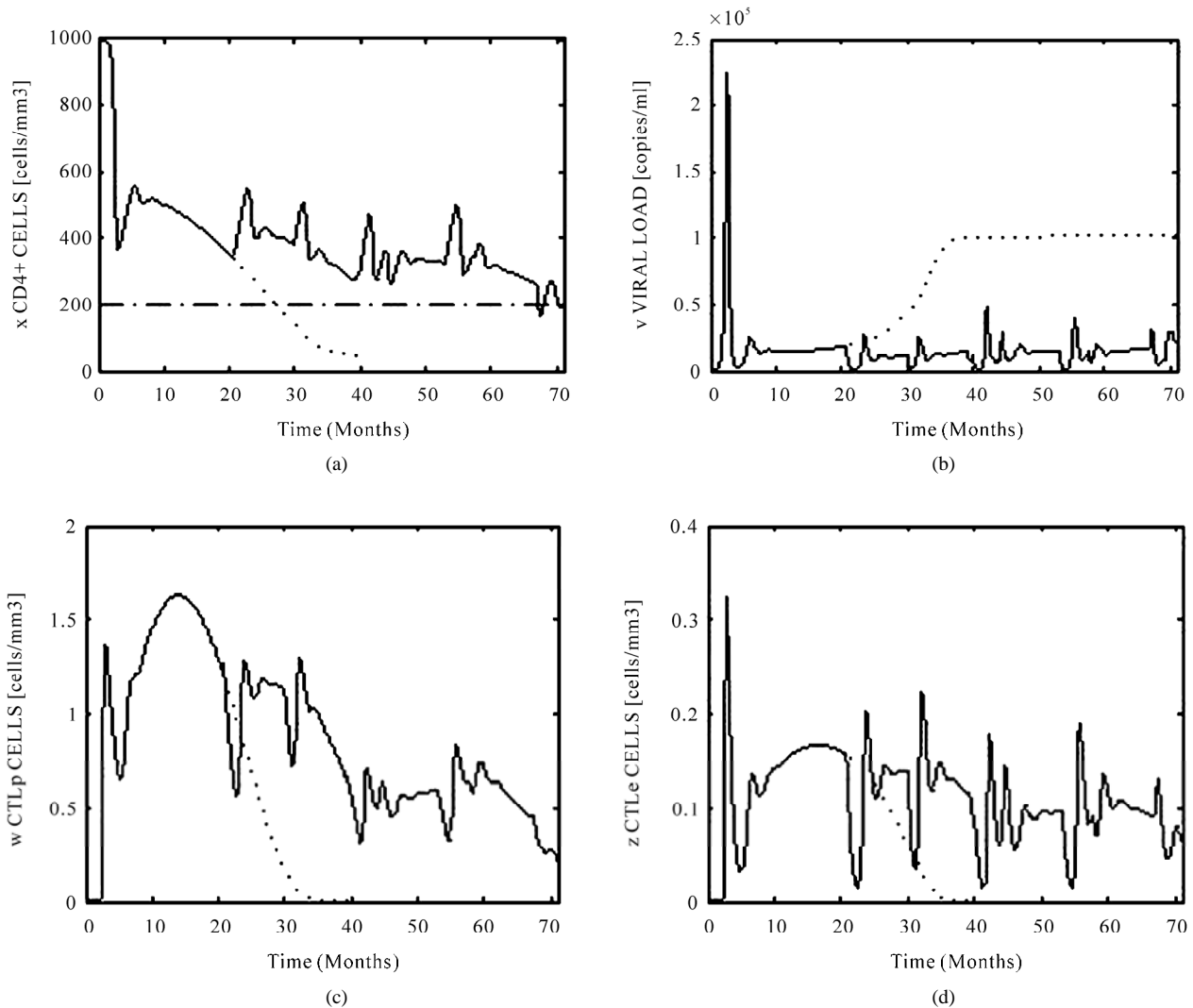


**Figure 2. Dynamic behavior of the state variables  $x$ ,  $v$ ,  $w$  and  $z$  versus time in the case of untreated (dotted line) and treated infected patients (solid line).**

presence of CD4+ T-cell help. **Figures 2(a) and 2(b)** show that, in presence of treatment the virus is controlled to very low levels and CD4+ T-cells are maintained above the critical levels for relatively long time. Therefore, immune response expands for relatively long time successfully. Furthermore, these figures indicate inverse-coloration between viral load and CD4+ T-cells level. From **Figures 2(c) and 2(d)** interestingly, a decrease in CTL's occurs in response to therapy can be observed. The extent of the decrease is directly correlated with the increase in treatment effectiveness which is consistent with experimental findings [37].

## 6. Conclusions

In this paper, we considered a system of ordinary differ-

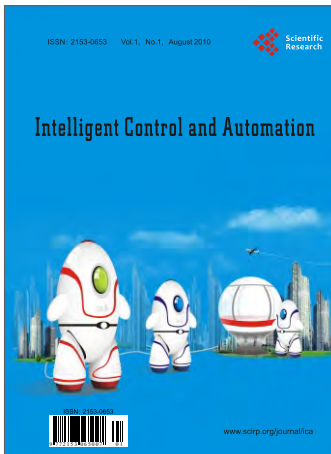
ential equations, which describe various aspects of the interaction of HIV with healthy cells in fast progressive patient, for constructing a time optimal control problem which maximizes asymptomatic stage of patient. A measure theoretical method is used to solve such kind of problems, and numerical results, confirmed the effectiveness of this approach.

## 7. References

- [1] T. W. Chun, L. Stuyver, S. B. Mizell, L. A. Ehler, J. A. Mican, M. Baseler, A. L. Lloyd, M. A. Nowak and A. S. Fauci, "Presence of an Inducible HIV-1 Latent Reservoir During Highly Active Antiretroviral Therapy," *Proceedings of the National Academy of Sciences*, Vol. 94, No. 24, 1997, pp. 13193-13197.
- [2] D. Finzi, M. Hermankova, T. Pierson, L. M. Carruth, C.

- Buck, R. E. Chaisson, T. C. Quinn, K. Chadwick, J. Margolick, R. Brookmeyer, *et al.*, "Identification of a Reservoir for HIV-1 in Patients on Highly Active Antiretroviral Therapy," *Science*, Vol. 278, No. 5341, 1997, pp. 1295-1300
- [3] J. K. Wong, M. Hezareh, H. F. Gunthard, D. V. Havlir, C. C. Ignacio, C. A. Spina and D. D. Richman, "Recovery of Replication-Competent HIV Despite Prolonged Suppression of Plasma Viremia," *Science*, Vol. 278, No. 5341, 1997, pp. 1291-1295.
- [4] M. M. Hadjiandreou, R. Conejeros and V. S. Vassiliadis, "Towards a Long-Term Model Construction for the Dynamic Simulation of HIV Infection," *Mathematical Biosciences and Engineering*, Vol. 4, No. 3, 2007, pp. 489-504.
- [5] A. S. Perelson, A. U. Neumann, M. Markowitz, *et al.*, "HIV-1 Dynamics in Vivo: Virion Clearance Rate, Infected Cell Life-Span, and Viral Generation Time," *Science*, Vol. 271, No. 5255, 1996, pp. 1582-1586.
- [6] D. Wodarz and M. A. Nowak, "Specific Therapy Regimes Could Lead to Long-Term Immunological Control of HIV," *Proceedings of the National Academy of Sciences*, Vol. 96, No. 6, 1999, pp. 14464-14469.
- [7] A. Landi, A. Mazzoldi, C. Andreoni, M. Bianchi, A. Cavallini, M. Laurino, L. Ricotti, R. Iuliano, B. Matteoli and L. Ceccherini-Nelli, "Modelling and Control of HIV Dynamics," *Computer Methods and Programs in Biomedicine*, Vol. 89, No. 2, 2008, pp. 162-168.
- [8] K. R. Fister, S. Lenhart and J. S. McNally, "Optimizing Chemotherapy in an HIV Model," *Electronic Journal of Differential Equations*, Vol. 1998, No. 32, 1998, pp. 1-12.
- [9] M. M. Hadjiandreou, R. Conejeros and D. I. Wilson, "Long-Term HIV Dynamics Subject to Continuous Therapy and Structured Treatment Interruptions," *Chemical Engineering Science*, Vol. 64, No. 7, 2009, pp. 1600-1617.
- [10] W. Garira, D. S. Musekwa and T. Shiri, "Optimal Control of Combined Therapy in a Single Strain HIV-1 Model," *Electronic Journal of Differential Equations*, Vol. 2005, No. 52, 2005, pp. 1-22.
- [11] J. Karrakchou, M. Rachik and S. Gourari, "Optimal Control and Infectiology: Application to an HIV/AIDS Model," *Journal of Applied Mathematics and Computing*, Vol. 177, No. 2, 2006, pp. 807-818.
- [12] A. Heydari, M. H. Farahi and A. A. Heydari, "Chemotherapy in an HIV Model by a Pair of Optimal Control," *Proceedings of the 7th WSEAS International Conference on Simulation, Modelling and Optimization*, Beijing, 2007, pp. 58-63.
- [13] B. M. Adams, H. T. Banks, H. D. Kwon and H. T. Tran, "Dynamic Multidrug Therapies for HIV: Optimal and STI Control Approaches," *Mathematical Biosciences and Engineering*, Vol. 1, No. 2, 2004, pp. 223-241.
- [14] F. Neri, J. Toivanen and R. A. E. Mäkinen, "An Adaptive Evolutionary Algorithm with Intelligent Mutation Local Searchers for Designing Multidrug Therapies for HIV," *Applied Intelligence*, Vol. 27, No. 3, 2007, pp. 219-235.
- [15] R. Culshaw, S. Ruan and R. J. Spiteri, "Optimal HIV Treatment by Maximizing Immune Response," *Journal of Mathematical Biology*, Vol. 48, No. 5, 2004, pp. 545-562.
- [16] O. Krakovska and L. M. Wahl, "Costs Versus Benefits: Best Possible and Best Practical Treatment Regimens for HIV," *Journal of Mathematical Biology*, Vol. 54, No. 3, 2007, pp. 385-406.
- [17] C. D. Myburgh and K. H. Wong, "An Optimal Control Approach to Therapeutic Intervention in HIV Infected Individuals," *Proceedings of the Third International Conference on Control Theory and Applications*, Pretoria, South Africa, 2001.
- [18] B. M. Adams, H. T. Banks, M. Davidian, H. D. Kwon, H. T. Tran, S. N. Wynne and E. S. Rosenberg, "HIV Dynamics: Modeling, Data Analysis, and Optimal Treatment Protocols," *Journal of Computational and Applied Mathematics*, Vol. 184, No. 1, 2005, pp. 10-49.
- [19] J. Alvarez-Ramirez, M. Meraz and J. X. Velasco-Hernandez, "Feedback Control of the Chemotherapy of HIV," *International Journal of Bifurcation and Chaos*, Vol. 10, No. 9, 2000, pp. 2207-2219.
- [20] S. Butler, D. Kirschner and S. Lenhart, "Optimal Control of Chemotherapy Affecting the Infectivity of HIV," In: O. Arino, D. Axelrod, M. Kimmel and M. Langlais, Eds., *Advances in Mathematical Population Dynamics: Molecules, Cells, Man*, World Scientific, Singapore, pp. 104-120.
- [21] H. Shim, S. J. Han, C. C. Chung, S. Nam and J. H. Seo, "Optimal Scheduling of Drug Treatment for HIV Infection: Continuous dose Control and Receding Horizon Control," *International Journal of Control, Automation, and Systems*, Vol. 1, No. 3, 2003, pp. 401-407.
- [22] D. Kirschner, S. Lenhart and S. Serbin, "Optimal Control of the Chemotherapy of HIV Infection: Scheduling, Amounts and Initiation of Treatment," *Journal of Mathematical Biology*, Vol. 35, No. 7, 1997, pp. 775-792.
- [23] U. Ledzewicz and H. Schättler, "On Optimal Controls for a General Mathematical Model for Chemotherapy of HIV," *Proceedings of the 2002 American Control Conference*, Anchorage, Vol. 5, 2002, pp. 3454-3459.
- [24] R. Zurawski, M. J. Messina, S. E. Tuna and A. R. Teel, "HIV Treatment Scheduling Via Robust Nonlinear Model Predictive Control," *Proceedings of the 5th Asian Control Conference*, Melbourne, Vol. 1, 2004, pp. 25-32.
- [25] R. Zurawski and A. R. Teel, "Enhancing Immune Response to HIV Infection Using MPC-Based Treatment Scheduling," *Proceedings of the 2003 American Control Conference*, Denver, Vol. 2, 2003, pp. 1182-1187.
- [26] R. Zurawski, A. R. Teel and D. Wodarz, "Utilizing Alternate Target Cells in Treating HIV Infection through Scheduled Treatment Interruptions," *Proceedings of the 2004 American Control Conference*, Melbourne, Vol. 1, 2004, pp. 946-951.
- [27] R. Zurawski and A. R. Teel, "A Model Predictive Control Based Scheduling Method for HIV Therapy," *Journal of Theoretical Biology*, Vol. 238, No. 2, 2006, pp. 368-382.
- [28] H. T. Banks, H. D. Kwon, J. Toivanen and H. T. Tran,

- “An State Dependent Riccati Equation Based Estimator Approach for HIV Feedback Control,” *Optimal Control Applications and Methods*, Vol. 27, No. 2, 2006, pp. 93-121.
- [29] M. A. L. Caetano and T. Yoneyama, “Short and Long Period Optimization of Drug Doses in the Treatment of AIDS,” *Anais da Academia Brasileira de Ciências*, Vol. 74, No. 3, 2002, pp. 379-392.
- [30] A. M. Jeffrey, X. Xia and I. K. Craig, “When to Initiate HIV Therapy: A Control Theoretic Approach,” *IEEE Transactions on Biomedical Engineering*, Vol. 50, No. 11, 2003, pp. 1213-1220.
- [31] J. J. Kutch, P. Gurfil, “Optimal Control of HIV Infection with a Continuously-Mutating Viral Population,” *Proceedings of the 2002 American Control Conference*, Anchorage, Vol. 5, 2002, pp. 4033-4038.
- [32] P. Borrow, A. Tishon, S. Lee, J. Xu, I. S. Grewal, M. B. Oldstone and R. A. Flavell, “CD40L-Deficient Mice Show Deficits in Antiviral Immunity and Have an Impaired Memory CD8 CTL,” *Journal of Experimental Medicine*, Vol. 183, No. 5, 1996, pp. 2129-2142.
- [33] C. Young, “Calculus of Variations and Optimal Control Theory,” Saunders, Philadelphia, 1969.
- [34] D. A. Wilson and J. E. Rubio, “Existence of Optimal Controls for the Diffusion Equation,” *Journal of Optimization Theory and Applications*, Vol. 22, 1977, pp. 91-101.
- [35] J. E. Rubio, “Control and Optimization: The Linear Treatment of Non-linear Problems,” Manchester University Press, Manchester, 1986.
- [36] H. H. Mehne, M. H. Farahi and A. V. Kamyad, “MILP Modelling for the Time Optimal Control Problem in The Case of Multiple Targets,” *Optimal Control Applications and Methods*, Vol. 27, No. 2, 2005, pp. 77-91.
- [37] X. Jin, *et al.*, “An Antigenic Threshold for Maintaining Human Immunodeficiency Virus Type 1-Specific Cytotoxic T Lymphocytes,” *Molecular Medicine*, Vol. 6, 2000, pp. 803-809.



# Intelligent Control and Automation (ICA)

ISSN: 2153-0653 (Print), 2153-0661 (Online)

<http://www.scirp.org/journal/ica>

Intelligent Control and Automation is an open access, peer-reviewed and fully refereed journal focusing on theories, methods and applications in intelligent control and automation. The goal of this journal is to provide a platform for scientists and academicians all over the world to promote, share, and discuss various new issues and developments in different areas of intelligent control and automation.

## Editor-in-Chief

**Prof. Theodore B. Trafalis**

University of Oklahoma, USA

## Subject Coverage

All manuscripts must be prepared in English, and are subject to a rigorous and fair peer-review process. Accepted papers will immediately appear online followed by printed hard copy. The journal publishes original papers including but not limited to the following fields:

- Advanced Control Algorithms and Applications
- Artificial Intelligence and Knowledge Engineering
- Complex Systems and Intelligent Robots
- Complex Systems, Logistics, and Supply Chain
- Computational Intelligence and Applications
- Control Theory and Control Engineering
- Electronic Commerce and Office Automation
- Industrial Automation and On-line Monitoring
- Integrated and Complex Automation Systems
- Intelligent Automation and Manufacturing
- Intelligent Control Theory and Applications
- Intelligent Management and Decision Making
- Modeling, Identification, and Fault Diagnosis
- Network Intelligence and Network Control
- Robotics, Service and Medical Robotics
- Systems Engineering and Engineering Optimization
- Systems and Control Theory and Applications

We are also interested in short papers (letters) that clearly address a specific problem, and short survey or position papers that sketch the results or problems on a specific topic. Authors of selected short papers would be invited to write a regular paper on the same topic for future issues of the *ICA*.

## Notes for Intending Authors

Submitted papers should not be previously published nor be currently under consideration for publication elsewhere. Paper submission will be handled electronically through the website. All papers will be peer reviewed. For more details about the submissions, please access the website.

## Website and E-Mail

<http://www.scirp.org/journal/ica>

E-mail: [ica@scirp.org](mailto:ica@scirp.org)

## TABLE OF CONTENTS

Volume 1 Number 1

August 2010

|   |    |
|---|----|
| <b>Parametric Tolerance Analysis of Mechanical Assembly by Developing Direct Constraint Model in CAD and Cost Competent Tolerance Synthesis</b><br>G. Jayaprakash, K. Sivakumar, M. Thilak..... | 1  |
| <b>Optimal Control Strategy for a Fully Determined HIV Model</b><br>M. Shirazian, M. H. Farahi.....   | 15 |
| <b>Weightlifting Motion Generation for a Stance Robot with Repeatedly Direct Kinematics</b><br>J. Liu, Y. Kamiya, H. Seki, M. Hikizu.....   | 20 |
| <b>A Nonmonotone Line Search Method for Symmetric Nonlinear Equations</b><br>G. L. Yuan, L. S. Yu.....  | 28 |
| <b>Stability Analysis and Hadamard Synergic Control for a Class of Dynamical Networks</b><br>X. J. Liu, Y. Zou.....   | 36 |
| <b>Maximizing of Asymptomatic Stage of Fast Progressive HIV Infected Patient Using Embedding Method</b><br>H. Zarei, A. V. Kamyad, S. Effati.....   | 48 |